8-2016

MECHANISTIC AND FUNCTIONAL CHARACTERIZATION OF B AND T LYMPHOCYTE ATTENUATOR (BTLA) IN CD8 TUMOR INFILTRATING LYMPHOCYTES

krit ritthipichai

MECHANISTIC AND FUNCTIONAL CHARACTERIZATION OF B AND T LYMPHOCYTE ATTENUATOR (BTLA) IN CD8 TUMOR INFILTRATING LYMPHOCYTES

by

Krit Ritthipichai, D.V.M., M.S.

APPROVED:

_____
Patrick Hwu, M.D.
Supervisory Professor

_____
Chantale Bernatchez, Ph.D

_____
Greg Lizee, Ph.D

_____
Roza Nurieva, Ph.D

_____
Thomas Cooper, M.D.

APPROVED:

_____
Dean, The University of Texas
Graduate School of Biomedical Sciences at Houston

MECHANISTIC AND FUNCTIONAL CHARACTERIZATION OF B AND T LYMPHOCYTE ATTENUATOR (BTLA) IN CD8 TUMOR INFILTRATING LYMPHOCYTES

A

DISSERTATION

Presented to the Faculty of

The University of Texas

Health Science Center at Houston

and

The University of Texas

M. D. Anderson Cancer Center

Graduate School of Biomedical Sciences

in Partial Fulfillment

of the Requirements

for the Degree of

DOCTOR OF PHILOSOPHY

By

Krit Ritthipichai, D.V.M., M.S.

Houston, Texas

August, 2016

DEDICATION

To my father, thank you for inspiring me to work on cancer immunology.

To my mother, thank you for your sacrifice, support, and encouragement.

To my brothers, thank you for your patience and encouragement.

ACKNOWLEDGEMENTS

I would like to thank my advisors, Drs. Patrick Hwu, Chantale Bernatchez, and Laszlo Radvanyi for their guidance. Dr. Hwu, thank you for your patience and support, you always challenge me to do the best. Thank you Chantale for always being there for me. Your support and encouragement have helped me surpass obstacles. Thank you Laszlo for giving me an opportunity to be in the field of adoptive T cell therapy.

I would also like to thank my committee members: Thank you Drs. Roza Nurieva Greg Lizee and Thomas Cooper for your great support and encouragement.

Thank you to previous and current members of the Bernatchez and Radvanyi lab: Cara Haymaker, Marie Andree Forget, Geok Choo Sim, Jessica Chacon, Michiko Harao, Richard Wu, Charuta Kale, Caitlin Creasy, Kelly Bowen, Young Uk Kim, Donald Sakellariou-Thompson, and Lorenzo Federico. Thank you for all your wonderful support and unforgettable memories.

Thank you to my fellowship advisors (Drs. Ness, Mullen, and Loose) and past and current CPRIT fellows.

MECHANISTIC AND FUNCTIONAL CHARACTERIZATION OF B AND T LYMPHOCYTE ATTENUATOR (BTLA) IN CD8 TUMOR INFILTRATING LYMPHOCYTES

Krit Ritthipichai, D.V.M., M.S.

Supervisory Professor: Patrick Hwu, MD

This dissertation project focused on understanding the functional role of BTLA on $CD8^+$ Tumor Infiltrating Lymphocytes (TIL) from metastatic melanoma patients. Clinical trials of adoptive T-cell therapy (ACT) using autologous *ex vivo* expanded TIL have demonstrated the great potential of this immunotherapy with an overall clinical response rate 40-50% for stage IV metastatic melanoma patients. We have investigated a number of biomarkers in both the infused TIL and the tumor microenvironment for their association with clinical response. Surprisingly, a subset of $CD8^+$ TIL expressing the co-inhibitory molecule BTLA (B-and-T lymphocyte attenuator) was highly associated with clinical response, while expression of other co-inhibitory molecules such as PD-1, TIM-3, and Lag3 did not associate with response. BTLA is expressed by T cells, B cells, and NK cells and serves as a T cell differentiation maker whereby high expression of BTLA associates with less differentiated T cell phenotype. While the suppressive function of the ITIM and ITSM motifs of BTLA are well described, the Grb2 motif's function remains understudied.

In this study, we sought to determine the functional characteristics of the $CD8^+BTLA^+$TIL subset and define the contribution of the Grb2 motif of BTLA in T cell co-stimulation. We have uncovered a survival advantages of the $BTLA^+$ subset that allows for serial killing of target tumor cells, which may explain our previous

correlation between this subset and response to TIL ACT. BTLA-HVEM interaction during T cell activation led to the specific activation of SRC kinase. In addition, our results unveiled a role for the BTLA-associated Grb2-binding motif in T cell proliferation and IL-2 production following TCR engagement that was independent of the inhibitory function of ITIM/ITSM motifs.

Overall, our study first unveil the dual role of BTLA as both a co-stimulatory and co-inhibitory molecule. The integration of the positive and negative signals transduced by BTLA promotes IL-2 secretion while reducing certain effector function of T cell. Altogether, the combination of both BTLA signaling and inherent attributes of less differentiated T cells could promote T cell survival, persistence, and anti-tumor function.

TABLE OF CONTENTS

LIST OF FIGURES

CHAPTER 1.

CHAPTER 2.

CHAPTER 3.

LIST OF TABLES

ABBREVIATIONS

aAPC: Artificial Antigen Presenting Cell

ACT: Adoptive T-cell Therapy

ADCC: Antibody-dependent cell-mediated cytotoxicity

AICD: Activation Induced Cell Death

AIH: Autoimmune Hepatitis

BCG: bacillus calmette-guerin

BMS: Bristol myers squibb

BTLA: B and T lymphocyte attenuator

CAR: Chimeric Antigen Receptor

CCR: C-C Chemokine receptor

CD: Cluster of Differentiation

CEA: Carcinoembryonic antigen

CFSE: Carboxylfluorescein Succinimidyl Ester

Chk: Checkpoint kinase

CRD: cysteine-rich domain

CRISPR/Cas9: Clustered regularly interspaced short palindromic repeats/Caspase-9

CTL: Cytotoxic T lymphocyte

CTLA-4: Cytotoxic T-lymphocyte-associated protein 4

CXCR: C-X-C chemokine receptor

DC: Dendritic Cell

DNA: Deoxyribonucleic acid

DNAM-1: DNAX Accessory Molecule-1

EMD serono: Emanuel Merck Darmstadt serono

ERK: Extracellular signal-regulated kinases

FBL-3: Friend virus-induced leukemia of B6 origin

FDA: Food and Drug Administration

FOXP3: Forkhead box P3

GADS: Grb2-homologous adapter protein

GM-CSF: Granulocyte-macrophage colony stimulating factors

Gp-100: Glycoprotein-100

Grb2: Growth factor receptor bound protein2

GVHD: Graft Versus Host Disease

HER-2: Human Epidermal growth factor receptor

HLA: Human Leukocyte Antigen

HPV: Human Papilloma Virus

HSV1 gD: Herpes virus 1 glycoprotein D

HVEM: Herpes virus entry mediator

I.P.: Intraperitoneal

I.V.: Intravenous

ICOS: Inducible T-cell Co-Stimulator

IFN: Interferon

IHC: Immunohistochemistry

IL-2: Interleukin-2

IL-4: Interleukin-4

IL-7: Interleukin-7

IL-9: Interleukin-9

IL-10: Interleukin-10

IL-15: Interleukin-15

IL-18: Interleukin-18

IL-21: Interleukin-21

ITIM: Immunoreceptor tyrosin-based inihibitory motif

ITSM: Immunoreceptor tyrosin-based switch motif

IU: International Unit

JAK/STAT: Janus Kinase/Signal Transducer and Activator of Transcription

JNK: Jun Nuclear Kinase

KIR2DL1: Killer-cell immunoglobulin-like receptor 2DL1

KLRG-1: Killer cell lectin-like receptor subfamily G member 1

LAG-3: Lymphocyte-activation gene 3

LAK: Lymphokine-activated killer

LCK: Lymphocyte-specific protein tyrosine kinase

LPS: Lipopolysaccharide

MAGE: Melanoma Associated Antigen

MAPK: Mitogen-activated protein kinases

MART: Melanoma Antigen Recognized by T cells

MDACC: M.D. Anderson Cancer Center

MDSC: Myeloid Derived Suppressor Cell

MFI: Mean Fluorescence Intensity

MHC: Major Histocompatibility Complex

mTOR: mammalian Target of Rapamycin complex

MUC1: Mucine-1

NCI: National Cancer Institute

NK: Natural Killer

NKG2D: Natural-killer group 2, member D

NMN: Non-myeloabaltive regimens

NOD: Non-obese diabetic

NSG: NOD Scid IL2 receptor gamma chain knockout mice

NY-ESO-1: New York esophageal cancer-1

PAP: Prostate acid phosphatase

PBMC: Peripheral Blood Mononuclear Cell

PD-1: Program cell death protein 1

PDA: Pancreatic ductal adenocarcinoma

PI3-AKT: Phosphatidylinositol-3-Kinase and Protein Kinase B

PKB: Protein Kinase B

PLCγ: Phospholipase C gamma

pRAS40: proline-rich Akt substrate of 40

PTEN: Phosphatase and Tensin homolog

RAG: Recombination-activating-gene

REP: Rapid Expansion Protocol

RNA: Ribonucleic acid

RPPA: Reverse Phase Protein Array

SCF: Stem cell growth factor

scFV: single chain variable fragment

SCID: Severe Combined Immunodeficiency

SHP: Src homology region 2 domain-containing phosphatase-1

SLE: Systemic Lupus Erythematosus

SLP76: SH2 domain-containing lymphocyte protein

Src: Sarcoma-family kinases

SRC: Spare Respiratory Capacity

STAT5: Signal Transducer and Activator of Transcription

TAA: Tumor associated antigen

TBI: Total Body Irradiation

TCGA: The Cancer Genome Atlas

TCM: Central Memory T-cell

TCR: T-cell Receptor

TEF: Effector T-cell

TEM: Effector memory T-cell

TEMRA: Terminally differentiated T-cell

TGF-β: Transforming growth factor-beta

TIL: Tumor-Infiltrating Lymphocyte

TIM-3: T cell immunoglobulin and mucin domain-3

TIMING: Timelapse Imaging Microscopy In Nanowell Grids (TIMING)

TLR: Toll right receptor

TNF: Tumor Necrosis Factor

TNFR: Tumor Necrosis Factor Receptor

TNFRSF: tumor necrosis factor receptor superfamily member

TNM: Tumor Node Metastasis

Treg cell: T regulatory cell

TYROBP: TYRO protein kinase-binding protein

USDA: United States Department of Agriculture

Vav1: Vav guanine nucleotide exchange factor 1

VISTA: V-domain Ig suppressor of T cell activation

ZAP70: Zeta-chain-associated protein kinase 70

CHAPTER 1

General Introduction

1.1 Cancer Immunotherapy

Recently, the second edition of hallmarks of cancer proposed by Robert Weinberg and Douglas Hanahan have included evading immune system destruction as one of the biological properties that transformed cells require during multistep carcinogenesis (1, 2). In the past two decades, our extensive gain in knowledge of cancer immunology has solidly proved that the immune system plays both a positive and negative role during cancer development. The first evidence of the immune system's role in tumor control was demonstrated by William B. Coley in 1893 when he treated inoperable malignant sarcoma with inactivated bacterial lysates that consisted of *Streptococcus pyogenes* and *Bacillus prodigiosus*, which triggered an immune response resulting in tumor regression in a patient for almost 26 years until his death (3). Although the finding suggested that the activated immune system could promote tumor regression, there was no strong evidence to support this clinical observation.

In early 1909, Paul Ehrlich first postulated that the immune system could recognize and destroy cancerous cells (4). Five decades later, Lewis Thomas and MacFarlane Burnet proposed their immunosurveillance hypothesis, which suggested the existence of effector cells that can sentinel the transformed cells in the body and eliminate them through a specific mechanism (4-6). Later on, a number of extensive *in vivo* and *in vitro* studies have refined and included immunosurveillance as a part of "cancer immunoediting", which more precisely defines the involvement of the immune system in tumor development in three phases; elimination, equilibrium, and escape. Elimination (or immunosurveillance) is the first step, in which immune cells recognize

tumor cells and destroy cancer cells. In the equilibrium phase, some tumor cells are not targeted by immune-mediated killing. Emerging new tumor cell variants are then selected to grow and flee from immune detection in the escape phase (7-9).

1.1 a) Highlights of major discoveries in cancer immunotherapy

***1950*:** Evidence from Llyod Old, and other scientists emphasized the importance of the immune system in tumor control (10, 11).

***1961 to 1970*:**

- Hellstorm and colleagues demonstrated specific tumor recognition by immune cells (12).
- Alpha fetoprotein (AFP) was identified as the first tumor-specific antigen by Irlin's group (13).
- Gershon and Kondo revealed the suppressive role of T cells, leading to immunotolerance theory (14).

1971 to 1980

- Discovery of dendritic cells by Ralph Steinman, leading to cancer vaccine study (15).
- Identification of Natural killer cells by Eva Klein and Hans Wigzell, leading to the development of NK cell therapy (16).
- Francis W. Ruscetti, Doris A. Morgan, Robert Gallo and colleague discovered Interleukin-2, the first effective immunotherapy in cancer treatment and also used in combination with other immunotherapies (17-19).

1981 to 1990

- FDA approved Rituxan, the first monoclonal antibody for B cell lymphoma treatment developed and tested by Ronal Levy. A few years later, Greg Winter successfully generated the world's first humanized antibody (20, 21).
- Dr. Steven Rosenberg first used high-dose IL-2 as a single therapy for cancer patients with advanced diseases and treated the first melanoma patient with tumor infiltrating lymphocytes (TILs) (22).
- Discovery of T cell receptor by Phillippa Marrack, John Kappler, and James Allison (23).
- CTLA-4 was identified by Golstein and colleagues (24).

1991 to 2000

- Tyrosinase was the first tumor antigen on melanoma cells recognized by HLA-A2 restricted tumor reactive T cells (25).
- Drew Pardoll demonstrated the effectiveness of the cancer vaccine GVAX to stimulate a long-lasting anti-tumor response in a phase I clinical trial (26).
- The first report of using dendritic cells as a cancer vaccine in melanoma by Bijay Mukherji (27)
- James Allison and colleagues first revealed the effect of anti-CTLA-4 antibody in tumor control using murine model (28, 29).
- FDA approved Transtuzumab (Herceptin) for metastatic breast cancer treatment (30).

2001 to 2010

- Fully humanized monoclonal antibody (anti-human Epidermal Growth Factor Receptor, Ranitumumab) was approved by FDA for metastatic colorectal cancer (31).
- FDA approved Gardasil and Cervarix vaccines protecting against the Human Papilloma Virus (HPV), which causes approximately 70% of cervical cancer cases (32).
- Immunoscore was firstly introduced as a novel approach to evaluate cancer progression (33).
- Strong evidence demonstrating the effectiveness of the anti-CTLA-4 antibody in tumor regression in human studies (34).

2010 to present

- First dendritic cell vaccine (Sipuleucel-T) was approved by FDA for the treatment of prostate cancer (35)
- Clinical studies demonstrated an improved survival with ipilimumab metastatic melanoma patients that led to FDA approval (36, 37).
- Clinical trials of using anti-PD-1 blockade successfully showed improved clinical outcomes in metastatic melanoma, renal cancer, lung cancer, and colon cancer which led to FDA approval for anti-PD-1 antibody, Nivolumab and Pembrolizumab (38, 39).
- Success of CAR T cell therapy trials led by Carl June and Steven Rosenberg demonstrated approximately 90% objective clinical response in Hematological (40).

Current strategies in cancer immunotherapy

On the basis of our current knowledge, the immune system plays a protective role in pathogen infection as well as cancer control. Although the immune system is powerful enough to protect and control tumors, the remaining question is why cancers still occurs in normal people with healthy immune system. Indeed, tumors are able create a microenvironment that inhibits immune mediated cancer cell killing. Overcoming the immunosuppressive environment requires the coordination between antigen-presenting cells and T cells. Antigen-specific T cells need to receive an optimal priming in order to develop robust effector functions as well as long-lasting immune response. Several strategies have been extensively investigated to improve the function of immune cells including enhancing tumor antigen presentation and promoting effector function and memory development of antigen-specific T cells. Several types of tumor immunotherapy have been investigated and employed to foster innate and adaptive immune system. Here, four major types of cancer immunotherapy are discussed including; cytokine, checkpoint blockade inhibitor, vaccine, and cell-based therapy (**Figure 1.1**)

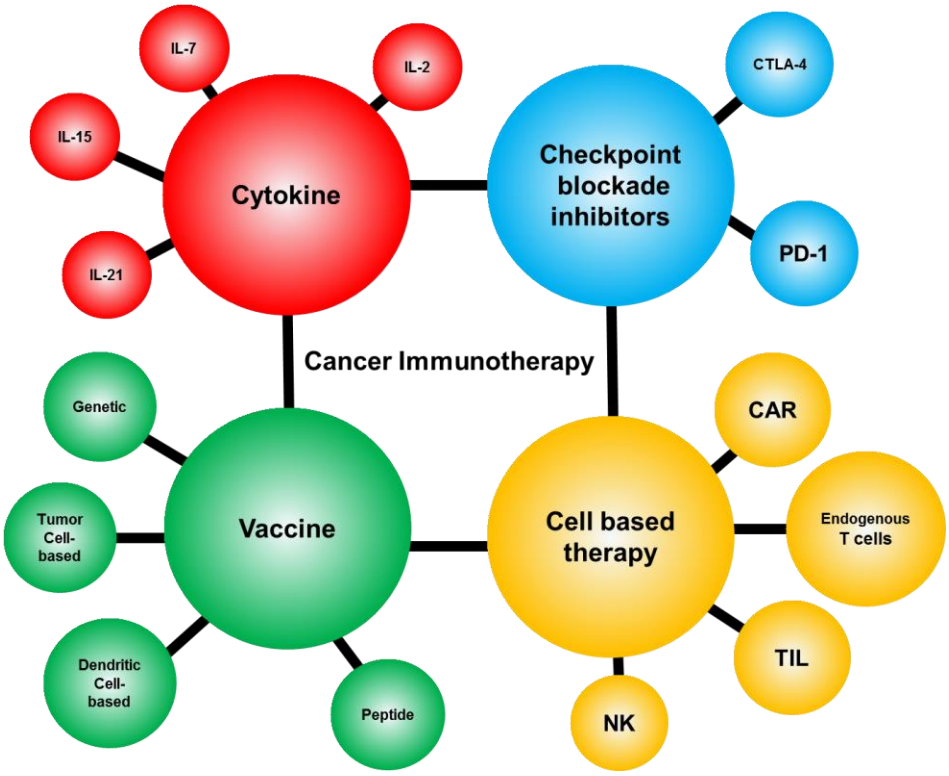

Figure 1.1. Schematic diagram demonstrates four major types of cancer immunotherapy.

1.1 b) Checkpoint blockade inhibitors

The effector functions of T cells, including cytokine production, proliferation, and target cell killing are regulated by the coordination between co-stimulatory and co-inhibitory molecules after encountering tumor antigens (41). Immune checkpoints are pivotal for the maintenance of self-tolerance and preventing an overreacting immune response (42, 43). However, excessive function of co-inhibitory molecules can benefit tumor cells to escape the immune response. Blockade of co-stimulatory molecules potentially breaks the physiological tolerance and enhances the anti-tumor response (42). Using antagonist antibodies against T cell co-inhibitory molecules has proved promising in cancer therapy. Targeting checkpoint molecules does not directly affect tumor cell death itself, instead this strategy prevents T cell from receiving inhibitory signal from tumor cells, resulting in improvement of its effector function in mediating tumor killing (42, 43). Currently, the effect of immune checkpoints' blockade on immune response has been widely investigated at both pre-clinical and clinical models. Targeting different inhibitory molecules have provided a great potential to manipulate immune response by different mechanisms such as enhancing effector T cell function, depleting regulatory T cells from tumor microenvironment, and facilitating T cell migration. Thus, combinatorial blockade is a worthwhile strategy for cancer immunotherapy.

CTLA-4

CTLA-4 was initially reported following the discovery of the first co-stimulatory molecules, CD80 and CD86, in 1991 (24). Due to the high sequence similarity between CTLA-4 and CD28 it was initially believed that CTLA-4 was a positive T cell co-stimulatory receptor (44). However, the inhibitory function of CTLA-

4 on T cells was revealed by James Allison's laboratory later in 1995 (45). CTLA-4 was shown to strongly suppress T cell proliferation by outcompeting CD28 from binding CD80 and 86 expressed by APCs during antigen stimulation (46). Thus far, the specific signaling pathway of T cells targeted by CTLA-4 has not been identified. Some studies suggest that the downstream pathway of CD28 might be dampened by CTLA-4 via activation of SHP2 proteins, a phosphatase protein that attenuates proximal TCR signals (47). In addition, the cytotoxic lymphocytes (CTL) proliferative dysregulation observed in in CTLA-4 knock-out mice confirmed its inhibitory role(48). The inhibitory function of CTLA-4 strongly affects the effector function of $CD8^+$ T cells, however CTLA-4 was found to directly enhance the suppressive function of $CD4^+CD25^+Foxp3^+$ T reg (Regulatory T cell, Treg). Thus, blockade of CTLA-4 can improve effector function of $CD8^+$ and attenuate the inhibitory function of T regulatory T cells (49). This results in boosting anti-tumor immunity in the tumor microenvironment. Preclinical studies demonstrated improvement of the antitumor response in partially immunogenic tumor-bearing mice when treated with anti-CTLA-4 as a single therapy (28). However, in poorly immunogenic tumor models, vaccination in conjunction with anti-CTLA-4 blockade was required to achieve a similar anti-tumor response (28, 50).

Based on preclinical evidence, two pharmaceutical companies have developed antibodies targeting CTLA-4, including Bristol Myer Squibb (ipilimumab) and Pfizer (tremelimumab). In phase III clinical trials, approximately 20% of patients with metastatic melanoma had achieved long-term-survival of at least two years when combined CTLA-4 treatment with gp100 vaccination (36, 51). Interestingly, ten-year

survival was also reported in some patients. On the basis of overall survival benefit for patients with advanced melanoma, ipilimumab was approved by FDA in 2011 (52). However, phase I and II clinical trials for melanoma with tremelimumab were discontinued in 2008 due to no statistical significance for improving overall survival (53). The successful story of CTLA-4 blockade has strengthened the concept of checkpoint blockade in cancer immunotherapy and fostered the needs for further studies on other checkpoint inhibitors such as PD-1, TIM-3, and LAG-3.

PD-1

PD-1 is characterized as a co-inhibitory molecule expressed by T cells. PD-L1 and PD-L2 are the two identified PD-1 ligands. Recruitment of phosphatase (SHP1 and 2) into ITIM and ITSM motifs is responsible for an inhibitory function of PD-1 (54, 55). It has been shown that PD-1 specifically targeted Akt and cell cycle pathways to suppress T cell proliferation (56). Although PD-1 and CTLA-4 are both negative stimulatory molecules, it is believed that their downstream targets are relatively distinct. CTLA-4 predominantly inhibits T cells during early activation, supposedly during T cell priming phase, while PD-1 mainly suppresses effector functions of T cells primarily residing in peripheral tissues and tumor bed due to the presence of its ligand (PD-L1) highly expressed by tumor cells.

PD-1 is widely expressed by several immune cells including B and NK cells, and its ligand is expressed by tumors. In contrast, expression of CTLA-4 is limited in T lymphocytes, and its ligand is mostly expressed by APCs (54). Thus, blockade of the PD-1 pathway is likely to affect more broad-range targets than CTLA-4. PD-1 blockade, considered to enhance effector T cell function, may also improve the function

of natural killer cells in mediating tumor regression, and indirectly boost humoral immunity against tumors mediated by B cells as well (57).

In several chronic diseases such as some viral infections and cancers, T cells are repetitively stimulated by antigens due to the persistence of diseases. This condition can induce high expression of PD-1 on T cells, resulting in T cell anergy or exhaustion (58). In murine models, it has been shown that blockade of PD-1 partially reversed the effector function of T cells during chronic viral infection (59).

Expression of PD-L1 has been indentified in several human tumors including melanoma, breast cancer, glioblastoma, and ovarian cancer. IFN-γ secreted by CTL was found to up-regulate PD-L1 on tumor cells, epithelial cells, and stromal cells (60). It was thought that the PD-L1 ligand itself had no role in tumor cell signaling based on the fact that the cytoplasmic domain is relatively short. However, a recent report in glioblastoma has demonstrated that PD-L1 enhanced PTEN degradation resulting in constitutive activation of the AKT pathway (61).

Suppression of anti-tumor immunity upon ligation between PD-L1 and PD-1 has been noted in several murine models. Defects in T cell-mediated tumor immunity were observed upon overexpression of PD-L1 in mouse tumor cells (62, 63). The use of PD-L1 expression as a prognostic marker in clinical trials using PD-1 blockade antibody has been controversial. This might be due to some difficulties in performing cross comparisons with variations in technique, type and stage of cancers, and prior treatment.

Strong evidence from mouse models demonstrating the effect of PD-1 blockade in improving tumor control combined with the observation of high expression of PD-

L1 in several cancers has led to the development of several human therapeutic antibodies targeting the PD-1 pathway including anti-PD-1 antibodies; (nivolumab (BMS) and pembrolizumab (Merck)), and anti-PD-L1 antibodies; (BMS-936558 (BMS), MPDL3280A (Genentech), MEDI4736 (Medimmune), MSB0010718C (EMD serono)) (38, 64). In phase I studies, nivolumab successfully improved the three-year survival rate to 40% among 107 treated melanoma patients (65). In 2014, FDA has approved nivolumab for the treatment of patients with metastatic melanoma with no response to prior treatment as well as squamous non-small cell carcinoma. Comparison of nivolumab and conventional chemotherapy (dacarbazine) in phase III clinical trails has successfully confirmed the phase 1 result with a superior response rate (40% versus 13%) (65).

1.1 c) Cancer vaccine

A knowledge of tumor antigens recognized by the immune system has shed light on developing vaccines as an alternative approach for cancer therapy. On the basis of vaccine components, it can be classified into three categories: cell-based, peptide-based, and genetically-based vaccines.

Cell based vaccine

Tumors derived from patients were first used as a vaccine to test the proof of principle that providing tumor antigens with an adjuvant (BCG) can boost the anti-tumor response. The patients vaccinated with irradiated autologous tumors alone did not achieve a favorable clinical response (66). However, tumors engineered to secrete granulocyte-macrophage colony-stimulating factors (GM-CSF) was found to trigger tumor regression when combined with anti-CTLA-4 antibodies (50). Autologous tumor cell preparation is labor intensive and limited to only some solid tumors. Hence, an

alternative approach of using an allogenic whole tumor cell vaccine was developed to overcome this limitation. The use of canavaxin, irradiated whole cells from three melanoma cell lines in combination with BCG, has been evaluated in phase III clinical trials and witnessed slightly improved overall survival rate in metastatic melanoma patients as compared to the control (49% versus 37%) (67). However, this approach was discontinued later on since two independent randomized trials failed to prove anti-tumor efficacy. Because tumor antigens from tumor cell lysate require effective antigen processing and presentation, another strategy of using dendritic cells for active immunotherapy has been developed. Sipuleucel-T (Dendreon Corporation) is the first dendritic cell vaccine approved by FDA for the treatment of asymptomatic and minimally symptomatic metastatic castration-resistant prostate cancer (35). Phase III trials have demonstrated a slightly improved median overall survival in patients treated with Sipuleucel-T as compared with a placebo control (25.8 months versus 21.7 months) (68). In our TIL therapy program at M.D. Anderson Cancer Center, we have observed that the combination of TIL therapy using TIL products containing MART-1 reactive $CD8^+$ TIL with the infusion of autologous dendritic cells pulsed with MART-1 peptide did not improve the efficacy of treatment from what is seen with the infusion of TIL alone in a small cohort of 19 patients (data not shown, personal communication from the TIL program).

Peptide vaccine

Several tumor-associated antigens (TAAs) are identified in many types of cancers such as MAGE, NY-ESO-1, gp100, MART-1, E75, and so forth. TAAs can be up-taken, processed, and presented on the cell surface of mature APCs (69). It is crucial

for dendritic cells to receive appropriate signals for maturation, migration to the regional lymph node, and presentation of TAAs to naïve T cells. Thus, the adjuvant is required for appropriate TAAs priming by APCs. Mimicking innate immune alarm using synthetic pathogen-associated molecular patterns (PAMPs) such as TLR agonists can activate APCs and enhance the desired anti-tumor response. Investigating the use of TLR agonists for cancer vaccine is currently under way in clinical trials, including TLR3, TLR4, and TLR9. So far, only three TLR agonists are approved by FDA for therapeutic use in humans including BCG (TLR 2, and 4 agonists), monophosphoryl lipid A (MPL, TLR4 agonist), and imiquimod (TLR7 agonist) (70). Identification of melanoma TAAs recognized by T cells including gp100, MART-1, NY-ESO-1, and survivin strengthens the use of vaccine as an alternative therapy for cancer. In phase III clinical trials, a combination of gp100 and IL-2 has demonstrated improved response rate in relative to IL-2 alone (16% versus 6%) (71). However, vaccination of melanoma stage III patients with MAGE-A3 failed to prolong disease-free survival in phase III clinical studies. Recent study on cocktail antigen vaccination with melanoma antigens, including gp100, MAGE-A1, MAGE-A2 and MART-1 and tyrosine kinase, exhibited extended survival time as compared with placebo controls (21 months versus 8 months) (72). In pancreatic adenocarcinoma (PDA), phase III clinical studies of telomerase vaccine (GV1001) with chemotherapy demonstrated no improvement in survival as opposed to chemotherapy alone (73). Immunization with IMA901 vaccine in conjunction with cyclophosphamide and GM-CSF increased overall survival rate in patients with reactive T cells against peptide IMA901, but did not benefit patients who had no pre-existing immune response (74).

Genetically based vaccines

Recombinant DNA vectors are carriers for protein overexpression in mammalian cells. This gene delivery approach can be used to deliver and express TAAs to enhance antigen recognition by T cells. Using optimization of codon usage can improve TAA expression when its gene-containing codons have rare tRNA. The major advantages of DNA vaccines are simple and flexible design, lack of adverse effects, heat labile, and cost effectiveness. In addition, DNA structure itself can also act as an adjuvant to activate innate immune systems through TLR, which can provide optimal priming to elicit potent adaptive immune (75). The introduction of DNA vaccines through intradermal and intramuscular injections was shown to have limited DNA up-taking, and resulted in low transfection efficiency. A novel technology using the Gene Gun to deliver DNA coated with gold particles can increase DNA uptake, which makes it feasible for clinical applications. Another approach to increase the uptake of DNA plasmid is the use of electroporation which works by permeabilizing the cell membrane with electric pulses. By this mean, not only does the efficiency of DNA delivery can increase approximately 1,000-fold, but also lead to the recruitment of APCs at the vaccination site due to tissue damage (76).

The first successful DNA vaccine (Oncept, Merial) was initially tested in canine spontaneous melanoma using a human tyrosinase recombinant DNA vector. The use of Oncept has demonstrated prolonged survival in dogs with advanced melanoma without toxicity. Thus far, Oncept is one-and only DNA vaccine approved by USDA. In human, DNA vaccine for cancer treatment has not yet been approved by FDA (77). However, several clinical trials are being extensively conducted in different types of cancers. In

melanoma, using the gp100 DNA vaccine has shown no benefit in progression-free survival regardless of patient immune response. Only a subtle increase in IFN-γ in $CD8^+gp100^+$ T cells has been observed in some patients (78). A number of studies of tumor antigens in other cancers are currently ongoing including human epidermal growth factor receptor 2 (HER2), carinoembryonic antigen (CEA), prostate acid phosphatase (PAP), and E6/E7 (human papilloma viral proteins). An increase in effector function of tumor-specific antigen reactive T cells was found in breast cancer and colorectal cancer patients, but failed to prolong the survival time (79).

An application of mRNA vaccines is another approach used extensively in small animal models. RNA structure can be recognized by TLR and help prime an innate immune response. Because RNA is vulnerably instable and prone to degrade upon delivery, several strategies have been focused on protecting RNA from degradation such as RNA-loaded nanoparticles, protamine-condensed RNA, and encapsulated RNA. Instead of immunization with naked RNA, adoptive transfer of autologous dendritic cells transfected with the RNA of target antigens has also been studied in several types of cancers including melanoma, lung cancer, colorectal cancer, prostate cancer, and pancreatic cancer. In a study in humans, transfection of DCs with RNA directly isolated from autologous tumors has demonstrated the expansion of tumor-reactive T cells mediating autologous tumor cell lysis (80). Currently, the clinical study of RNA vaccines is still limited to phase I/II trials. In melanoma, using naked RNA purified from an autologous tumor improved clinical response rates, mixed response (15%) and no evidence of disease (23%) (81). In renal cell carcinoma, patients immunized with a cocktail of RNA of tumor antigens (MUC1, CEA, HER-2/neu,

telomerase, surviving, and MAGE-1) has illustrated only 7% partial response and 40% stable disease, and an increase in the effector function of $CD8^+$ and $CD4^+$ T cells was also observed in some patients (82).

1.1 d) Cytokine therapy for cancers

Cytokine, a small molecule secreted from cells, can act as a mediator for intercellular communication. Engagement of cytokine and receptors on immune cells can rapidly stimulate cell signaling and function in multiple facets including cell proliferation, migration, and cytotoxicity. In cancer immunology, cytokines are very critical to enhance maturation of innate immune cells such as dendritic cells as well as the effector function of cytotoxicity T cells (CTLs). Nevertheless, some cytokines such as IL-10 and TGF-β can inhibit effector function of CTLs. Currently, only two cytokines have been approved by FDA through the use of cancer therapy, including IL-2 and IFN-α (83). In addition, a number of several cytokines such as IL-7, IL-15, IL-18, and IL-21 are being focused in both preclinical and clinical studies for cancer treatment.

IL-2

IL-2 is a cytokine mainly secreted by activated $CD4^+$ T cells. IL-2 mediates T cell proliferation similar to the cytokines that share common gamma chain receptors such as IL-4, IL-7, IL-9, IL-15, and IL-21. The IL-2 receptor consists of three subunits; alpha (CD25), beta (CD122), and gamma (CD132). The alpha subunit is involved in binding, while the other subunits play an important role in downstream signaling. Unlike T cells, IL-2 receptor in NK cells and B cells contains only gamma and beta subunits, thus mediate less binding affinity than T cells (84). Engagement of IL-2 and its receptor on

T cells does not only stimulate cell proliferation, but also promotes T cell differentiation into different subsets such as memory, effector, and terminally-differentiated subsets (85).

Discovery of IL-2 has unleashed new possibilities for *in vitro* expansion of T cells for functional study. Successfully shown to be effective in tumor control in murine model, the use of IL-2 was then quickly applied into cancer therapy (19). High dose IL-2 was given intravenously at 600,000 to 720,000 IU/kg every eight hours for two cycles; first and second cycle began on D1 to D5 and D15 to D19 respectively. Clinical response was evaluated within a month following the second cycle of treatment. It has been demonstrated that IL-2 treatments in melanoma patients with advanced stages achieved approximately 20% clinical response, and intriguingly 5 to 7% had a durable complete response (86). The success of high dose IL-2 therapy in metastatic melanoma and renal cell carcinoma has eventually led FDA approval in 1998. Currently, the use of high dose IL-2 treatment becomes a conventional therapy used concurrently with other types of immunotherapy such as T cell therapy and cancer vaccination. Patients administered IL-2 require an intensive monitoring due to its toxicity, including febrile, hypotension, and capillary leak syndrome (87). Although major toxicities of IL-2 can be harmful, this effect is completely reversible following the completion of treatment. With proper management, IL-2 can be safely used either as a single treatment or in conjunction with other immunotherapies.

IL-7

IL-7 is known as a cytokine promoting the growth of hematopoietic cells. It is majorly produced by epithelial cells in thymus and stromal cells in bone marrow, but not

lymphocytes. Its receptor contains a gamma subunit commonly shared with IL-2. IL-7 plays a critical role in promoting differentiation of hematopoietic stem cells into lymphoid lineage cells (88). It has been also shown that IL-7 enhanced cell survival and proliferation of B cells and NK cells (89, 90). In T cells, IL-7 is critical for early development of thymocytes during double-negative stage (91). Together with stem cell factor (SCF), IL-7 promotes proliferation of TN precursors and provides survival signals through regulation of bcl-2 family members (92). It is known that IL-7 also enhances T cell activation, particularly in suboptimal conditions. IL-7 preferentially stimulates a type I immune response resulting in an increased IFN-γ and IL-2. A recent report also indicated that IL-7 directly boosts the cytolytic capacity of CTL as well as NK cells, NKT cells, and γδ T cells (93). Functional studies of IL-7 are still limited to *in vitro* settings and preclinical murine models. Two clinical trials are currently underway regarding the role of IL-7 in cancer immunotherapy. Early results have shown the promise of IL-7 in enhancing T recovery following chemotherapy treatment with minimal toxicity (94-96).

IL-15

IL-15 is a unique cytokine that is secreted in a complex form of IL-15 and IL-15 receptor alpha (IL-15Rα) (97). Monocytes are a major source for IL-15 production (98). Upon activation with the IFN or engagement of the CD40 ligand, dendritic cells can upregulate IL-15 and IL-15Rα expression, and to trans-present to $CD8^+$ memory T cells or NK cells expressing IL2/IL-15 receptor beta (IL-15Rβ) (99). Similar to other cytokines in the gamma receptor family, IL-15 stimulates proliferation of T cells and NK cells, and also enhances immunoglobulin production in activated B cells.

Downstream signal of IL-15 through the JAK/STAT pathway can promote phosphorylation of Src family proteins and the PI3K/Akt pathway (100). This results in an increased Bcl-2 and Bcl-xL proteins, which help protect memory CD8 T cells against apoptosis from activation-induced cell death mechanism (AICD) (101).

IL-21

IL-21 is a type I cytokine predominately produced by NKT cells, T follicular helper cells (Tfh), and Th17 cells (102). Unlike other cytokines in the type I receptor superfamily, IL-21 mainly activates STAT1 and STAT3 instead of STAT5 (103). IL-21 has a pleotropic effect as its receptor is expressed by a broad range of several immune cells, including lymphoid lineage as well as myeloid cells. In B cells, IL-21 can enhance immunoglobulin G production by promoting class switching (104). IL-21 can also promote both NK cells and T cell proliferation and cytotoxic function without causing AICD, but suppresses FOXP3 expression in Treg cells (105). It has been evident that IL-21 promoted cytotoxic function of NK cells through antibody-dependent cell cytotoxicity (ADCC), and effector function of T cells by enhancing granzyme and IFN-γ production (106). In our observation, IL-21 at low dose tends to preferentially promote $CD8^+$TIL expansion, while attenuation of TIL proliferation has been observed with those expanded with IL-21 at high doses. Interestingly, recent findings showed that IL-27 can stimulate $CD8^+$ T cells to secrete IL-21, which act as an autocrine regulator (107). In murine models, IL-21 has been shown to suppress the growth of melanoma and fibrosarcoma by enhancing the function of NK and $CD8^+$T cells. Because IL-21 effectively promotes the function of CTL and NK cells, the use of IL-21 become attractive for an application in cancer treatment as either single therapy

or combination with other treatments. Systemic administration of IL-21 is likely to benefit tumor regression by enhancing the function of $CD8^+$ and NK cells without vascular leakage, which provide an advantage over high dose IL-2 therapy. However, an adverse effect in enhancing pro-inflammation cytokine such as IL-6 and IL-17 might raise some concerns in clinical use. An alternative approach is adoptive transfer of autologous dendritic cells transfected with IL-21 transcript. Transferred dendritic cells can provide IL-21 locally to TIL in tumor microenvironments with minimal unwanted side effects (108). Another approach is to use IL-21 for *ex-vivo* expansion of TIL for Adoptive T cell therapy (ACT). Analysis of the immunophenotype of TIL expanded with IL-21 revealed a less differentiated phenotype (CD27hi and CD28hi) with increased cytotoxic capacity. Because poorly differentiated TIL is associated with persistence following TIL transfer, the expansion TIL with IL-21 could be a potential approach to improve TIL quality and clinical response (109).

1.2 Cell based therapy for malignant diseases

1.2 a) NK cell therapy

Natural killer cells (NK) are innate immune cells derived from lymphoid progenitor cells in the bone marrow. As they are derived from a lymphoid lineage, NK cells can be defined as $CD45^+CD3^-CD56^+$ cells. The expression level of CD56 can further classify NK cells into to two subsets; $CD56brightCD16^-$ and $CD56dimCD16^+$. Peripheral blood is highly enriched for the $CD56dimCD16^+$ subset, while $CD56brightCD16^-$ subset primarily resides in the lymph nodes and tonsils. Unlike T cells, NK cells recognize transformed cells such as virus-infected cells, stressed cells, and tumor cells in non-MHC-restricted settings. The mechanism of NK-mediated target cell killing relies on the balance between activating signals and inhibitory signals from

cell surface receptors (110). The activating receptor, such as NKG2D, NKp30, and DNAM-1, can trigger signals by phosphorylating the immunoreceptor tyrosine-based activating motif (ITAM) in the cytoplasmic domain. This results in recruitment of Syk and ZAP70, leading to degranulation of perforin and granzymes as well as cytotoxic cytokines such as IFN-γ and TNF-α. On the other hand, inhibitory receptors, such as Ly49C, KIR2DL1, and KLRG1, attenuate signals through immunoreceptor tyrosine-based inhibitory molecules (ITIMs), resulting in sequestration of phosphatase SHP1 or 2 and dephosphorylation of phosphoproteins in activating pathways. Under normal physiological condition, the cytotoxic activity of NK cells is suppressed by engagement of NK cell inhibitory receptors and MHC expressed by normal cells. Down-regulation of MHC expression in tumor cells and can relieve the suppressive function of the inhibitory receptor, which allows NK cells to become activated and destroy target cells. Moreover, up-regulation of danger signals by tumor cells can enhance the cytolytic capacity of NK through engagement of activating receptors (111). Under the selective pressure in tumor microenvironments, tumor cells tend to escape T cell recognition by down-regulation of MHC class I. This mechanism somehow aids NK cells to become more activated and attack tumor cells better. On the basis of its anti-tumor activity, several strategies have been developed to use adoptive transfer of NK cells for cancer treatment (112).

NK cells can be generated from different sources such as peripheral blood, bone marrow, umbilical cord blood, and stem cells. The combination of IL-15 and hydrocortisone to propagate NK cells has become general practice guideline for *ex vivo* NK cell expansion. Although autologous NK can be successfully expanded for clinical

treatment, these expanded cells do not develop full cytolytic function following adoptive transfer, resulting in an unfavorable clinical outcome (113). It has been suggested that some tumor cells still maintain MHC class I expression, which is effective enough to suppress cytotoxic function of NK cells. Thus, another strategy is the use of allogenic NK cells with KIR mismatch which could circumvent the suppressive effect of MHC I and allow activating receptors to exhibit positive signals mediating tumor killing. It has been demonstrated that the KIR haplotype of the donor is associated with a survival benefit. Patients who received donor KIR haplotype group B have been shown to have improved overall survival as compared to those who received the KIRT haplotype group, mainly due to the high enrichment for activating receptors in the KIRT haplotype. Nevertheless, allogenic NK cells are eventually eliminated by the host immune system due to MHC mismatch (114). Currently, early clinical trials in adoptive NK cell therapy are under way in several countries, including the United States, Korea, France, Spain, and Singapore. The efficacy of NK cell therapy is evaluated mainly in hematological malignancies including leukemia, lymphoma, and multiple myelomas. A clinical trial conducted at Masonic Cancer Center in acute myeloid leukemia (AML) demonstrated that 26% of patients receiving haploidentical NK cells exhibited durable clinical outcomes. Recent studies have also demonstrated NK cell therapy in some solid tumors such as non-small cell carcinoma, hepatocellular carcinoma, and neuroblastoma. The clinical outcome of trials conducted in multiple institutions are promising for NK cells therapy (115). A more in-depth understanding of the signaling that regulates cytotoxic function is warranted for further improvements in NK cell therapy.

1.2 b) T cell therapy

Discovery of the TCR in early 1980 has driven a leap in understanding T cell biology in the context of antigen recognition through MHC. This knowledge does not only foster basic immunology research, but also extends a great benefit for cancer immunotherapy. Based on the fact that T cells can recognize and destroy tumor cells, this notion has attracted scientists and physicians to utilize T cells for cancer treatment.

Adoptive T cell therapy can be categorized on the basis of the source of T cells and type of gene modification approach used. T cells used for therapy can be derived from different sources, including the Tumor infiltrating lymphocytes (TIL), sorted antigen-specific T cells from peripheral blood, and normal peripheral blood mononuclear cells (PBMC). T cells can also be genetically modified to overexpress either chimeric antigen receptors or T cell receptors specific for tumor antigens by using bioengineering methods.

TIL therapy (ACT)

History of ACT

In late 1987, a progress study on adoptive transfer of lymphokine-activated killer (LAK) cells with IL-2 was first investigated in 157 patients with metastatic melanoma. A combination of LAK and IL-2 was found to have advantages over IL-2 alone due to the durable complete responses (22). The limited efficacy of LAK has suggested the used of TIL, which are already present in tumor bed and more enriched for tumor-reactivity (116).

Several efforts were made to conduct adoptive transfer T cells for cancer therapy in murine models. One of the most successful murine models was established

in Dr. Alex Fefer's lab in Fred Hutchinson Cancer Research Center. Adoptive transfer of T cells from immunized mice with the Friend virus-induced leukemia, FBL-3 was shown to be effective following intravenous administration in both local tumors and disseminated metastasis (117). Although the concept of using adoptive transfer of tumor-specific T cells to destroy cancer was proved, incapability of expanding antigen-specific T cells against spontaneously growing human cancers was a major hindrance. The approach of using adoptive transfer of TIL as an immunotherapy of cancer was proposed shortly after the success of using syngeneic TIL plus IL-2 therapy in murine model to eradicate established hepatic metastasis (118).

The observation that specific tumor-reactive T cells can be grown from resected metastatic melanoma tumor with IL-2 was a critical step to support further investigation of large scale TIL expansion for therapeutic use. TIL expansion protocol initially used only IL-2 to grow TIL from digested tumor fragments. The fold expansion ranged from 3 to 9 X 10^8-fold over 14 to 100 days (119). Shortly after, a pilot study using a combination of IL-2 and TILs was first reported from the Surgery Branch at the NCI (120). This report was considered as a huge leap for cancer immunotherapy and the beginning of the era of TIL ACT.

Current TIL ACT therapy

ACT is an effective immunotherapy for cancer using autologous tumor-infiltrating lymphocytes (TIL) isolated from cancer patients. TIL can be generated from either small pieces of resected tumor fragments (approximately more than 1 cm) or tumor digestion followed by density gradient centrifugation. TILs are initially grown in 24-well plates with high dose IL-2 (6,000 IU/ml) for approximately three to five

weeks. The cells are then further propagated with a rapid expansion protocol (REP) using irradiated peripheral blood mononuclear feeder cells as feeders, anti-CD3, and high dose IL-2, for 14 days (**Figure 1.2**) (121). Recent studies have shown that genetically modified artificial antigen-presenting cells derived from K562 cells overexpressing CD19, CD64, CD86, and CD137L could be substituted for the feeder cells without perturbing REP fold expansion (122).

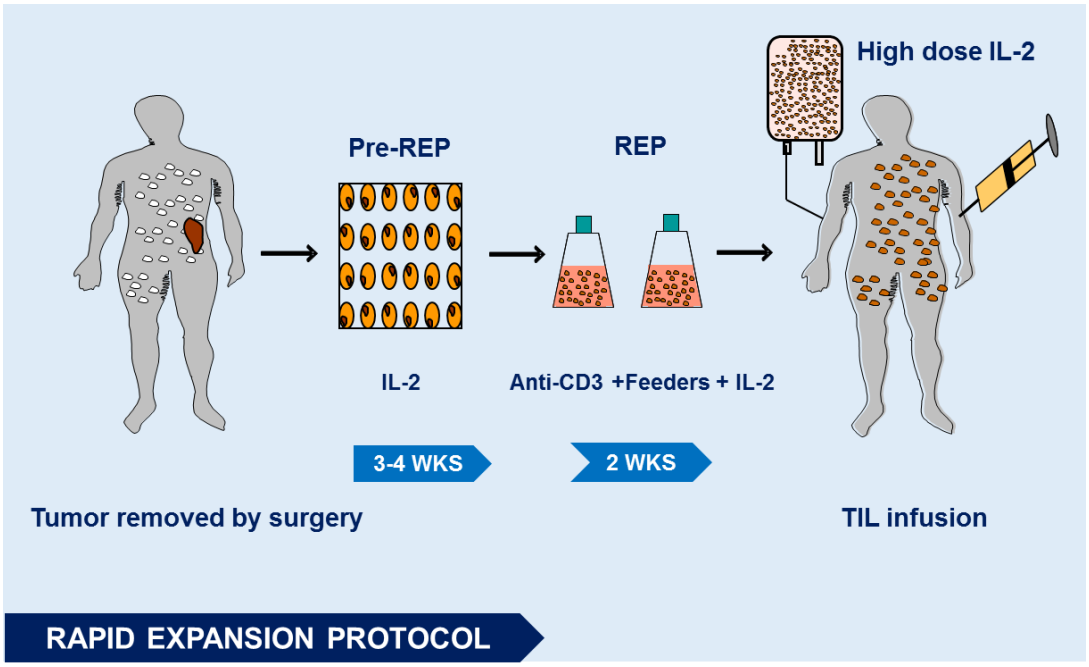

Figure 1.2. Schematic diagram of the TIL expansion (Pre-expansion and Rapid expansion) and TIL therapy.

Based on the studies in animal models, lymphodepletion in combination with ACT was shown to be critical for an effectiveness of transferred TIL. This helps eliminate the Treg cells and myeloid-derived suppressive cells (MDSCs) and preparing space for transferred cells (123). Currently, lymphodepletion prior to ACT has become a conventional practice widely used in multiple institutions including the Surgery Branch at NCI, M.D. Anderson Cancer Center, Moffit Cancer Center, and Sheba Medical Center in Israel. In non-myeloablative regimens (NMA), patients with metastatic disease undergo lymphodepletion with cyclophasphamide (30 or 60 mg/kg per day) and fludarabine (25 mg/m^2 per day) for two and five days, respectively, prior to TIL transfer. High dose IL-2 (720,000 IU/kg) is administered starting one day after TIL infusion every 8 hours to tolerance (124). In myeloablative regimens, patients are given total body irradiation (TBI) in combination with cyclophosphamide and fludarabine followed by $CD34^+$ hematopoietic stem cell transfer (125).

TIL: tumor recognition in melanoma tumor cells

Identification of tumor-specific cytolysis in human melanoma TIL was evident based on the existence of tumor-specific antigens recognized by T cells. The expression of T cell co-stimulatory molecules such as 4-1BB, ICOS and OX40, as well as co-inhibitory molecules like PD-1, is triggered upon antigen stimulation and therefore is a marker of activation. The observation that TIL contain subpopulations of recently activated T cells ($CD8^+4\text{-}1BB^+$), and are enriched for chronically activated T cells ($CD8^+PD\text{-}1^+$) as compared to the blood suggests that a high fraction of TIL are recognizing tumor antigens. In addition, secretion of cytotoxic cytokines such as IFN-

γ, TNF-α, and/or GM-CSF upon stimulation with autologous tumors also indicates tumor recognition by TIL (126).

Most tumor-associated antigenic peptides identified are restricted by commonly shared HLA subtypes such as HLA-A1, -A2, -A24, -A31, -B8, and –Cw. However, HLA-2 is the most intensively studied due to high prevalence in Caucasian populations (approximate 45%) (127). It has been shown that TIL clones from HLA-$A2^+$ patients were able to lyse HLA-$A2^+$ melanoma cell lines derived from different patients, but did not lyse non-melanoma cells lines and other types of cancers. This suggested that melanoma tumor-associated antigen peptides in melanoma cells are commonly shared among patients in a HLA-A2 restricted fashion. In addition, overexpression of HLA-A2 in HLA-A2 negative melanoma cell lines enables HLA-$A2^+$ TIL to mediate tumor cytolysis (128). Melanoma associated antigen 1 (MAGE) was identified as the first melanoma antigen recognized by HLA-A1 restricted melanoma TIL. Although MAGE-1 is also expressed by non HLA-A1 melanoma tumors, HLA-A2 specific CTL has never been reported. In addition, HLA-A2 antigen specific TIL were found not to lyse HLA-$A2^+$ fibroblast cell lines overexpressing the MAGE-1 gene. Several HLA-A2-restricted melanoma cytotoxic T lymphocytes derived from TIL recognizing other tumor antigens were also identified, including MART-1, gp100, and tyrosinase. Although most tumor antigen-specific CTLs were described in the HLA-2 restricted subtype, the MAGE-3 antigen expressed by melanoma and other types of cancers such as breast cancer, colon cancer, and lung cancer, was also recognized by the HLA-1 restricted CTLs (129).

Effectiveness of ACT in melanoma and other cancers

ACT is one of the most effective treatments in metastatic melanoma in inducing durable clinical responses as compared with other types of immunotherapy. The first preliminary report in 1988 of adoptive transfer of TIL was conducted in 12 patients with metastatic melanoma at the Surgery Branch, NCI. Objective tumor regressions occurred in 60% (9/15) of patients who had never been treated with IL-2 and 40% (2/5) of patients who were refractory to IL-2 therapy (130). In another trial in 2002 at the NCI, it was shown that 13 HLA-$A2^{+}$ metastatic melanomas treated with TIL ACT had 40% (6/13) objective clinical response to treatment. Rapid clonal repopulation of MART-1 reactive T cells was observed in two patients, resulting in the off-target destruction of normal cells expressing the MART-1 antigen (131). Several studies both in murine models and humans suggested that lymphodepletion is a critical factor for the positive clinical outcome of ACT (124). The NMA regimen using cyclophosphamide and fludarabine treatment prior to adoptive transfer was included in the standardized ACT protocol (132). In a recent study, myeloabalation using total body irradiation (TBI) concurrently with ACT has been investigated in 93 patients at the Surgery Branch, NCI. The clinical trial was assigned to patients into three cohorts; 1) NMA regimen (n=45), 2) myleoablation with TBI 2 Gy (n=25) 3) myeloablation with TBI12 Gy (n=25). Overall objective response rates in each cohorts were 49% (21/49), 52% (13/25), and 72% (18/25) respectively. In the NMA cohort, the complete response rate was around 10%, however in the TBI groups, over 20% of the patients achieved a complete response 20% underwent a complete remission more than 3 years. In a subsequent randomized study with more patients (101 patients; NMA (n=51) and

NMA plus TBI (n=50), the addition of TBI to the regimen did not improve the incidence of complete responses (133). Overall objective clinical response across multiple institutions is relatively similar to NCI, including M.D. Anderson Cancer Center (Houston, TX) (48%, 15/31 patients), Moffitt Cancer Center (Tampa, FL) (38%, 5/13), and Sheba Cancer Research Center, (Israel) (40%, 23/34) (121).

Functional role of TIL subsets in ACT: Tumor reactivity and persistence

Different T cell lineage in TIL

A high proportion of $CD8^+$ TIL in infused TIL has been shown to associate with clinical response in melanoma TIL-treated patients (134). It is known that $CD8^+$ T cells have a predominant role in the cell-mediated cytotoxic capability to induce cell death in pathogen-infected cells and transformed cells. The superior advantage of T cells over innate immune cells, which also mediate cell death, such as NK cells, is due to their specificity, adaptability, and durability. These properties allow $CD8^+$ TIL to recognize both tumor specific antigens and mutated peptides and provide long lasting immune response. The mechanism used by $CD8^+$ TIL to mediate tumor killing in has been well characterized. Following TCR recognition of peptide presented by tumor cells, both perforin (a membrane disrupting protein) and granzymes (serine proteases) secreted from effector TIL can cooperatively activate caspase-3 mediating tumor cell death (135). Occasionally, we have observed that TIL-treated patients somehow respond to the therapy even though the proportion of $CD4^+$TIL is relatively high. $CD4^+$T cells are generally not considered as key players in cell-mediated cell death, but coordinately facilitate $CD8^+$ function by providing cytokines such as IL-2, TNF-α, and IFN-γ that are critical for proliferation and effector functions of $CD8^+$TIL. On the other hand, Treg

can also suppress the anti-tumor function of $CD8^+$ by secreting immunosuppressive cytokines such as IL-10 and TGF-β (135).

We have occasionally observed outgrowth of γδ TIL during initial expansion, but the dominant outgrowth of this subset following REP is rarely observed. Zoledronate was reported to facilitate expansion of γδ TIL. A Phase I ACT clinical trial in several cancer patients with metastasis using γδ TIL expanded with zoledronate has shown no clinical response even though the migration of transferred T cells into the tumor bed was observed due to high expression of chemokine receptors such as CXCR3, CXCR5, CCR5, and CCR7 (136). This suggests that these cells were capable of trafficking into the tumor site, but might not be able to recognize tumor cells or might lack the effector function.

T cell differentiation and T cell persistence following adoptive transfer.

Although the $CD8^+$ TIL subset is pivotal for tumor-mediated regression, only a subset of TIL-treated patients with a high number of $CD8^+$ achieved a complete remission. It remains inconclusive as to what exact $CD8^+$TIL subset(s) is/are responsible for the clinical response. After encountering tumor antigens presented by APC, naïve T cells undergo clonal expansion and further differentiate into effector T cells (TEF), followed by the development of effector memory T cells (TEM) and central memory T cells (TCM) for long-term recall response. Effector T cells will then undergo further differentiation and become terminally differentiated and eventually undergo clonal deletion. It has been controversial whether memory development involves a transition to effector phase prior to memory commitment or if memory cells are exclusively arising from pluripotent effector cells (137). It remains unclear what signals control the

decision fate in memory development, but recent studies suggest that the strength of antigen stimulation and cytokines might be critically involved (138). In human $CD8^+$ T cells, the combination of CD45RA and CCR7 markers is most commonly used to distinguish different memory T cells into the following subsets: naïve ($CD45RA^+CCR7^+$), effector memory (TEM) ($CD45RA^-CCR7^-$), terminally differentiated (TEMRA) ($CD45RA^+CCR7^-$), and central memory (TCM) ($CD45RA^-CCR7^+$) (139). In addition, the combination of co-stimulation molecules such as CD28 and CD27 is also used to further characterize the differentiation status of CD8 into three stages; undifferentiated (CD28+CD27+), intermediate differentiated (CD28-CD27+), terminally differentiated (CD28-CD27-) (140). Recently, we and others demonstrated that B and T lymphocyte attenuator, a co-inhibitory molecule, also serve a T cell differentiation marker, where high expression of BTLA is observed in less differentiated T cell (141, 142). Persistence of infused TIL in the peripheral blood one month following adoptive transfer has shown to be associated with clinical response (134, 143). A recent study unveiled the phenotype of a memory T cell subset with stem cell-like properties (TSM) which exhibited a least differentiated phenotype with enhanced proliferative capacity (144). Adoptive transfer of this T cell subset showed improved memory T cell survival and superior anti-tumor immunity. A report from the NCI indicated that the $CD28^+CD27^+$ TIL subset had longer telomeres with enhanced persistence in circulation after adoptive transfer (140). In line with this observation, we found that a high proportion of $CD8^+BTLA^+$ (less differentiated $CD8^+$ TIL phenotype) in infusion product positively correlate with improved clinical response of TIL ACT treated patients (134).

Chimeric antigen receptor T cell therapy (CAR)

TIL from several tumors have been shown to recognize and destroy the autologous tumor cells, but very few tumor-reactive T cells recognizing more broadly antigens have been identified. Most tumor antigens appear to be unique to the patients. This limitation strongly hampers the selection and enrichment of tumor-specific T cells for adoptive T cell therapy. Several shared cell surface tumor-associated antigens in several types of cancer have been more extensively identified. This type of antigen can be targeted by an antibody. One approach to improve recognition of these antigens is to couple the high affinity recognition of an antibody to the killing machinery of a T cell by engineering an artificial T cell receptor on a T cell made up of an antibody linked to the intracellular domains of the TCR and its co-stimulation molecules. Therefore, the use of genetic engineering method to overexpress chimeric antigen receptor (CAR) on T cells can be used to improve tumor specific antigen recognition and enhance tumor killing (145).

Chimeric antigen receptors (CAR) contain two major parts; 1) an extracellular binding region of target proteins and 2) an intracellular signaling domain. The extracellular part contains a single chain variable fragment (scFv), variable regions of light chain and heavy chain of immunoglubin. scFV is designed to interact with the potential tumor antigen targets expressed by tumor cells. The intracellular signaling domain consists of a CD3 ξ chain, which exhibit the downstream signal mimicking TCR activation signals during the engagement of the extracellular part and the potential target. In the second and third-generation of CAR, its intracellular domain has been further modified with additional of signaling domains of CD28 and co-stimulatory

molecules such as OX-40 (CD134) and 4-1BB (CD137). Second-generation CAR has been found to be more effective than the first-generation because co-stimulatory signal can enhance cell survival and prevent T cell exhaustion. Generation of CAR T cells is far more complicated than TIL therapy, as T cells are required to undergo genetic modification prior T cell expansion. Several approaches are used to deliver modified genes including viral transduction, sleeping beauty, and CRISPR/Cas9 gene editing. Once modified genes are inserted, T cells then undergo propagation with artificial antigen-presenting cells (aAPC), which can provide a proper co-stimulatory signal, prior to adoptive transfer into the patients (145, 146).

CAR T cell therapy has been widely used in hematological malignancies, including B cell malignancy, T cell malignancy, and myeloma. The durable clinical outcome in B cell malignancy patients treated with anti-CD19 CAR T cell therapy has demonstrated a promising model for other types of cancer. A number of targets of CAR T cell therapy for acute myeloid leukemia (AML) that are currently under investigation in an early phase clinical trials include CD33 (myeloid specific lectin), CD123 (IL-3 receptor alpha chain), CD44v6 (adhesion molecule expressed by some subset of AML and multiple myeloma) (147-149). Clinical trials of CAR T therapy also are currently expanding into solid tumors, including glioblastoma multiforme, mesothelioma, ovarian cancer, and pancreatic cancer (145). Selection of targets can be very challenging, as solid tumors are much more heterogenous as opposed to hematological cancers. Because of a few instances of treatment-related fatal toxicity, such as in colon cancer patients treated by anti-HER-2/neu CAR T cell therapy, off-target toxicity from

targeting antigens commonly present in normal tissue is also a major safety concern for CAR therapy (150).

Endogenous T cell therapy

Detection of tumor-reactive T cells in the peripheral blood of cancer patients has provided a rationale for attempting their selection and expansion for adoptive T cell therapy. Tumor-reactive T cells in circulation are present at a very low frequency (less than 0.5%), which presents a challenge (151). If the tumor antigen is known, the T cells can be stained with fluorescence conjugated peptide-MHC tetramer and sorted by flow cytometry. A current strategy used to amplify circulating antigen-specific T cells is to stimulate PBMCs with APCs or insect cells expressing MHC class II pulsed with the peptide of interest. This helps expand and enrich tumor-reactive T cells prior to further selection processes by cell sorting, cloning, or performing immuonmagnetic selection (152).. If amplification of unselected tumor-reactive T cells is desired, hundreds of T cell clones can be screened for tumor reactivity and immunomagnetic selection methods can be performed to capture cytokine-secreting cells using dual-specific antibodies that can bind both $CD45^+$ (lymphocyte marker) and IFN-γ (151). The enrichment and selection method can increase the number of cells to 1 to 5 millions of $CD8^+$ T cells with the frequency greater than 80% of tumor-reactive T cells. The final expansion with high dose IL-2, anti-CD3, and feeders can rapidly increase the number of tumor-specific T cells to a billion cells with 90% specificity within two weeks. Unlike TIL adoptive transfer, patients are treated with low dose IL-2 without or minimal lymphodepletion, thus endogenous T cell therapy confer less adverse effects (153).

There have been several attempts to improve T cell quality with enhanced *in vivo* persistence. It is known that persistence of T cells following transfer is critical for positive clinical outcomes in adoptive T cell therapy. It has been shown that lymphodepletion with fludarabine alone or high dose cyoclophosphamide alone could improve engraftment and persistence of transferred T cells (133). Another report has indicated that central memory (TCM)-derived CTLs were the only phenotypes that exhibited *in vivo* long-term persistence (154). Consistently, a murine model also demonstrated that Tcm-derived CTLs were much more effective for tumor control due to superior replicative capacity when compared with effector and effector memory subset (144). In a recent study in human, $CD8^{+}MART^{+}$T cells expanded with IL-21 up-regulated CD28 and IL-7R and maintained the expression for several weeks following adoptive transfer. In addition, cancer patients treated with endogenous T cells expanded with IL-21 exhibited better tumor control and some of those underwent a complete durable response (155).

A major challenge of endogenous T cell therapy is to develop a novel approach to identify, select, and enrich tumor antigen-specific T cells that are of very low frequency in circulation. T cells recognizing well characterized shared tumor antigens such as MART-1, gp100, NY-ESO can be selected for treatment. However, tumors may not uniformly express those antigens and therefore the development of alternative methods such as cloning and immunomagnetic selection to enrich tumor-reactive T cells will be warranted. Moreover the transfer of T cells specific for one antigen may initiate an immunoselective pressure which allows immune escape through antigen loss and the development of resistance.

1.3 Biomarker of immune cell: Immunoscore

The TNM (Tumor Node Metastasis) system, a standard criteria to evaluate the degree of tumor spread, has been widely used in cancer centers all over the world. This classification system aids physicians in planning treatment, making prognoses, and evaluating effectiveness of therapy. Disease progression used in TNM solely relies on the spreading of the tumor itself and does not include other factors in the tumor microenvironment. In recent years, it has become clear that the immune system plays a critical role in tumor control and progression (156). Thus, immune cells should also be included in evaluation of tumor progression criteria. Recently, Jerome Galon, a scientist at INSERM laboratory in France, has proposed a novel method to incorporate immune cells into the clinical assessment of cancer patients (157).

The concept of "immunoscore" has emerged from a meta-analysis of more than 120 independent studies on the impact of immune cells in tumor microenvironments. It has been demonstrated that the presence of CTL, memory T cells, and the CD4 Th1 subset in all types of cancers is associated with extended survival time. On the basis of these analyses, the quantification of three surface markers on T cells including CD3, CD8, and CD45RO in combination with location in the tumor bed, the core of the tumor (CT) and the invasive margin (IM) are used to tabulate the immunoscore. The score is graded on the density of immune cells diffused in both the core tumor and the invasive margin from "no" or lowest (Immunscore 0, I0) to the highest (Immunoscore 4, I4) (157). A recent report from two independent cohort studies has demonstrated the ability to predict the recurrence of colorectal cancer in patients who had no detectable metastasis in either lymph nodes or distant organs. It appeared that patients with a high immune score (I4) exhibited a low chance of tumor recurrence (less than 5%), while

patients with a low immune score (I1) were very likely to develop recurrence (approximately 72%) (158). Based on the fact that Immunoscore is the only system that helps predict disease recurrence, the critical role of the immune system in the tumor microenvironment becomes very clear.

Immunoscore is a task force established in collaboration with multiple institutions worldwide. The method standardization of immunohistochemistry and analysis software is currently being validated to ensure the accuracy and reproducibility across laboratories. Immunohistochemistry of immune markers is already routinely performed in the diagnostic pathology laboratory, it is possible that immunoscore will become a part of a conventional system for cancer treatment in the near future. Together with the TNM system, immunoscore can enhance the ability to evaluate disease progression, prognosis, as well as aid in developing a decisive plan for immunotherapy.

1.4 Co-signaling molecules on T cells

Co-signaling molecules on T cells

Engagement of TCR by peptide-MHC class I or II complexes determines the strength of TCR activation. Without additional co-signaling, T cells become unresponsive and undergo clonal deletion eventually. It is known that co-signaling molecules play a key role in steering the outcome of TCR signaling by either enhancing or inhibiting the downstream signals during TCR activation. This outcome is crucial for regulating the fate of T cell differentiation, effector function, cell proliferation and survival (159).

1.4 a) Co-stimulatory molecules

A co-stimulatory molecule is a receptor expressed on T cells whose signaling provides positive effect on T cell functions. On a structural basis, co-stimulatory molecules can be classified into two major groups; the Tumor Necrosis Factor Receptor superfamily (TNFRSF) and the Immunoglobulin super family (IgSF). TNFRSF requires a cluster formation of at least two molecules for the full activation, while only one molecule of IgSF is sufficient for the full function (159).

Tumor Necrosis Factor Receptor superfamily (*TNFRSF)*

TNFRSF family members consist of at least one subunit of extracellular cysteine-rich domains (CRDs). Most TNFRSF members such as 4-1BB, CD40, OX40, and HVEM exhibit signals through NF-kB and mitogen-activated protein kinases (MAPK) pathways. However, some TNFRSF receptors contains dead domains (DD) such as Fas and TRAIL and are able to promote apoptosis. TNFRSF members expressed by T cells mostly synergize with T cell survival function rather than promote T cell apoptosis. A number of TNFRSF have been extensively studied in T cell and other cell types. Here,

only selected TNFRSFs that have potential in clinical application for cancer immunotherapy will be discussed (160).

4-1BB

4-1BB is an inducible molecule, which is up-regulated within only a few hours following T activation, and its expression declines within a few days. 4-1BB is preferentially expressed by activated $CD8^+$, NK cells, and dendritic cells. Although 4-1BB can be shed from the cell surface, the soluble form is not able to exert signals when engaged with its ligand (161). It has been shown that the soluble form of 4-1BB is highly associated with severity of patients with rheumatoid arthritis (162). In T cells, 4-1BB mediates signals through NF-kB and activating protein-1 (AP-1), which triggers several downstream pathways including MEK, and JNK. 4-1BBL, identified as a binding partner for 4-1BB, is mainly expressed by antigen-presenting cells including dendritic cells, B cells, and macrophages. It has been demonstrated that the 4-1BB pathway in T cells enhances T cell proliferation and cell survival and prevents AICD (163). Although the 4-1BB pathway plays an important role in enhancing TCR activation signals, the 4-1BB pathway might not be a substitute for CD28 for long term protective tumor immunity. In murine lymphoma models, engagement of 4-1BB and 4-1BBL did not rescue the killing capacity of T cells against T cell lymphoma cell line A20. When lacking CD28 signaling, cytotoxicity and survival of T cells were significantly impaired, resulting in a decrease in cytokine production, particularly IL-2 (164). Thus far, 4-1BB is a key target for immunotherapy, with agonistic antibodies in clinical development for systemic use and for *in vitro* selection of antigen specific T cells. It has been shown that co-expression of PD-1 and 4-1BB serves as a marker for

tumor-reactive T cells, thus developing selection methods to expand $CD8^+$4-1BB^+PD-1^+ becomes critical to enrich tumor antigen-specific T cells for T cell therapy (126). In addition, agonistic anti 4-1BB antibody has also been used to expand T cells from tumor fragments as well as REP as it provides a great benefit in selective expansion of $CD8^+$ subset expansion. TIL expanded with anti-4-1BB antibody also demonstrated protective capacity against AICD (165).

CD40

CD40 is TNFRSF receptor expressed by antigen-presenting cells, particularly in B cells and dendritic cells. CD40L expression, a ligand for CD40, is observed in activated T cells as well as non-immune cells such as endothelial cells, and epithelial cells. Interaction between CD40L and CD40 plays a critical role in the maturation of dendritic cells and the development of plasma cells and memory B cells. Like other TNFRSF members, engagement of CD40 and CD40L requires clustering of CD40 receptors for the recruitment of TNFR-associated factors (TRAF) into the cytoplasmic domain, which leads to the activation of NF-kB, MAPK, PI3K, and PLCy pathways (166). In addition, JAK3 was shown to interact with the CD40 cytoplasmic region through the STAT5 pathway (167). CD40/CD40L engagement is known enhance both humoral and cell-mediated immune response. It has been shown that activated T helper cells promote B cell differentiation, antibody production, and memory development through CD40 signaling pathway (168). In addition, disruption of CD40L and CD40 engagement was found to down-regulate expression of CD28 by dendritic cells, which directly attenuated T cell priming due to insufficient co-stimulatory signal (169). The CD40/CD40L pathway has been demonstrated to promote an optimal anti-tumor

responses both in vitro and in murine models. A number of studies have demonstrated that CD40 activation enhanced dendritic cell maturation and optimal priming, which is critical for developing a long term anti-tumor response (170).

CD27

CD27 is mainly expressed by T cells, NK cells, and memory B cells. CD70 expression, known as a CD27 ligand in TNFSR, is constrained in only activated T or B cells, and mature dendritic cells (171). Although CD27 is expressed at the baseline level in naïve T cells, its expression is further up-regulated following T cell activation. In addition, CD27 can be shed from the cell surface of activated T cells and competitively prevent CD70 from binding the membrane-bound form of CD27. Upon engagement with CD70, CD27 recruits TRAF 2 and 5 into the cytoplasmic domain, which then activates the NF-kb and JNK pathways. CD27 plays an important role in promoting T cell priming, clonal expansion following recent activation, and memory T cell generation (172). CD27/CD70 interaction prevents T cells from apoptosis through increasing anti-apoptosis protein expression, such as B cell lymphoma-extra large (Bcl-xL) as well as suppressing FasL expression by $CD4^{+}$T cells (173). In a murine model, engagement of CD27 and CD70 could harness Treg expansion, thus could suppress with the CTL function of $CD8^{+}$ in the tumor microenvironment (174). Expression of CD70 by antigen-presenting cells such as B cells and dendritic cells was found to improve antitumor immunity against murine lymphoma (EL4) and murine melanoma (B16) (175). Based on studies conducted in a non-human primate model, anti-CD27 (1F5) has shown no toxicity and caused a decrease in Treg subset. In humans, a fully humanized agonistic anti-CD27 antibody (1F5) is currently under investigation in

phase I clinical trials in several cancers including renal cell carcinoma, melanoma, and B cell malignancies (176).

Immunoglobulin superfamily (IgSF)

CD28

CD28 is classified into the immunoglobulin superfamily and the CD28 subfamily. It contains a single extracellular immunoglobulin variable-like domain with a short cytoplasmic domain. This structure is also observed in other CD28 subfamilies including ICOS, CTLA-4, PD-1, VISTA, and BTLA. CD28 is abundantly expressed by naïve $CD4^+$ and $CD8^+$ and down-regulated following T cell activation. Two receptors in the B7 subfamily (CD80 and CD86) are identified as ligands of CD28. CD80 and CD86 are mainly expressed by activated antigen-presenting cells, but also observed in activated T cells as well (177). The CD28 cytoplasmic region consists of YMNM and PYAP motifs. YMNM of CD28 was shown to interact with the SH2 domain of PI3K, Grb2, and the Grb2-related adaptor downstream of Src (GADS). Recruitment of the p85 subunit of PI3K subsequently results in activation of protein kinase B (PKB) and the Akt pathway. The PKB pathway is involved in a broad range of downstream targets including mTOR, Glycogen synthase kinase 3 (GSK3), and anti-apoptotic proteins (Bcl-XL and BAD). Moreover, interaction between PI3K with adaptor proteins VAv and SLP-76 can also enhance gene transcription and stabilization of IL-2 mRNA, which helps promote cell proliferation and survival. PYAP is known to interact with LCK, Grb2, and GADS. It has been shown that PYAP plays a role in cell proliferation and IL-2 production through the interaction of Vav and LCK (178). CD28 is considered one of the most important signals required during T cell priming.

Upon ligation with CD80/CD86, CD28 exhibits positive signals that enhance cell proliferation, cytokine production (particularly IL-2 and IL-4), and protection from activation-induced cell death (AICD) (179). In addition, CD28 also plays a critical role in T cell differentiation and T-cell subset generation.

ICOS

ICOS is a co-stimulatory molecule in the CD28 subfamily. Its expression is up-regulated following T cell actvation. ICOS expression is found in activated T cells (particularly the $CD4^+$subset), memory T cells, and activated NK cells, but not in naïve T cells. ICOS-L, an ICOS ligand, is expressed by immune cells such as $CD33^+$ cells in bone marrow, B cells, dendritic cells, and T cells. Its expression was also found in non-immune cells including epithelial cells, endothelial cells, and liver, kidney, and lung cells. IFN-γ can induce ICOS-L expression in B cells and dendritic cells, while GM-CSF/TNF-α enhance ICOS-L expression in $CD33^+$ cells in bone marrow. The cytoplasmic domain of ICOS contains the YMFM motif, which is also present in the CD28 and CTLA-4 (180). Engagement of ICOS and ICOS-L was shown to recruit p50 alpha and p85 subunits of PI3K, which then activated PDK1, PKB, and GSK3 (181). Although the downstream pathway of ICOS shares some similarity with CD28, lacking Asn residue in the YMFM motif disables ICOS to activate JNK pathway and IL-2 production through interaction with the Grb2 adaptor protein. Moreover, the TCR-induced transcriptional profile of ligation of CD28 and ICOS receptors demonstrated that CD28 induced gene expression much more than ICOS. However, some genes were selectively induced by ICOS, but not CD28, such as unconventional myosin (MYL1) and T-lymphocyte maturation-associated protein (MAL), suggesting that the

downstream pathway of ICOS is somehow distinct from CD28 even though overlap in signaling pathways has been demonstrated (180).

1.4 b) Co-inhibitory molecules

Co-inhibitory molecule is considered as a checkpoint to negatively regulate T cell function including cell proliferation, cytokine production, and effector function. Because phosphorylation of downstream T cell signaling proteins is critical for T cell activation, the commonly shared suppressive mechanism by co-inhibitory molecules mainly through dephosphorylation by phosphatase. Unlike co-stimulatory molecules, the all co-inhibitory molecule belong to Immunoglobulin superfamily, consisting of an immunoglobulin variable (IgV)-like domain and immunoglobulin constant (IgC)-like domain in the extracellular region (182).

PD-1

PD-1 is an inhibitory molecule in the CD 28 subfamily of the Ig superfamily. PD-1 is up-regulated upon T cell activation. Its expression is also found in activated B cells, activated natural killer cells, and TIL from different cancers. PD-L1 and PD-L2 are known as ligands for PD-1. PD-L1 is expressed in broad range of cell types including T and B cells, macrophages, dendritic cells, and tumor cells (60). PD-L1 is constitutively expressed by tumor cells and IFN-γ was found to enhance PD-L1 expression (183). Up-regulation of PD-L1 expression in tumor cells is thought to be a protective mechanism from T cell killing. Basal expression level of PD-L2 is restricted in dendritic cells and macrophages at low level (64).

Two cytoplasmic motifs of PD-1, ITIM and ITSM, were shown to suppress T cell function. Upon PD-1/PD-L1 ligation, SHP1/2 are recruited into ITIM and ITSM

motifs and attenuate proximal TCR activation. This inhibits T cell proliferation, cytotoxic function and cell survival (55). Downstream targets of PD-1 pathway are partially known. It has been demonstrated that the recruitment of SHP2 inhibited PI3K/AKT3, Ras, and MEK-ERK pathways (56). PD-1 pathway is known to exhibit an inhibitory function in $CD8^+$ antigen-specific T cells, but instead enhances the generation of Treg cells. PD-1 expression is up-regulated following antigen exposure and down-regulated when stimuli no longer exists. Under chronic stimulation such as in cancer or latent infection, PD-1 expression can be maintained and affect the effector function of T cell. This condition is defined as "T cell exhaustion" (58). In tumor microenvironments, high PD-L1 expression by tumor cells and myeloid cells can suppress the effector function of T cells and prevent tumor killing. A novel strategy to block PD-1/PD-L1 engagement is the use of blocking anti-PD-1 antibodies. This approach led to improved tumor burden control and survival in several murine tumor models as well as multiple cancer types including melanoma, non-small cell lung carcinoma, and renal cell carcinoma. At present, anti-PD-1 agents have been FDA approved for the treatment of melanoma and lung cancer and more clinical trials are under investigation in multiple institutions to gain a better understanding about mechanisms involved in blockade of the PD-1 pathway and clinical response (62).

CTLA-4

CTLA-4 is known as a member of the Ig superfamily. CTLA-4 is highly expressed in T cells following activation, similar to PD-1. Constitutive expression of CTLA-4 was also reported in T regulatory cells. Interestingly, intracellular CTLA-4 is highly abundant in memory T cells and can translocate to the cell surface membrane

during T cell activation (184). CTLA-4 gene transcription is controlled by nuclear factor of activated T cells (NFAT). Down-regulation of CTLA-4 expression is enhanced when NFAT is inactivated by cylclosporine A. CTLA-4 shares amino acid sequence similarity with CD28, and also interact with CD28 ligands, CD80 and 86 (44). Initially, it was thought that CTLA-4 was a co-stimulatory molecule, as the YVKM motif has been demonstrated to interact with PI3K. Later, it was found that this motif can also interact with SHP2, which can recruit phosphatase and attenuate TCR activation (47). In addition, CTLA-4 was shown to inhibit lipid raft formation and prevent microcluster of Zap70 during T cell activation. Moreover, CTLA-4 was shown to attenuate CD28 signal by competitive binding to CD80 and 86, which prevent T cell from full activation during priming (45). In murine models, CTLA-4 deficient mice developed severe myocarditis, pancreatitis, and lymphadenopathy with massive infiltration of activated T cells with high expression of CD69 and CD44. In addition, $CTLA^{-/-}$ T cells exhibited high proliferative capacity upon activation and were also susceptible to FasL mediated apoptosis. Altogether, these finding support the inhibitory effect of CTLA-4 (28).

CTLA-4 plays a critical role during T cell priming, which is critical for memory T cell generation. Thus, CTLA-4 blockade can be used to enhance the memory T cell pool generation under immunosuppressive environment in tumor bed. Several preclinical models have shown effectiveness in tumor control in both solid and hematological malignancies. The use of anti-CTLA-4 as a single agent in the clinic was very successful with the significant improvement in overall survival seen in melanoma patients leading to FDA approval in 2011 (185).

1.5 B and T lymphocyte attenuator (BTLA)

1.5 a) Discovery of BTLA and its ligand

B and T lymphocyte attenuator (BTLA) was first identified from the microarray analysis of T helper type 1 cells treated with IL-12 and IL-18 (186). BTLA transcripts were highly abundant in lymphoid organs such as the spleen and lymph node, but not in somatic tissues. BTLA is considered as the third co-inhibitory receptor found following the discovery of CTLA-4 and PD-1, respectively. BTLA belongs to the immunoglobulin superfamily as well as CD-28, ICOS, PD-1, and CTLA-4. The first report on the discovery of BTLA demonstrated that an orphan B7 (B7X) was a natural ligand for BTLA due to specific interaction between B7X-Ig fusion protein and with T cells overexpressing BTLA (186). Later, Sedy et al. found no direct interaction between NIHT3 cells overexpressing B7X and Fc fusion proteins of BTLA. A functional cloning strategy was used to indicate the actual ligand of BTLA. Cells transduced with retroviral cDNA libraries generated from mouse splenocytes were screened with tetramers of the extracellular domain of BTLA. Plasmon resonance imaging assay was used to confirm the direct interaction at the molecular level (187). From these results, HVEM (Herpes Virus Entry Mediator) was found to have a specific interaction with BTLA, and defined as an actual BTLA ligand. In addition, engagement of BTLA and HVEM triggered phosphorylation of tyrosine residues and inhibited T cell function. This finding unveils a novel concept of cross interaction between receptor in the immunoglobulin family and TNFR superfamily.

HVEM as well as other TNFR family members consists of three subunits of TNF ligands. The extracellular domain contains three cystein-rich domains (CRDs),

CRD1, CRD2, and CRD3, which can interact with its binding partners including LIGHT, lymphotoxin, Herpes virus 1 glycoprotien D (HSV1 gD), and BTLA. CRD2 and CRD3 have been shown to interact with LIGHT and lymphotoxin, while HSV1 gD and BTLA bind to CRD1 and CRD2 subunits. BTLA and LIGHT can interact with HVEM at distinct areas in a non-competitive fashion. It is possible that BTLA and LIGHT can bind HVEM concomitantly. It is known that UL144, a viral protein derived from human cytomegalovirus (CMV) can also bind to BTLA due to the shared structure with the first two CRDs of HVEM (188, 189). It has been proved that UL144 effectively suppresses T cell function upon ligation with BTLA, but recruitment of SHP1 and SHP2 has not been elucidated.

BTLA and HVEM expression in immune cells

BTLA expression was first observed in B and T cells, but later evidence was found that dendritic cells, macrophages, and NK cells also express BTLA. In mouse T cells, BTLA is up regulated upon T cell activation, particularly in Th1 cells, but not Th2 cells (190). It remains unclear what transcription factors controls BTLA expression in conventional T cells. On the other hand, it was indicated that transcription factor retinoid-related orphan receptor gamma (RORγt) dampens the expression of BTLA, whereas IL-7 augments BTLA expression, which helps maintain homeostasis of the normal gamma delta T cell subset (191). BTLA is expressed at low level in early stages of B cell development (pro-B cells and pre-B cells) and gradually increases upon maturation stages. High expression of BTLA is generally found in circulating B cells. HVEM is highly expressed in naïve T cells, and its expression gradually decreases following T cell activation. High expression of HVEM is observed in naïve and

memory human B cells, but not on germinal center B cells (188). On the other hand, mouse B cells express HVEM at low level. Upon ligation with LIGHT, B cells become activated and down-regulate HVEM expression. In immature dendritic cells, HVEM expression decreases upon engagement with LIGHT. Typically, HVEM expression is high in naïve immune cells, but the expression declines following cell activation (190).

1.5 b) BTLA structure and functions

The cytoplasmic region of BTLA consists of three signaling motifs including Grb2, ITIM and ITSM. Grb2 motif is present in CD28, and ITIM and ITSM motifs are commonly found in other co-inhibitory molecules such as PD-1 (186). Based on the BTLA gene sequence analysis, the three signaling motifs are highly conserved across different species including humans, mice, rats, dogs, and non-human primates. It was shown that a few tyrosines in BTLA signaling motifs were phosphorylated following cross-linking of BTLA at the cell surface with anti-BTLA antibodies, suggesting that these motifs might contribute in regulating downstream signaling pathways during TCR activation (189). The Immunoreceptor tyrosine-based inhibitory motif (ITIM) and Immunoreceptor tyrosine-based switch motif (ITSM) contain two tyrosine residues in both mice and humans. Similar to PD-1, ITIM and ITSM of BTLA could recruit and phosphorylate SHP1 and SHP2 tyrosine phosphatases, resulting in attenuation of TCR activation. It has been shown that T cell proliferation was suppressed following engagement of BTLA by HVEM, suggesting that BTLA functions as a co-inhibitory molecule by suppressing TCR activation (187).

The downstream signaling pathway of BTLA inhibited by SHP1 and SHP2 remains understudied. It has been suggested that the downstream targets of SHP1 and

SHP2 might be phosphorylated proteins involved in proximal TCR signals. A recent report has demonstrated that ITIM and ITSM motifs of PD-1 targeted the PI3K-AKT pathway, resulting in inhibition of T cell proliferation. Besides inhibitory motifs, BTLA also contains Growth factor receptor bound protein 2 (Grb2) motifs, commonly shared in co-stimulatory molecules like CD28. A biochemical assay using synthetic peptide demonstrated that Grb2 motifs of BTLA interacted with the p85 subunit of PI3K. Although using BTLA phosphotyrosile-containing peptide might not reflect the physiological binding of cellular protein during BTLA–HVEM interaction, it could provide indirect evidence leading to further study. The Grb2 motif of BTLA contains YXN, but not the YMNM sequence found in CD28. It has been well understood that Grb2 of CD28 could activate the PI3K-AKT pathway, resulting in an increased IL-2 production and cell proliferation (192). Thus far, there is no direct evidence that supports a positive role for the Grb2 motif of BTLA. Immunoprecipication assay and functional studies in cell lines or primary immune cells are required to determine an actual interaction between phosphorylated Grb2 motifs and Grb2 protein or PI3K. This will aid in gaining a better understanding of the role and regulation of the positive and negative motifs resulting in the physiological function of BTLA in T cells.

An early report on mouse and human BTLA indicated a highly conserved protein sequence in the three signaling motifs. In addition, inhibition of the function of BTLA on T cells and B cells were also consistent in both species. The study led by Riley's laboratory showed that the conserved ITIM sequences in both human and mouse BTLA was necessary for the suppressive function of BTLA. BTLA expression at high levels is observed in human naïve and central memory T cells, with a gradual

decrease of BTLA expression as T cell differentiation occurs (193). In contrast, there is no BTLA expression in naïve mouse T cells, but up-regulation of BTLA is seen following TCR activation. These marked differences between the kinetics of BTLA expression between mouse and human T cells suggest that the gene regulation of BTLA in mice and humans is completely different.

1.5 c) BTLA in murine disease models

Multiple studies have been demonstrated the role of BTLA in innate immune response. A report in acute experimental sepsis induction in mice (CLP) has revealed the role of BTLA in the $CD11C^+$ and $CD11B^+$ innate immune cell subsets, which generally are macrophages, dendritic cells, and monocytes. An increase in $BTLA^+HVEM^+$ innate inflammatory cells in the peritoneum contributed to worsened mortality and morbidity in mice administered with lipopolysacccharide (LPS). BTLA expression hindered activation of innate inflammatory cells with increased IL-10, but not of other pro-inflammatory cytokine production. This resulted in inhibiting the recruitment of innate inflammatory cells and limiting bacterial clearance from the body (194). Furthermore, an increased BTLA expression by innate inflammatory cells such as macrophages, dendritic cells, and granulocytes was also observed in septic ICU patients, suggesting a link between mouse models and human studies. In agreement with another study, there was a significant increase in $CD4^+BTLA^+$ in peripheral blood of ICU patients with septicemia as compared with non-septic individuals. Furthermore, more than 80% of patients with high $CD4^+BTLA^+$ in circulation experienced extended hospital stays as they became more susceptible to nosocomial infections (195). Another study using a NOD (non-obese diabetic) murine model, BTLA was expressed by

dendritic cells and mediated $CD8^+$ T cell tolerance which reduced the severity of diabetes. T cell proliferation and cytokine production were suppressed by dendritic cells overexpressing BTLA. In addition, NOD mice immunized with dendritic cells overexpressing BTLA reduced the incidence of diabetes. This results indicated inhibitory effect of BTLA on dendritic cell function (196, 197).

In an experimental malaria models, BTLA was found to impair both adaptive and innate immune responses to *Plasmodium yoelii* strain 17NL during blood stage infection. Humoral immune response, considered as a key mechanism for controlling infection, was suppressed by BTLA expression. Furthermore, BTLA also inhibited the innate immune compartment, as double deficient RAG1 and BTLA improved the capability to control parasitemia over RAG1 deficient animals (198). On the other hand, another study demonstrated the favorable role of BTLA in preventing the pathogenesis of cerebral malaria. BTLA was shown to increase in peripheral blood as well as in the brain during the blood stage infection of *Plasmodium berhei*. The incidence of cerebral malaria significantly diminished when mice treated with agonistic anti-BTLA (clone 6A6), which correlated with the reduction of infiltrating T cells in brain tissue. It was confirmed that anti-BTLA agonist antibody attenuates the cytokine production including IL-6, IL-18, and IFN-γ (198). This suggests that the inhibitory function of BTLA helped prevent brain destruction due to strong immune reaction.

Consistent with the graft-versus-host disease (GVHD) model, targeting BTLA with agonistic anti-BTLA (clone 6A6) has been shown to prevent GVHD regardless of the presence of HVEM. The agonistic anti-BTLA antibody was shown to directly inhibit cytokine production and cell proliferation of the donor effector $CD4^+Foxp3^-$ T

cells, resulting in expansion of the pre-existing donor Treg population. This created a new balance between the effector and Treg population that helped prevent GVHD without global immunosuppression (199). In addition, the inhibitory function of BTLA has been shown to extend the survival of mice with partial MHC class I and II mismatches in cardiac allograft, whereas PD-1 played a critical role in full MHC mismatch settings. Both BTLA and PD-1 were up-regulated upon allogenic antigen stimulation and high expression of HVEM and PD-L1 were observed in cardiac transplant tissues. Engagement of BTLA and PD-1 to their ligands could attenuate T cell responses to alloantigen by inhibiting T cell proliferation and Th1 cytokine production, resulting in alleviation of allograft rejection (200).

Interestingly, the role of BTLA in T cell survival has also been observed in the non-irradiated parental-into-F1 mouse model of acute GVHD. BTLA knockout (BTLA KO) donor lymphocytes were unsuccessfully engrafted in the host body. A similar finding was also observed when engagement of BTLA and HVEM was blocked using anti-BTLA antibody (clone 6A6). Donor lymphocytes lacking BTLA had less proliferative capacity prior to contraction as compared with wild type, resulting in engraftment failure. In addition, BTLA KO also impaired the re-expression of IL-7R alpha, considered as an important factor for homeostasis in naïve T cells. Another study has also shown that anti-HVEM antibodies specifically blocking HVEM and BTLA interaction ameliorated the graft versus host reaction in lethally irradiated parental-into-F1 murine models of GVHD. Blockade of HVEM and BTLA dampened donor $CD8^+$ T cell activation and IFN-γ secretion, which helped minimize donor anti-host rejection (201).

Previous studies in adaptive immune cells have shown that BTLA KO mice were able to produce more pro-inflammatory cytokine for the clearance of pathogen infections in several models such as malaria and listeria. However, it has been shown that macrophages lacking BTLA alleviated liver destruction in fulminant hepatitis models, caused by murine hepatitis virus strain-3. Macrophages were responsible for the pathogenesis of hepatitis as they carried and spread the virus during migration to the liver. A rapid increase in macrophage apoptosis mediated by the TRAIL receptor following virus infection was found to lower of the viral load and attenuate inflammatory response in the liver (202).

It has been shown that MRL/Mp-Fas (MRL-Ipr) mice, a systemic autoimmune disease model for systemic lupus erythematosus (SLE) in humans, become exacerbated when lacking BTLA. High infiltration of lymphocytes in salivary glands, lungs, pancreas, kidneys, and joints was observed in BTLA$^{-/-}$MRL-*lpr/lpr* mice as compared with the wild type counterparts. In addition, BTLA$^{-/-}$MRL-*lpr/lpr* mice developed necrotizing hepatitis with increased autoantibodies, which was similar to autoimmune hepatitis (AIH)-like disease. This suggests that BTLA plays an important role in protection against autoimmune diseases (203).

Although BTLA signaling itself is known to suppress immune cell function, a recent report has shown that BTLA could provide HVEM-dependent signals that harness T cell survival during bacterial infection. In *Listeria monocytogenes* infection models, engagement of HVEM expressed by CD8^{+}T cells and BTLA expression in the host microenvironment was critical for CD8^{+}T cell expansion and survival (204). This

suggests that BTLA can mediate positive signals through HVEM in *trans* con figurations, but inhibits HVEM signal in *cis* interactions.

1.6 Main theoretical questions posed in this dissertation

An emerging checkpoint blockade strategy has successfully demonstrated ameliorated clinical outcomes for cancers in an advanced stage. Targetting co-inhibitory molecules using monoclonal antibodies clearly improves T cell function, resulting in tumor regression. It is known that $CD8^+$T cells are prone to dysfunction in the tumor microenvironment due to high expression of inhibitory receptors such as PD-1, BTLA, TIM-3, and LAG-3 on the cell surface. We have investigated a number of biomarkers in both T cells and the tumor microenvironment. These included T-lymphocyte subsets (CD4 and CD8), effector-memory differentiation markers (e.g., CD27, CD28, CD57, KLRG1, CD45RA, CD62L), positive (4-1BB, OX40, ICOS) and negative co-stimulatory molecules (PD-1, BTLA, TIM-3, LAG-3). As expected, the total number of TIL and the frequency of $CD8^+$ was associated with a favorable clinical response. It as a surprise when we found that BTLA, a negative co-stimulatory molecule appeared to be the only marker highly associated with clinical response, while other inhibitory molecules such as PD-1, TIM-3, and Lag3 did not. BTLA is known as a maker for T cell differentiation. BTLA is highly enriched in less differentiated T cells such as naïve and memory T cells, however its expression is progressively lost in CTL differentiation. This suggests that the association of patients receiving a high proportion of $CD8^+BTLA^+$ in TIL infusion products with favorable clinical response might be due to the multifunctional properties of less differentiated T cells. It has been reported that tumor-bearing mice adoptively transferred with minimally differentiated T cell phenotypes exhibited greater tumor control as these cells persisted much longer in the body when compared to more differentiated ones. Consistent with this data, we have

found that $CD8^{+}BTLA^{+}$TIL susbset is a less differentiated TIL subset that persists longer *in vivo* following TIL transfer in ACT treated patients. Thus far, it remains inconclusive whether the BTLA signaling pathway is also involved in the favorable clinical response to adoptive T cell therapy. The BTLA cytoplasmic domain consists of three signaling motifs including Grb2, ITIM, and ITSM. It is clearly known that ITIM and ITSM motifs are essential for BTLA to exert a suppressive effect by recruiting SHP1 and 2 during TCR activation. On the other hand, the BTLA cytoplasmic tail also contains a predicted recruitment site for Grb2, which is present in the cytoplasmic tail of costimulatory molecules such as CD28 and ICOS. Recent studies have shown that the predicted Grb2 binding site was not only able to recruit Grb2 protein, but also interacted with p85 PI3K even though there is no reported consensus motif for p85 recruitment.

Previous studies have suggested the roles of BTLA in T cell differentiation and co-inhibitory signal. However, it remains unclear how less differentiated T cell characteristics could contribute in improving the clinical outcome of ACT treated patients. In addition, several unanswered questions still remains concerning whether the Grb2 motif of BTLA could provide a positive signal. If so, mechanisms defining the integration of the inhibitory and positive signals during engagement of BTLA and HVEM remain to be elucidated.

1.7 Overall hypothesis and specific aims

Our goal is to characterize the function of the $CD8^+BTLA^+$TIL subset and the molecular mechanism and function of BTLA upon HVEM ligation. We are hypothesizing that the less differentiated T cell phenotype of $CD8^+BTLA^+$ TIL together with BTLA signalling may provide a survival advantage and translate in a better persistence of TIL following antigen restimulation. In this dissertation, we tested our hypothesis under the following specific aims;

Specific Aim #1: To characterize the survival and anti-tumor function of $CD8^+BTLA^+$TIL and $CD8^+BTLA^-$TIL subsets using *in vitro* assays and NSG mouse model for adoptive T cell therapy.

Specific Aim#2: To dissect the function and downstream signals of BTLA using BTLA mutant retroviral constructs.

Specific Aim #3: To investigate the role of BTLA in the generation of memory upon vaccination with gp100 in a Pmel-1 mouse model.

CHAPTER 2

Transcriptional analysis of BTLA in metastatic melanoma patients and comparative study of the kinetics of BTLA expression in $CD8^{+}$T lymphocyte

2.1 Rationale and Hypothesis

Our phase II clinical trials of adoptive T cell therapy at MD Anderson Cancer Center using autologous *ex vivo* expanded tumor infiltrating lymphocytes (TILs) have demonstrated the great potential of this immunotherapy for stage IV metastatic melanoma. We have investigated a number of biomarkers in infused TIL for their association with clinical response. These included markers of T lymphocyte subsets, effector-memory differentiation markers, as well as positive and negative costimulatory molecules. Unexpectedly, we observed that BTLA is the only maker that is associated with positive clinical response in TIL treated patients (134).

BTLA is characterized as a co-inhibitory receptor belonging to the Ig superfamily (186). It has been demonstrated that several co-inhibitory molecules including PD-1, CD160, TIM-3, LAG-3 are tightly associated with T cell exhaustion phenotype (205). As activated T cells progress toward exhaustion they gradually upregulate the expression of these co-inhibitory markers which results in a gradual loss of T cell effector function defining T cell exhaustion. By the same token, T cells expressing one of these molecules, for example $CD8^+PD\text{-}1^+$ T cells in peripheral blood of healthy donors or antigen-specific T cells circulating in melanoma patients are not essentially functionally defective. A recent report has clearly demonstrated that the majority of co-inhibitory receptors such as PD-1, CD160, 2B4, as well KLRG1 were inducible upon T cells activation. On the contrary, BTLA is highly enriched in naïve T cells and gradually down-regulated following T cell activation, suggesting that BTLA marks a "young T cell phenotype" (141). It was demonstrated that human effector $CD8^+$ T cells derived from naïve cells exhibit a minimally diferentiated phenotype with

superior ability to expand and retain longer telomere. These findings suggest that a less differentiated phenotype is tightly associated with enhanced proliferative capacity and persistence following T cell transfer, which is linked to an effective clinical response in ACT (206).

Thus far, the study of BTLA has been largely restricted to its inhibitiory function in studieusing models such as autoimmune diseases and infectious diseases (191, 202, 207, 208). Our unexpected findings suggest that BTLA could play an important role in tumor immunology, particulary for adoptive T cell therapy. We have witnessed an improved clinical response in patients treated with high proportion of $CD8^{+}BTLA^{+}$ in their infusion products. However, our findings are based on the expression of BTLA on *in vitro* expanded TIL and it is unclear whether high expression of BTLA in the tumor tissue could be associated with improved survival in metastatic melanoma patients. Although BTLA expression was preliminarily reported in human and mouse T cells, the kinetic expression of BTLA in different T cell subsets has not yet been investigated, particularly in murine T lymphocytes.

In this study, we aimed to investigate the transcription level of BTLA in stage III metastatic melanoma patients to investigate the association between BTLA trancription and patient survival. In addition, we also determined the kinetics of expression of BTLA in both human and mouse to comparatively examine BTLA regulation between two species.

2.2 Results

High CD8a and High BTLA gene expression strongly linked to an improved survival of stage III metastatic melanoma patients.

We previously demonstrated that $CD8^+BTLA^+$ subset is highly associated with favorable clinical response in TIL treated metastatic patients, but not other co-inhibitory molecules such as PD-1, TIM-3, as well as LAG-3 (141). It remains understudied whether metastatic melanoma patients with high expression of BTLA, CD8 or both markers, in the tumor tissue also conferred superior survival rate regardless of given therapy.

To further examine whether $CD8^+BTLA^+$ is linked with better survival, we analyzed integrated data generated by The Cancer Genome Atlas (TCGA) Research Network. The data from 96 stage III metastatic melanoma patients were retrieved from the database for survival analysis using a Kaplan-Meier analysis method. A non-parametric statistic was used to evaluate the fraction of patients alive for a period of time following therapeutic intervention. In this study, we performed transcription analysis by evaluating the association between transcripts of CD8a, CD19, NRC1, and BTLA, with survival in metastatic melanoma patients. Gene transcription level was categorized into high and low based on the expression being higher or lower than the median value respectively.

We found that the patients with high transcripts of either CD8a or BTLA had much superior survival when compared with either CD8a low or BTLA low (Log Rank; CD8a high vs CD8a low, $P=0.0007$, $N=42$; BTLA high vs BTLA low, $P=0.001$, $N=42$) (**Figure 2.1A and 2.1B**). When both CD8a and BTLA were considered, high transcription level of CD8a and BTLA was the strongest link with better survival.

Interestingly, patients with low CD8 but high BTLA had better survival as compared to high CD8 paired with low BTLA. (Log Rank; CD8a high BTLA high vs CD8a low BTLA low, P =0.0007, N =98) **(Figure 2.1C)**.

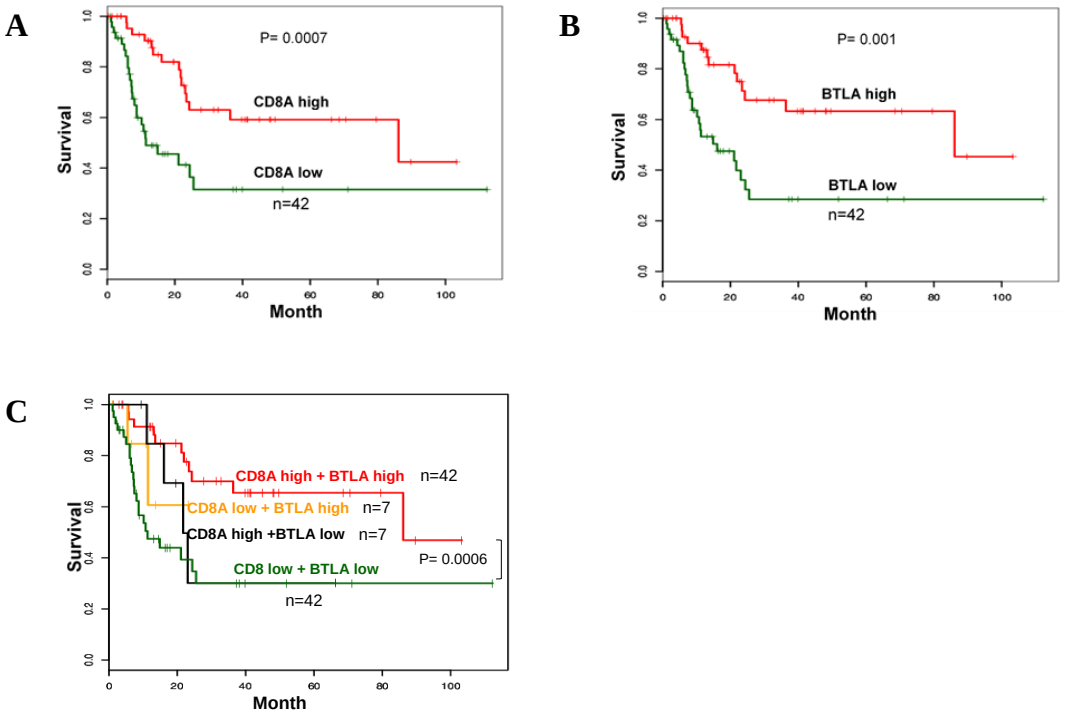

Figure 2.1. Association of high CD8a and high BTLA transcription level and improved patient survival in stage III metastatic melanoma.

Kaplan-Meier survival curves in stage III metastatic melanoma from The Cancer Genome Atlas (TCGA) consortium depicts; (**A**) CD8a expression; CD8a high versus CD8a low (**B**) BTLA expression; BTLA high versus BTLA low (**C**) Combined CD8 and BTLA expression; CD8a high BTLA high versus CD8a low BTLA high versus CD8a high BTLA low versus CD8a low BTLA low. Total number of patients=98, (high- above median, low-below median). Statistical significance was determined using a log-rank. (P <0.001 and P <0.0001). CD8a high BTLA high, N=42; CD8a high BTLA low, N=7; CD8a low BTLA high, N=7; CD8a low BTLA low, N=42.

Since BTLA can be expressed by other cell types, we also further investigated the association of BTLA with other immune cells such as B cells (defined as CD19) and NK cells (defined as asNCR1). We found that high CD19 transcription level was linked with better survival, particularly in combination with low BTLA **(Figure 2.2A)**. The worst survival was observed in the patients with low transcription level of both CD19 and BTLA; however, patients with low CD19 and high BTLA had much superior survival as compared with low CD19 and low BTLA P =0.024, N=40 (**Figure 2.2B**). Next, we determined the gene expression level of NK cells and BTLA, we observed that low NCR1 and high BTLA was correlated with the greatest survival. Within the BTLA high group, NCR1 expression defined worst survival. Overall the high expression of BTLA in conjunction with either high CD8, high/low CD19 or low NCR1 was most predictive of best survival, indicating that BTLA might be a good predictor for stage III metastatic melanoma patients.

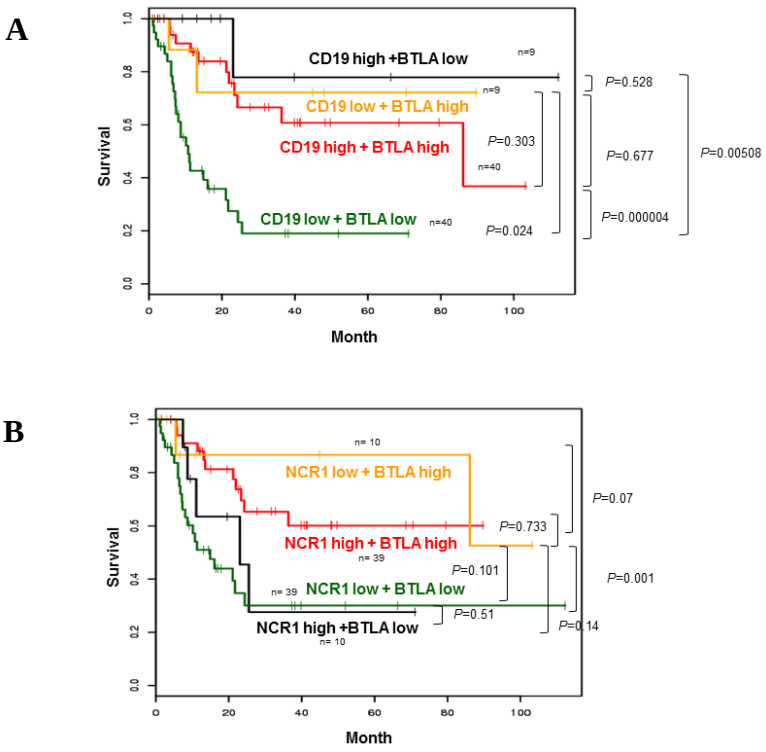

Figure 2.2. Correlation of CD19, NRC1, and BTLA transcription level with patients in stage III metastatic melanoma.

Kaplan-Meier survival curves in stage III metastatic melanoma from The Cancer Genome Atlas (TCGA) consortium depicts (**A**) CD19 and BTLA expression in the following combinations; CD19 high and BTLA low (black), CD19 low and BTLA high (yellow), CD19 high and BTLA high (red), and CD19 low and BTLA low (green). (**B**) NCR1 (NK cell marker) expression and BTLA expression in the following combinations; NCR1 low and BTLA high (yellow), NCR1 high and BTLA high (red), NCR1low and BTLA low (green), and NCR1 high and BTLA low (black). Total number of patients=98 (high-above median, low-below median). Statistical significance was determined using a log-rank. CD19 high and BTLA low, *N=9*; CD19 low and BTLA high, *N=9*; CD19 high and BTLA high, *N=40*; and CD19 low and

BTLA low, *N=40*. NCR1 low and BTLA high, *N=10*; NCR1 high and BTLA high, *N=39*; NCR1low and BTLA low, *N=39*; and NCR1 high and BTLA low, *N*=10.

Human BTLA is downregulated upon cell differentiation and expansion.

BTLA was first characterized as a co-inhibitory molecule expressed by B cells, T cells, dendritic cells, as well as NK cells (186). Several *in vitro* and *in vivo* studies have consistently shown that BTLA attenuated T activation through its inhibitory motifs, ITIM and ITSM. Unlike other inhibitory molecules, BTLA is down-regulated following T cell activation as opposed to the increased expression commonly seen with PD-1, TIM-3, and LAG-3. Transcriptional analysis of $CD8^+BTLA^+$ versus $CD8^+BTLA^+$ has indicated that $CD8^+BTLA^+$ T cell subset is highly enriched in genes associated with less differentiated T lymphocytes including CD28, whereas a gene signature typical of more differentiated T cells is highly up-regulated in $CD8^+BTLA^-$ T cell subset (142).

Based on this finding, we further performed immunophenotypic analysis of T cells in PBMCs to determine the expression level of BTLA in different T cells subsets. Human PBMCs isolated from five donors were stained with CD3, CD8, CD45RA, CCR7, and BTLA. $CD8^+$T cells were categorized into five subsets on the basis of the expression of CCR7 and CD45RA; Naïve ($CD45RA^+CCR7^+$), Central memory ($CD45RA^-CCR7^{+)}$, Effector memory ($CD45RA^-CCR7^-$), Effector memory intermediate ($CD45RA^{int}$, $CCR7^-$), and terminally differentiated ($CD45RA^+$, $CCR7^-$) (**Figure 2.3A**). Highest BTLA expression was observed in naïve T cells (non-differentiated cells), and terminally differentiated had the lowest BTLA expression. BTLA expression between naïve and central memory was comparable (P=0.06), but the expression was significantly higher than effector memory and terminally differentiated cells respectively (naïve versus effector memory, P= 0.028, N=6; naïve versus terminally differentiated, P =<0.001; central memory vs terminally

differentiated, *P*=0.03) (**Figure 2.3B and C**). This indicates that BTLA is highly enriched in less differentiated T cells, and that its expression level is down-regulated upon differentiation. Thus BTLA expression level marks T cell differentiation status.

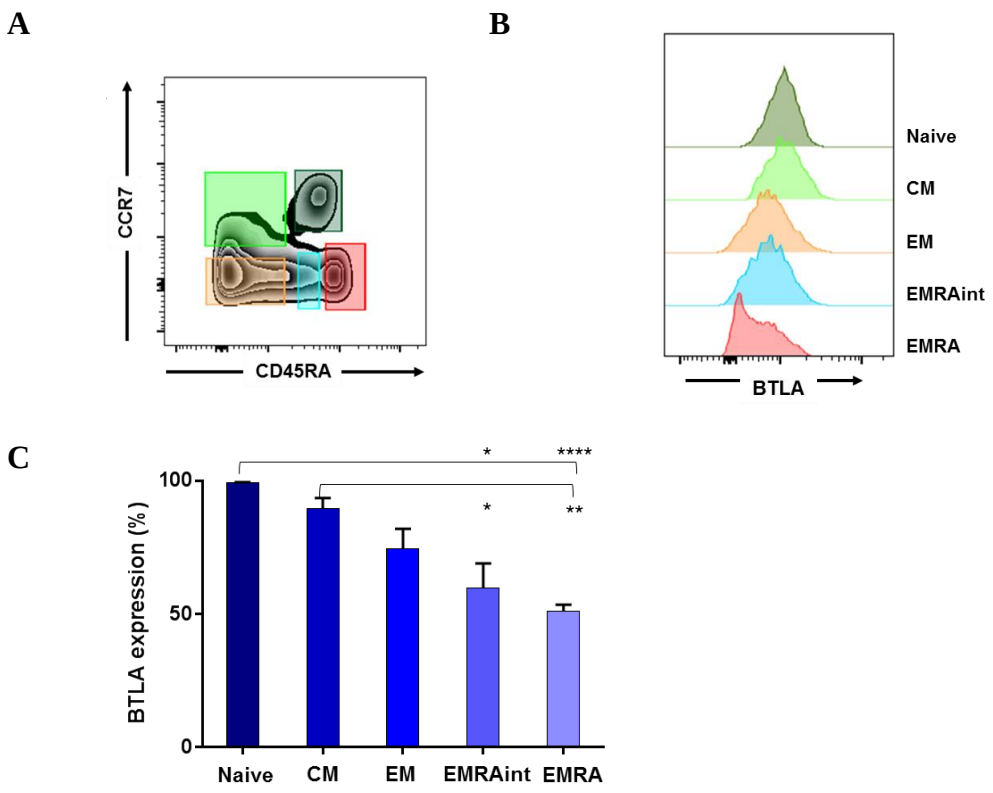

Figure 2.3. BTLA expression correlates with differentiation status of T cells.

PBMCs were isolated form five human donors. The cells were stained with anti-human CD3, CD8, CD45RA, CCR7, and BTLA. (**A**) Zebra plot depicts different $CD8^+$ T cell subsets defined by the expression of CD45RA and CCR7; Naïve ($CD45RA^+CCR7^+$), Central memory ($CD45RA^-CCR7^{+)}$, Effector memory ($CD45RA^-CCR7^-$), Effector memory intermediate ($CD45RA^{int}$, $CCR7^-$), and terminally differentiated ($CD45RA^+$, $CCR7^-$). (**B**) Histogram plot demonstrates mean fluorescence intensity (MFI) of BTLA expression in Naïve, Central memory (CM), Effector memory (EM), Effector memory intermediate ($EMRA^{int}$), and Terminally differentiated (TEMRA). (**C**) Bar graph depicts percentage expression of BTLA in different $CD8^+$T cell subsets. BTLA expression was down-regulated upon T cell differentiation.

Upon T cell activation, T cells undergo proliferation as well as differentiation. Because BTLA expression correlates with T cell differentiation, we further investigated whether T cell expansion could lead to BTLA down-regulation. BTLA expression level was compared between pre and post-expansion of sorted $BTLA^+$ TIL propagated using the REP protocol. BTLA was found to be significantly decreased in post-expansion of sorted BTLA TIL as compared to pre-expansion, indicating that BTLA is down-regulated upon T cell expansion and differentiation (P=0.001) (**Figure 2.4A and B**).

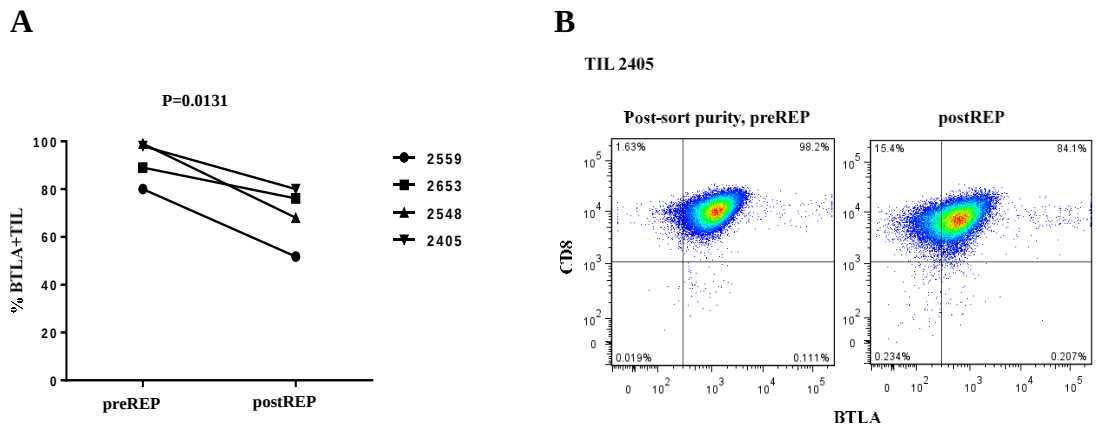

Figure 2.4. BTLA is down-regulated upon T cell expansion and differentiation.

$CD8^+BTLA^+$ TIL from four patients were sorted and propagated with the Rapid expansion protocol using irradiated PBMC, anti-human CD3, and IL-2 (6000 IU/ml) for 14 days. The cells were stained with anti-human CD8 and BTLA. The expression level of BTLA by CD8 TIL was assessed by flow cytometry. (**A**) BTLA expression was significantly decreased following TIL propagation using REP. (*N*=4, *P*=0.0131) (**B**) Pseudo color plots demonstrates BTLA expression. Representative example of $CD8^+$TIL (TIL #2405) demonstrates post-sort purity (left panel) and a decreased BTLA expression following REP (right panel).

Mouse BTLA is up-regulated upon T cell activation.

We previous demonstrated the expression of BTLA in different human T cell subset. In this study, we explored the kinetic of BTLA expression in different subset of mouse $CD8^+$T lymphocytes. Mouse $CD8^+$T cells were categorized into three subsets on the basis of the expression of CD62L and CD44; Naïve ($CD44^-CD62L^+$), Central memory ($CD44^+$high$CD62L^+$), Effector memory ($CD44^+CD62L^-$) (**Figure 2.5A**). Splenocytes from OT-1 mouse were stained with anti-CD3, anti-CD8, anti-CD44, anti-CD62L, and anti-BTLA.

High expression of BTLA was observed in $CD44^+CD8^+$ T cells, particularly in CD44high and $CD62L^+CD8^+$T cells, suggesting that BTLA expression correlates with T cell activation as $CD44^+$ is highly expressed by activated T lymphocytes (**Figure 2.5B and C**). Unlike human T cells, the expression of BTLA in mouse naïve T cells was undetectable.

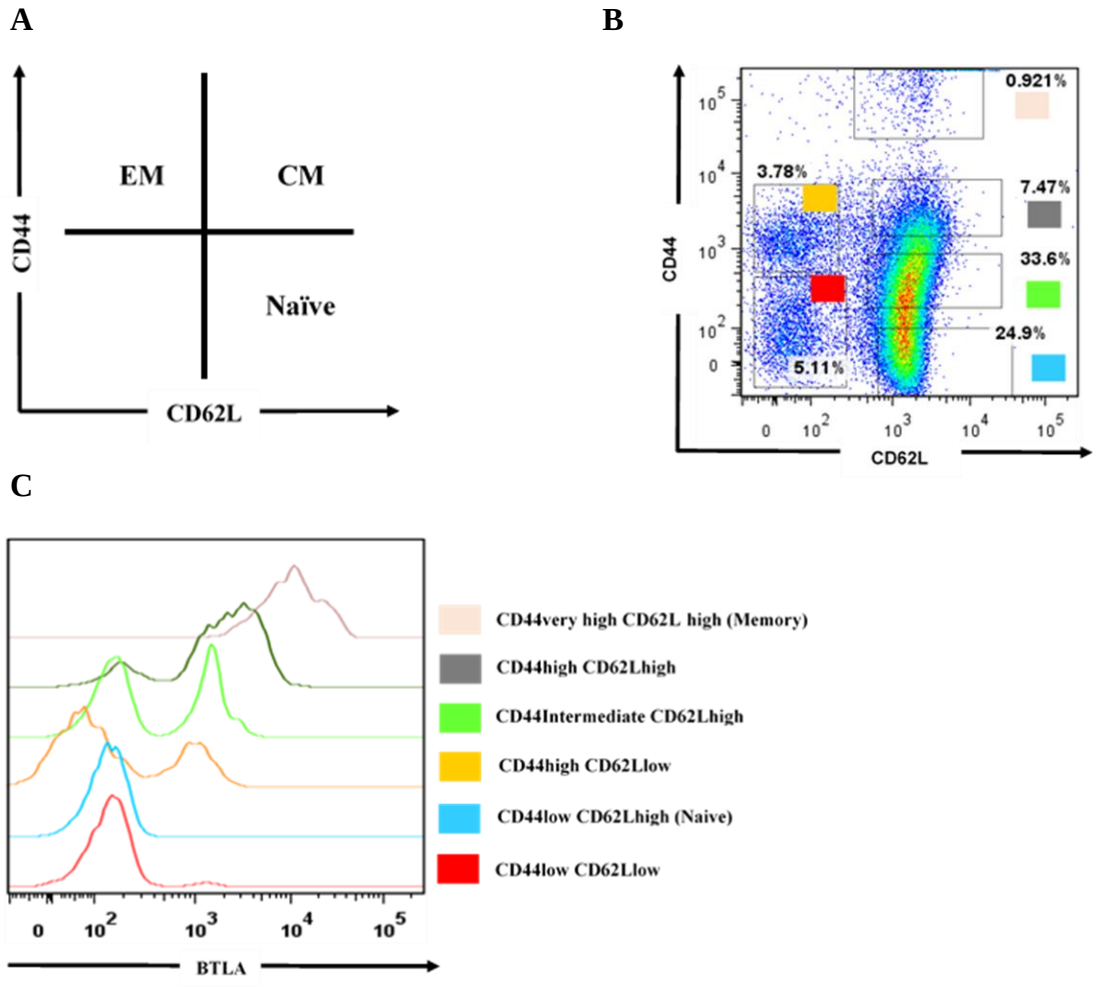

Figure 2.5. High expression of BTLA correlates with CD44.

Splenocytes were isolated from wild type OT-1 mouse, lysed with ACK buffer, then stained with anti-CD3, anti-CD8, anti-CD44, anti-CD62L, and anti-BTLA. (**A**) Mouse $CD8^+$ T cell subset defined by the expression of CD44 and CD62L; Naïve ($CD44^-$ $CD62L^+$), Central memory (CM, $CD44^+CD62L^+$), and Effector memory (EM, $CD44^+CD62L^-$). (**B**) High expression of BTLA correlates with CD44. (**C**) The highest BTLA expression was found in Memory T cell subset (CD44 very hi and CD62Lhi), while CD44 low and CD62L subset had the lowest expression of BTLA.

Next, we further examine the kinetic of BTLA expression in different mouse T cell subsets following T cell activation. Either sorted naïve T cells ($CD44^{-}CD62L^{+}$) or Memory T cells ($CD44^{+}CD62L^{+}$) were labeled with eflour®670 and stimulated by co-culturing with bulk splenocytes of OT-1 mouse and anti-mouse CD3 (**Figure 2.6A**). BTLA expression was determined every other days following T cell activation. Down-regulation of BTLA was observed in mouse T lymphocytes, which is similar to the kinetic of human T cells. In mouse naïve T cells, BTLA expression was inducible upon T cell activation, and gradually declined within five days (**Figure 2.6B**). Interestingly, re-stimulation with anti-mouse CD3 failed to trigger the expression of BTLA regardless of the dose of antibody (**Figure 2.6C**).

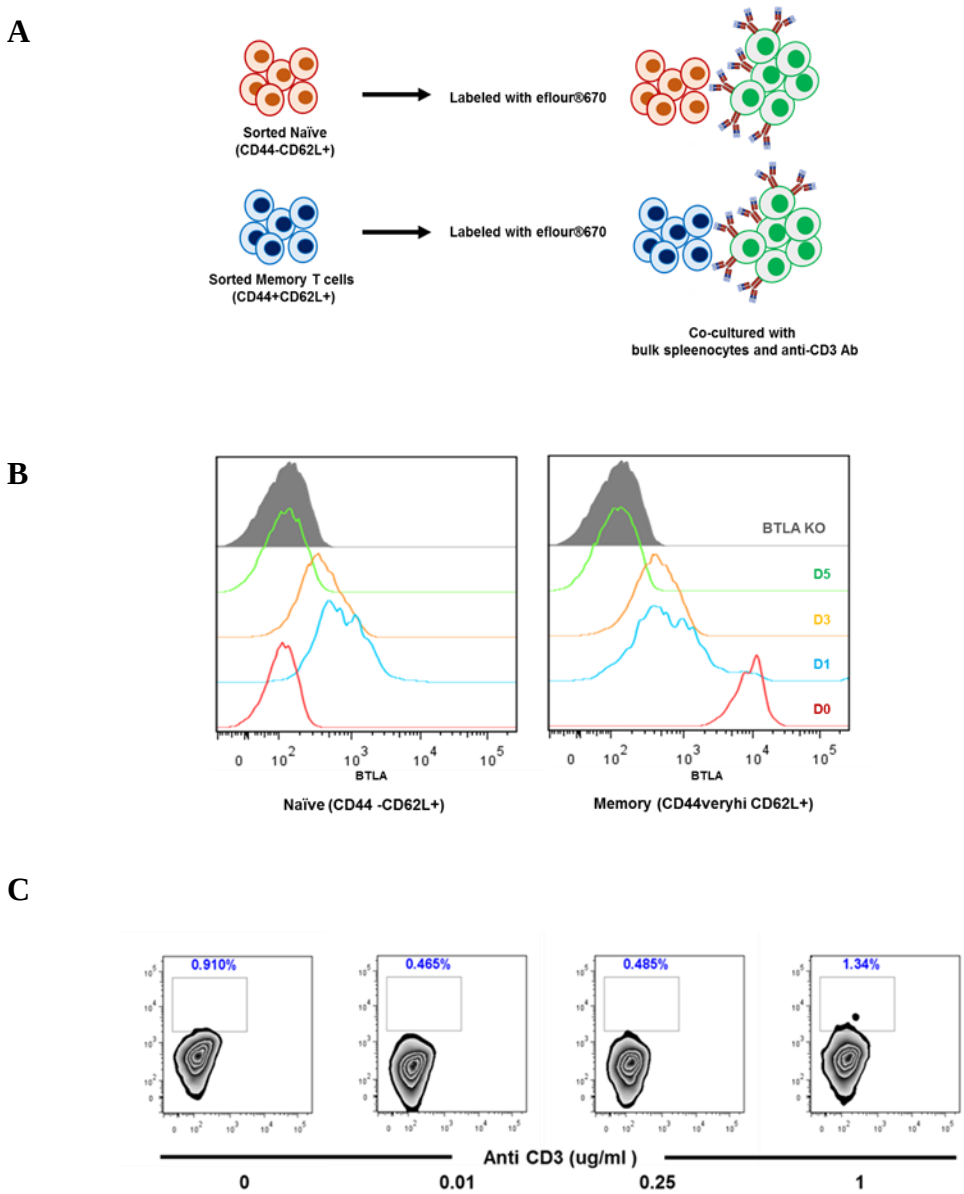

Figure 2.6. The kinetic of BTLA expression in mouse T cells.

(**A**) Naïve (CD44loCD62Lhi) and Memory T cells (CD44very hi and CD62L hi) were sorted from bulk splenocytes of OT-1 mouse, labeled with efluor670®, and activated by co-culturing with bulk splenocytes with mouse anti-mouse CD3 at concentration of 300 µg/ml. Activated T cells were harvested and stained with anti-CD44, anti-CD62L,

and anti-BTLA on day 0, 1, 3, and 5 respectively. (**B**) Sorted cells were gated on efluor670®$^{+}$CD3^{+}CD8^{+}cells and analyzed for expression of BTLA, CD44, and CD62L. BTLA in naïve T cell was up-regulated shortly after activation and return to basal level within 5 days, while BTLA expression in memory T cell subset was continuously decrease within a day upon activation. (**C**) On day 7, the cells were re-stimulated with antimouse-CD3 at concentration of 0.01, 0.25, and 1 mg/ml. There was no BTLA expression detected within 24 hours following re-stimulation.

2.3 Discussion

Transcriptional analysis has demonstrated that the gene expression of CD8a and BTLA in the tumor tissue is associated with an extended survival of stage III metastatic melanoma patients, while no correlation of survival benefit was seen with the co-expression of BTLA and other immune cells such as NK and DC cells. This finding is in agreement with our previous observation indicating that high proportion of $CD8^+BTLA^+$TIL in the infusion product associated with positive ACT clinical outcome (134). The association between the expression of BTLA and CD8 and survival from the TCGA data strengthens our results making the point that the co-expression of BTLA and CD8 is a good prognostic factor for patient survival regardless of the therapy they eventually receive.

Our data on correlation of the high expression of human BTLA in less differentiated T cells is in agreement with a previous report from Speiser's lab (142). A recent report also suggested that BTLA could be a maker for B cell differentiation as decreased BTLA expression was observed in aged B cells minimally responsive to influenza vaccination (209). Altogether, these results indicate that BTLA serves as a cell differentiation marker in both B and T cells.

We found that BTLA expression in mouse T cells did not correlate with cell differentiation. In fact, we did not observe BTLA expression in naïve T cells isolated from C57B6L mouse. During T cell activation, mouse BTLA expression is up-regulated rapidly within 24 hours, and the expression declines over 7 days. The kinetic of expression of BTLA in mouse is similar to the general expression pattern of co-inhibitory molecules such as PD-1 and CTLA-4 (184, 210).

In conclusion, human BTLA serves as a cell differentiation maker in both B and T cells. In contrast, the kinetic of expression of BTLA in mouse is similar to other co-inhibitory molecules and not considered as a differentiation marker. This finding suggest BTLA gene regulation in mouse and human is different, possibly result from dissimilar epigenetic regulation of gene expression.

CHAPTER 3

Characterization of the anti-tumor function of the $CD8^+BTLA^+$ TIL subset

3.1 Rationale and Hypothesis

In the previous chapter, we and other have demonstrated that BTLA is considered as a marker for human T cell differentiation. BTLA is highly enriched in minimally differentiated T cells such as naïve and central memory T cells, while low expression is found in more differentiated phenotype (142). $CD8^+BTLA^+$TIL abundantly contains gene signature of less differentiated T lymphocyte including CD28, CD127 (also known as IL7R), and CX3CR1 (also known as CX3C chemokine receptor 1), while $CD8^+BTLA^-$TIL are highly enriched in more differentiated T lymphocyte gene cluster such as TYROBP (TYRO protein tyrosine kinase-binding protein), KIR2DL-1, -2, and-3 (Killer cell immunoglobulin-like receptor) (141). It has been demonstrated that minimally differentiated CD8 T lymphocytes are less potent in effector cytokine production such as IFN-γ, perforin, and granzymes, as well as cytotoxic function as compared to the more differentiated CD8 T lymphocyte counterpart. Several studies have also indicated that more differentiated T lymphocyte are more effective in mediating cytotoxic killing (206). However, we have observed that our ACT treated patients who received high proportion of $CD8^+BTLA^+$ TIL subset achieved better clinical response relative to those who were infused with less proportion of $CD8^+BTLA^+$ TIL (141). Less differentiated T lymphocytes are thought to be less effective in effector mediating killing (141, 143). However, several studies have been reporting that less differentiated T lymphocyte subset have superior proliferative capacity and persistence as compared to more differentiated T lymphocyte (140, 143, 206). We hypothesized that $CD8^+BTLA^+$ TIL may be less potent effectors but may be

able to proliferate and survive longer to repeatedly mediate tumor killing and therefore be able to better control tumor growth than their $CD8^+BTLA^-$ counterpart.

In this study, we aimed to perform an extensive investigation of the cytotoxic function of both $CD8^+BTLA^+$ TIL subset and $CD8^+BTLA^-$TIL subset. We utilize *in vitro* tumor killing assay as well as an *in vivo* model of immunodeficient NOD-*scid* IL2Rgamma^{null} model for adoptive TIL transfer to evaluate tumor burden control. To extensively determine the dynamic interaction between tumor target cell and effector T cell in isolated killing events, we conducted single cell T cell/Tumor cell killing assay using TIME. This allowed us to gain a comprehensive understanding of the fate of the T cell after tumor killing at single cell level and helped us understand the outcome of the *in vivo* tumor challenge.

3.2 Results

In vitro tumor killing capacity is relatively comparable between $CD8^+BTLA^+$ and CD8+BTLA- subsets regardless of tumor antigen restricted setting.

It is known that more differentiated T lymphocytes are more effective in tumor killing relative to those of less differentiated T cell subset. Unexpectedly, we observed TIL treated patients who were infused with high percentage of less differentiated phenotype ($CD8^+BTLA^+$TIL subset) achieved superior clinical response instead of those patients who received high percentage of more differentiated phenotype ($CD8^+BTLA^+$TIL subset). We previously reported that the T cell repertoire of $CD8^+BTLA^+$TIL and $CD8^+BTLA^-$TIL subsets almost completely overlaps (>95% of the TCR CDR3 sequences are shared) using high throughput CDR3 sequencing. This suggests that tumor-reactive T cells are not selectively enriched in one subset and the assumption is that they are equally distributed among two subset. With this bias removed, the overall killing capacity of each subset is determined on the basis of intrinsic cytotoxicity. We performed an *in vitro* killing assay to evaluate the killing capability of $CD8^+BTLA^+$ and $CD8^+BTLA^-$ subsets in cultures where the antigen recognized by TIL are unknown (non-antigen restricted killing) and also with TIL that were sorted for HLA-A2 restricted recognition of MART-1 tumor antigen (antigen-restricted killing). To investigate CTL-mediated tumor killing in tumor antigen restricted setting, we selected two TIL lines containing MART-1 recognizing TCR population (TIL#2559 and 2765). We co-incubated either sorted $CD8^+BTLA^+$MART-1 tetramer positive or $CD8^+BTLA^-$ MART-1 tetramer positive TIL with MEL526 (human melanoma tumor cells expressing the MART-1 antigen) at the ratio of effector T cells to target tumor cells of

1:1, 1:3, and 1:10 (**Figure 3.1**). Percentage of caspase-3 positive MEL526 tumor cells was used to compare tumor killing capacity between the two subsets. We found that the killing capability in two MART-1 antigen specific TIL lines were equally comparable (TIL# 2559; 1:1, BTLA+ (33%) vs BTLA-(29.1%), 1:3, BTLA+(13.95%) vs BTLA-(16.2%), 1:10, BTLA+(5.5%) vs BTLA-(5.6%), TIL#2765; 1:1, BTLA+ (2.5%) vs BTLA-(2%), 1:3, BTLA+ (7.7%) vs BTLA- (7%), 1:10, BTLA+ (11.8%) vs BTLA-(13.7%). Consistently, we did not observe any difference in tumor killing capacity in using bulk TIL from another patient in a non-antigen restricted setting (TIL# 2549; 1:1, BTLA+ (64%) vs BTLA-(71%), 1:3, BTLA+(46%) vs BTLA-(63%), 1:10, BTLA+(38%) vs BTLA-(49%). In conclusion, CD8+BTLA+ and CD8+BTLA- exhibit equivalent *in vitro* tumor killing.

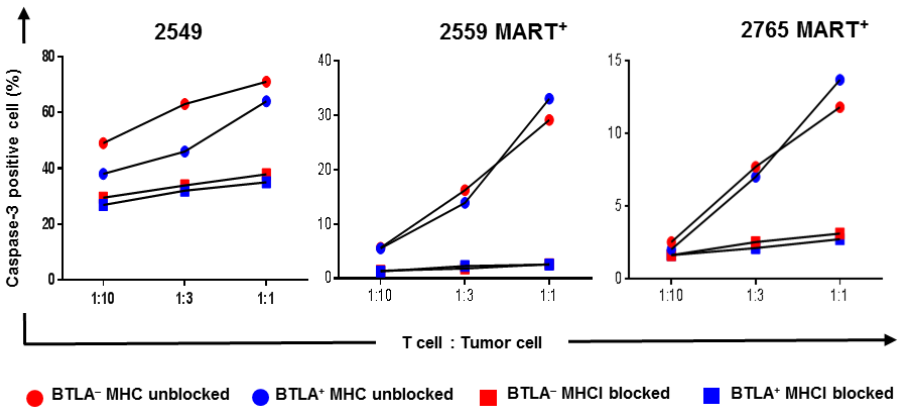

Figure 3.1. Evaluation of *in vitro* killing capacity between CD8$^+$BTLA$^+$TIL and CD8$^+$BTLA$^-$TIL subset.

MART1-reactive CD8$^+$ TIL (left and mid panel) and TIL 2549 (right panel) were sorted into BTLA$^+$ and BTLA$^-$ subsets. MEL 526 (melanoma tumor expressing MART-1 antigen, left and mid graph) or autologous tumor line 2549 (right graph) were stained with eFluor670® and co-cultured with TIL at the following TIL-to-tumor cell ratios (1:10, 1:3, and 1:1). Tumor cell death is measured by the percentage of caspase-3 positive cells. Comparable tumor killing capacity was found between two subsets.

$CD8^+BTLA^+$TIL subset confers superior tumor control in NSG mouse model for adoptive T cell therapy as compared to $CD8^+BTLA^-$TIL counterpart.

Our results indicated comparable intrinsic tumor killing ability between $CD8^+BTLA^+$ and $CD8^+BTLA^-$ subsets. This result disagreed with the previous knowledge demonstrating that more differentiated T cells are more effective in mediating tumor killing as compared to those less differentiated T lymphocyte phenotypes (211). Because *in vitro* killing capacity testing was conducted in short time (3 hours) and in a confined environment, this setting might not reflect an actual physiological interaction between tumor and TIL. We thus further determined the killing capability of TIL using an *in vivo* setting with the NOD-*scid* IL2Rgamma^{null} (NSG) mouse model for adoptive T cell therapy. NSG mice lack immune cells including mature T cells, B cells, as well as NK cells. In addition, the innate immune system and multiple cytokines are also defective in NSG mice (212). The NSG mouse model is widely used to examine the function of human T cell for the therapy of cancer, particularly in genetic modified T lymphocytes. In this study, we compared the potency of *in vivo* tumor control between $CD8^+BTLA^+$TIL versus $CD8^+BTLA^-$TIL subsets in both a tumor-antigen restricted manner (MART-1 antigen) and a non-tumor restricted setting. In the tumor-antigen restricted setting, two TIL lines containing MART-1 recognizing TCR populations (TIL#2559 and 2765) were sorted on either $CD8^+BTLA^+$MART-1 subset or $CD8^+BTLA^-$MART-1 TIL subset, and further propagated using the REP for 14 days. These expanded cells were adoptively transferred into NSG animals that were engrafted with 10 x 10^6 cells of MEL526 human melanoma tumor line expressing MART-1 antigen. IL-2 was administered immediately following T cell transfer and daily for

three days to support the *in vivo* TIL expansion. Tumor measurements were used to determine the potency of *in vivo* tumor control. Similarly, in the non-antigen restricted setting, TIL#2549 were sorted on either $CD8^+BTLA^+$ or $CD8^+BTLA^-$, propagated with the REP for 14 days, and adoptively transferred into NSG mice engrafted with autologous tumor generated from TIL#2549 patient. We found that the transfer of $CD8^+BTLA^+$ in tumor-bearing NSG mice conferred significantly better tumor control relative to those NSG mice infused with the $CD8^+BTLA^-$ TIL counterpart in both tumor-antigen restricted (TIL#2559; P = 0.002, 2765; P=0.04) and non-tumor-antigen restricted setting (TIL#2549; P=0.049). This suggests that the $CD8^+BTLA^+$ subset has a superior capability to mediate *in vivo* tumor control from an equivalent TCR repertoire therefore implying intrinsic differences (**Figure 3.2A**).

To evaluate the persistence of TIL in NSG mouse following TIL transfer, peripheral blood was collected every other day and stained with anti-human CD45 and anti-human $CD8^+$. We observed that TIL were barely or no longer detected in peripheral blood of NSG mice approximately 6 to 8 days following TIL transfer. This could suggest that TIL do not efficiently engraft in the NSG host. We found that NSG treated with $CD8^+BTLA^+MART^+$ had significant higher absolute number of $CD45^+CD8^+$ cells than those treated with $CD8^+BTLA^+MART^+$ (TIL#2559$MART^+$; D4, P=0.0021, TIL#2765$MART^+$; D2, P=0.0021, D4, P=0.02). In NSG treated with non-antigen restricted TIL, the absolute number of $CD45^+CD8^+$ cells in peripheral blood are comparable in NSG mice treated with either $CD8^+BTLA^+$ or $CD8^+BTLA^-$ (TIL#2549; D2, P=0.06) (**Figure 3.2B)**.

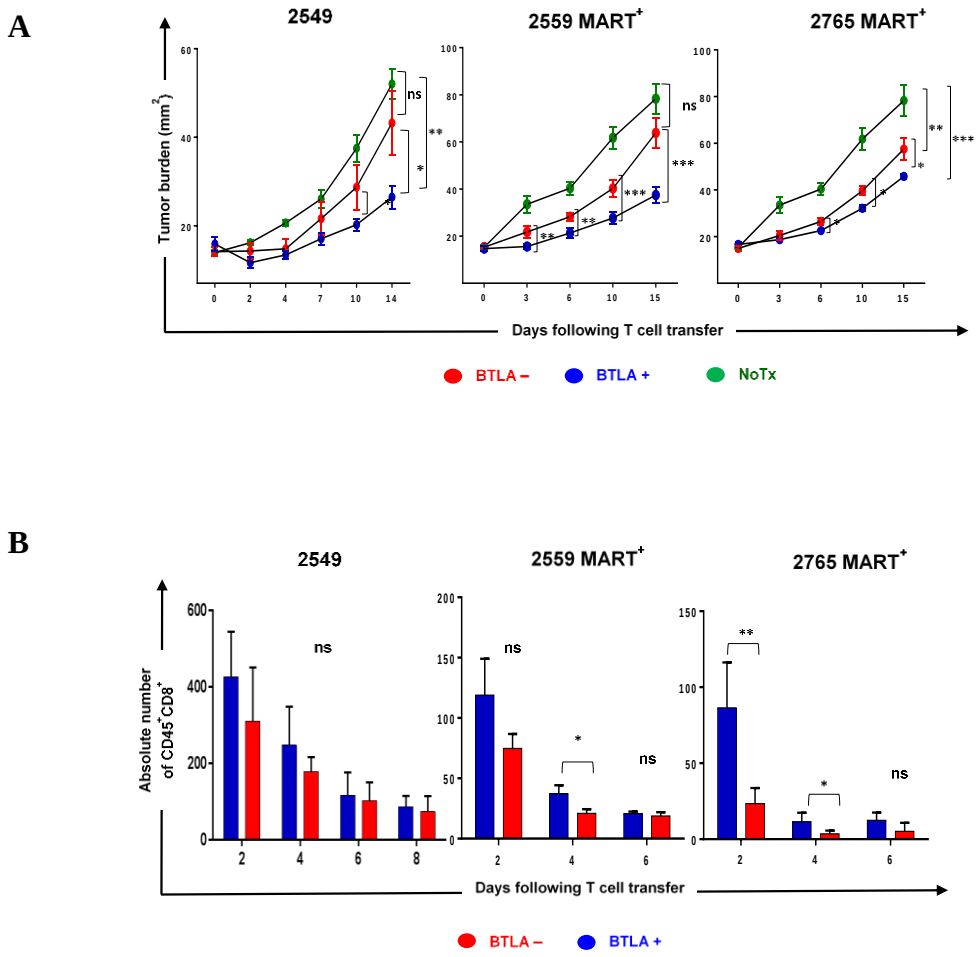

Figure 3.2. CD8$^+$BTLA$^+$ exhibits superior in vivo tumor control potency as compared to CD8$^+$BTLA$^-$.

(A) CD8$^+$BTLA$^+$TIL subset exhibited superior in vivo tumor control as compared to their CD8$^+$BTLA$^-$TIL counterpart. Ten million sorted CD8$^+$BTLA$^+$ or sorted CD8$^+$BTLA$^-$ TIL were intravenously injected into tumor bearing mice previously subcutaneously implanted with either MEL526 or autologous melanoma tumor line 2549. Tumor burden was measured for 15 days following TIL transfer using calipers and the diameter was graphed as mm^2. (**B**). To determine TIL persistence following TIL transfer, peripheral blood was collected every other day and lysed with lysed with

ACK buffer, then stained with anti-human CD45 and anti-human CD8. Bar graphs demonstrate percentage of absolute number of $CD45^{+}CD8^{+}$. $CD8^{+}BTLA^{+}$TIL subset persisted significantly longer following adoptive transfer in antigen-restricted TIL lines (2559 MART-1^{+} and 2765 MART-1^{+}).

Exploring the dynamic interaction between TIL and tumor cell at a single cell level using TIMING.

We observed that $CD8^+BTLA^+$ displayed superior *in vivo* tumor control using NSG mouse model as compared with their $CD8^+BTLA^-$ counterpart; however, no difference in *in vitro* tumor killing capacity was observed between these two subsets. The *in vivo* setting provides a broader picture relevant to an actual physiological situation and we chose to next look at the dynamic interaction between TIL and tumor at the cellular level over a longer period of time to elucidate functional differences between the two subsets. We utilized Timelapse Imaging Microscopy In Nanowell Grids (TIMING) to study the dynamic interactions between individual tumor targets and effector cells in a high-throughput setting. The nanofabricated array was used to restrict the effector TIL and tumor targets in small volumes. Functional features of TIL and tumor cells were sequentially monitored for 8 hours by automated time-lapse fluorescence microscope in each individual wells of nanofabricated array (213, 214).

In this study, we evaluated the tumor killing capacity of TIL by measuring the survival of tumor cells following the interaction with TIL and we also determined the survival of TIL after a killing event. MART-1 recognizing TIL line was used to reduce the bias of heterogeneity of the tumor recognition capacity. TIL (either sorted $CD8^+BTLA^+$MART-1 TIL or $CD8^+BTLA^-$MART-1 TIL) and MEL526 human melanoma tumor line were labeled with Vybrant Violet and Cell Tracker Red respectively, and loaded onto nanowell chip at two separate effector-to-target ratios of 1:1 and 1:2. Dynamic interaction between TIL and tumor was monitored for 500

minutes using digital fluorescence microscope attached underneath the nanowell chip (**Figure 3.3A and B**) (213, 214).

A

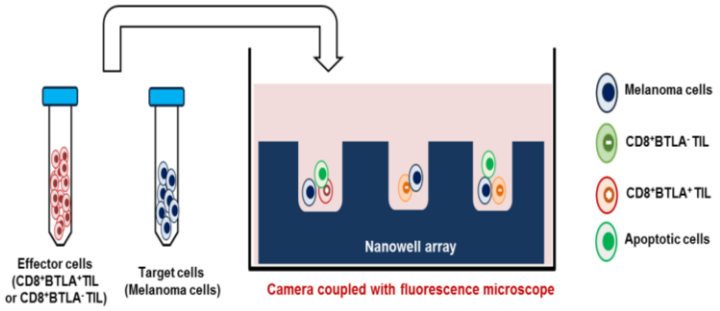

B

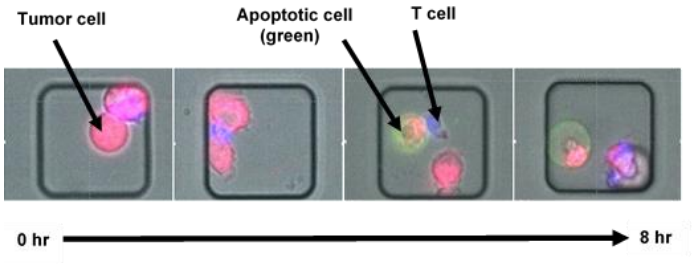

Figure 3.3. Schematic diagram demonstrating single-cell cytotoxic analysis using nanofabricated array based analysis.

Nanowell array-based cytolysis assay was used to determine tumor killing capacity at the single cell level. Effector cell and Tumor target are labeled in different colors and loaded into the nanowell at effector-to-target cell ratios of 1:1 and 1:2. Interaction between effector and target cells is monitored by automated time-lapse camera coupled with a fluorescence microscope. (**A**) Schematic diagram demonstrates nanowell chips loaded with effector cell and tumor target cells. (**B**) Timelapse images depict effector cells and tumor target cell interaction over 8 hours following co-incubation; tumor cell, T cells, and apoptotic cells are labeled in red, blue, and green respectively.

CD8+BTLA-TIL subset accelerates tumor cell death by shortening t contact and t death.

The kinetics between TIL and tumor were evaluated using these three following sequential parameters ($t_{seek,\ contact,\ and\ } t_{death}$).1) Time needed to establish conjugation between the T cell and tumor target (t_{seek}), 2) duration of the contact between the T cell and the tumor target ($t_{contact}$), and 3) time between the first T cell contact with the tumor cell and tumor cell apoptosis (t_{death}) (**Figure 3.4A**). Intriguingly, the $CD8^+BTLA^+$ subset was more effective in tumor seeking at effector-to-target cell ratios of 1:1 as time that T cell used to initiate first contact with tumor target was significantly less in $CD8^+BTLA^+$ as compared to $CD8^+BTLA^-$subset (N= 3319, tseek; ratio 1:1, P<0.0001) (**Figure 3.4B**). This difference was not observed when two targets were present in the well. (N= 3319, tseek; ratio 1:2, P<0.22) (**Figure 3.4B**). This finding could imply that $CD8^+BTLA^+$ TIL subset may be more bioenergetically efficient than the $CD8^+BTLA^-$ counterpart.

However, the $CD8^+BTLA^-$ subset was found to spend less time in contact with the tumor cell target ($t_{contact}$; 1:1 and 1:2, P<0.0001) and the time from first contact to apoptosis of the tumor target was considerably shorter for the $CD8^+BTLA^-$ subset at both E:T ratios (t_{death}; 1:1 and 1:2, P<0.0001) (**Figure 3.4C and D**). These findings support the functional role of BTLA in both signaling and cell differentiation. The co-inhibitory role of BTLA signal attenuate TCR activation, resulting in extending the time used for TIL to reach and initiate interaction with a tumor. In addition, shortened tdeath observed in $CD8^+BTLA^-$TIL subset is in agreement with the previous knowledge demonstrating that more differentiated T lymphocytes are more potent in cytotoxic function relative to those of less differentiated phenotype.

In summary, $CD8^+BTLA^+$TIL subset are more active in seeking the tumor cell than $CD8^+BTLA^-$TIL subset, but perform tumor cell death with slower kinetics. These behavioral features might be explained from both distinct differentiation status and BTLA signaling.

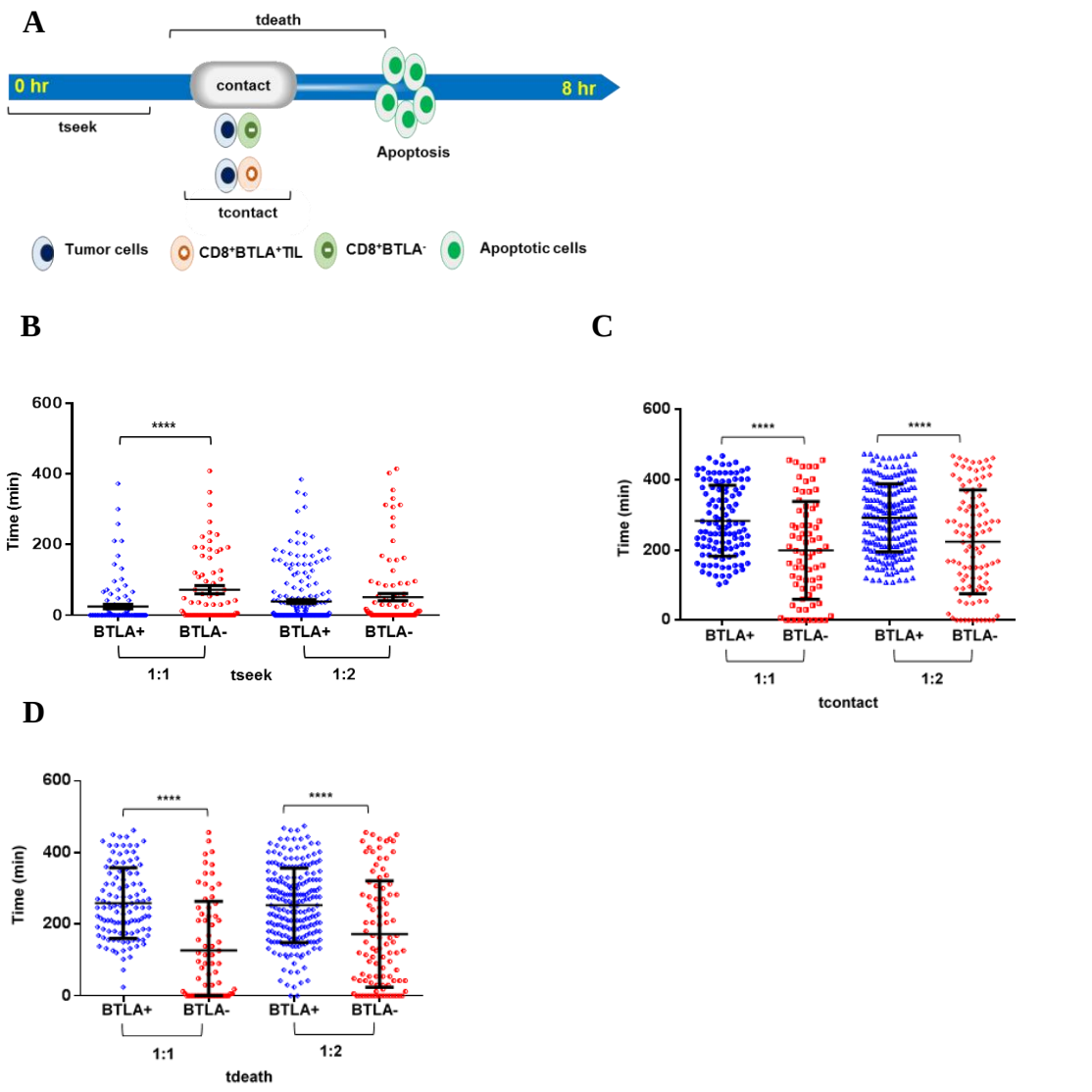

Figure 3.4. CD8$^+$BTLA$^-$TIL subset extend t seek, but shorten t contact and t death. (**A**) Schematic diagram demonstrating the sequential events in which effector cells seek (tseek), contact (tcontact), and mediate tumor cell death (tdeath). Either CD8$^+$MART1$^+$BTLA$^+$ or CD8$^+$MART1$^+$BTLA$^-$ subset was co-incubated with MEL 526. Time (min) between each sequential event is evaluated. Dot plots depict tseek (**B**), tcontact (**C**), tdeath (**D**) in comparison between CD8$^+$BTLA$^+$ (blue) and CD8$^+$BTLA$^-$

(red) subsets. All error bars depicts the mean ± s.e.m. All *P*-values were calculated using a two-tailed Student's *t*-test. (*N*=497).

$CD8^+BTLA^+$ subset conferred survival capacity that mediates tumor serial killing.

We previously have shown that $CD8^+BTLA^-$ TIL are effective in tumor killing as the time used to form contact (tcontact) and mediate tumor cell death (tdeath) was significantly less than $CD8^+BTLA^+$ subset. In contrast, we found that the two subsets had comparable tumor killing capacity when used for *in vitro* tumor killing in bulk setting.

We next examined whether the overall killing capacity between the two subsets was any different by evaluating tumor target cell survival following 8 hour of co-incubation with TIL. In general, we found that both T cell subsets equally killed tumor target (**Figure 3.5A**, 18% of tumor target killed at an E:T ratio of 1:1). Interestingly, at the E:T ratio of 1:2 the $CD8^+BTLA^+$ subset was able to kill a total of 21% of tumor targets upon contact as compared to only 14% for the $CD8^+BTLA^-$ **(Figure 3.5A)**. When two tumor targets were in the presence of one effector T cell, the $CD8^+BTLA^+$ subset was twice as likely to kill both targets (**Figure 3.5A**, 14% for the $BTLA^+$ versus 7% for the $BTLA^-$).

Next, we evaluated tumor target cell survival through time following effector target cell killing over 500 minutes. In the first 250 minutes, we found that the $CD8^+BTLA^-$ TIL subset was more potent in tumor killing capacity as survival of tumor cells being killed by $CD8^+BTLA^-$ TIL was significantly less than tumors co-incubated with the $CD8^+BTLA^+$ TIL counterpart at both effector TIL to target tumor cell ratio of 1:1 and 1:2 (**Figure 3.5B and C**, survival of contacted tumor target cells; 1:1, $P<0.03$, 1:2, $P<0.0001$). In the last 250 minutes, we found that the two subsets had comparable tumor killing capacity at effector TIL to target tumor cell ratio of 1:1; however,

$CD8^+BTLA^+$ became more effective in tumor killing when effector TIL to target tumor cell ratio increased to 1:2 (**Figure 3.5D and E**, survival of contacted tumor target cells; 1:1, $P<0.54$, 1:2, $P<0.0001$).

When we cautiously determined the survival capability of T cells following tumor killing events, we found that the $CD8^+BTLA^-$ subset was more susceptible to undergo apoptosis in comparison with the $CD8^+BTLA^+$ counterpart (**Figure 3.5D**, survival of effector cells following target tumor cell killing; ratio 1:1, $P<0.01$). This demonstrates that the $CD8^+BTLA^+$ subset is prone to survive better after tumor killing, and thus is able to repeatedly kill additional tumor cells.

Overall, our results suggest that $CD8^+BTLA^-$ is more effective in tumor killing, but also more susceptible to undergo apoptosis following killing as compared to $CD8^+BTLA^+$.

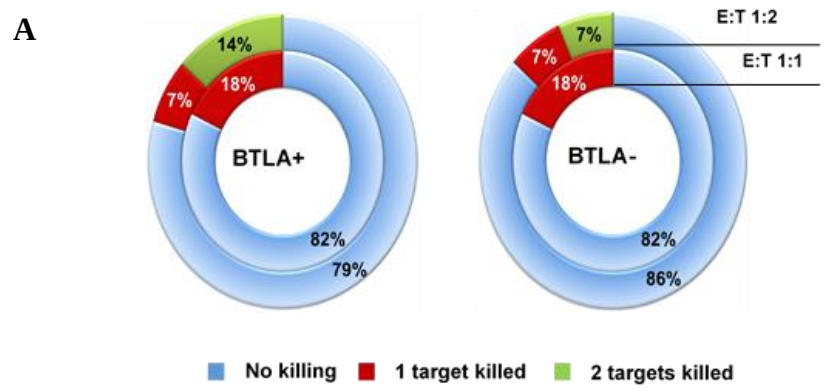
A
14%
18%
7%
BTLA+
82%
79%
E:T 1:2
E:T 1:1
7%
7%
18%
BTLA-
82%
86%
No killing
1 target killed
2 targets killed

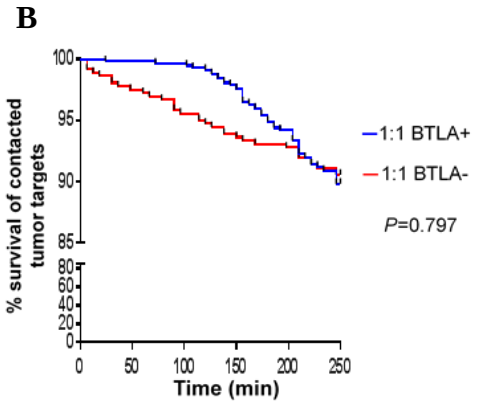
B
% survival of contacted tumor targets
Time (min)
1:1 BTLA+
1:1 BTLA-
P=0.797

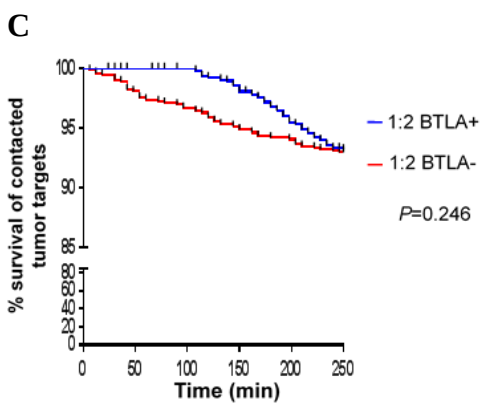
C
% survival of contacted tumor targets
Time (min)
1:2 BTLA+
1:2 BTLA-
P=0.246

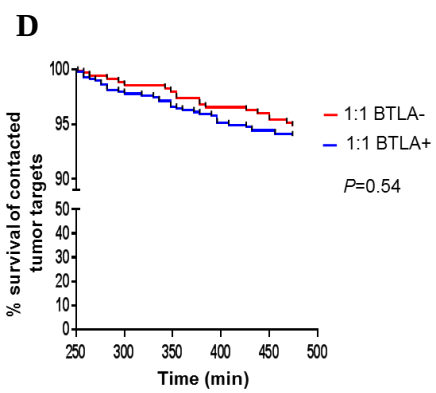
D
% survival of contacted tumor targets
Time (min)
1:1 BTLA-
1:1 BTLA+
P=0.54

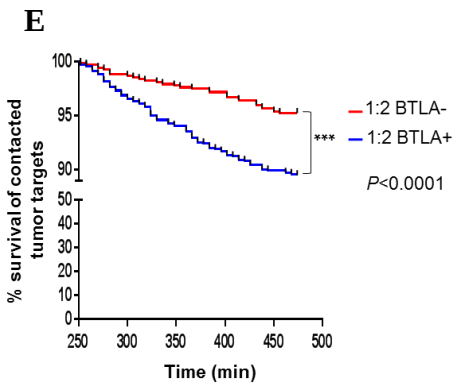
E
% survival of contacted tumor targets
Time (min)
1:2 BTLA-
1:2 BTLA+
***
P<0.0001

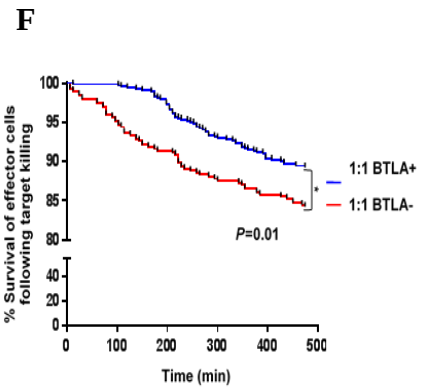
F
% Survival of effector cells following target killing
Time (min)
1:1 BTLA+
1:1 BTLA-
*
P=0.01

Figure 3.5. $CD8^+BTLA^+$ TIL subset exhibit improved survival following tumor target killing.

(A) Donut charts demonstrate the frequency of tumor cell death following effector cell killing by either $CD8^+BTLA^+$ (left) or $CD8^+BTLA^-$(right) subset. Inner circle and outer circle depict E:T ratio of 1:1 and 1:2 respectively. Kaplan-Meier survival curves of T cell-contacted tumor targets resulting in a killing event in the first 250 minutes in comparison between $CD8^+BTLA^+$ and $CD8^+BTLA^-$subsets at effector-to-target cells ratios of 1:1 (**B**) and 1:2 (**C**). Kaplan-Meier survival curves of T cell-contacted tumor target resulting in a killing event in the last 250 minutes; comparison between $CD8^+BTLA^+$ and $CD8^+BTLA^-$subset at effector-to-target cells ratios of 1:1 (**D**) and 1:2 (**E**). Statistical significance was determined using a log-rank. (N=3319). (***P <0.0001). (**F**) Kaplan-Meier survival curves of tumor-contacted effector cells following tumor cell death in comparison between $CD8^+BTLA^+$ and $CD8^+BTLA^-$ subsets at an effector-to-target ratio of 1:1. Statistical significance was determined using a log-rank. (N= 3319) (*P<0.05).

Discussion

Previous knowledge indicates that more differentiated T lymphocytes are more potent at performing effector function, suggesting that $CD8^+BTLA^-$ subset (more differentiated T cell) might be endowed with better tumor killing capacity as compared to the $CD8^+BTLA^+$ counterpart. However, we observed comparable *in vitro* tumor killing capacity between these two subsets regardless of tumor antigen recognition ability. A recent report showed that the BTLA blockade in γδ T cells had no effect on tumor killing (215). Because we did not observe difference in killing capacity between these two subset, we thus further examined the potency of *in vivo* tumor burden control using NSG mouse model. We observed that the $CD8^+BTLA^+$ TIL subset was significantly more potent at controlling *in vivo* tumor growth than its $CD8^+BTLA^-$ counterpart. In addition, we found that $CD8^+BTLA^+$TIL tended to persist longer following adoptive transfer. This finding is in accordance with our clinical observation indicating that $CD8^+BTLA^+$TIL persisted longer following TIL transfer (141).

Discerning the difference between the two BTLA subsets required to carry out the killing assay for a long period of time (8h) and looking at the fate of both T cells and tumor cells. Utilizing Timelapse Imaging Microscopy In Nanowell Grids (TIMING), we demonstrated that $CD8^+BTLA^+$ TIL subset has a heightened capability of killing multiple tumor targets through enhanced T cell survival. This finding provides a rationale for the improved *in vivo* efficacy of the $CD8^+BTLA^+$ TIL subset.

We previously demonstrated that $CD8^+BTLA^+$ TIL subset has superior mitochondrial function and spare respiratory capacity (SRC) as compared to its $CD8^+BTLA^-$ counterpart. It has been shown that memory $CD8^+$ T cells manifested high

SRC with increased number of mitochondria, which is distinct from naïve and effector T cell subset (216). This unique bioenergetic attribute was shown to play a role in cell survival and establishment of the memory T cell pool.

Overall, our findings suggest that BTLA signaling itself might not affect the tumor killing capability. In fact, the intrinsic attributes of the less differentiated phenotype of the $BTLA^{+}$ subset provide a pro-survival signal enhancing the "serial killing" capacity.

CHAPTER 4

Functional study of B and T lymphocyte attenuator in murine model

4.1 Rationale and Hypothesis

BTLA is well characterized as an inhibitory molecules belonging to the Ig superfamily. Its cytoplasmic domains composes of three motifs (Grb2, ITIM, and ITSM), which are highly conserved between mouse and human. As mentioned before the inhibitory role of ITIM and ITSM motifs of BTLA through recruitment of SHP1/2 is well documented (186, 189, 192, 207). BTLA also contains the Grb2 motif, which also exists as a cytoplasmic motif in CD28. It is known that Grb2 motif contributes to CD28 signaling pathway to promote T cell proliferation. However, the function of the Grb2 motif of BTLA has not been addressed. Evidence suggest that it might transduce a positive signal. An *in vitro* binding assay first demonstrated the potential interaction of the Grb2 binding motif with the Grb2 adaptor protein and the p85 subunit of phosphatidylinositol 3-kinase (p85 PI3K). Moreover gene expression analysis of mouse T cells following activation of anti-CD3 and anti-BTLA demonstrated a highly overlapping transcription profile with that produced by anti-CD3 in combination with positive co-stimulators but not inhibitory molecules (192).

We hypothesize that the **Grb2 motif might exert positive signal that could contribute to BTLA's function besides transducing an inhibitory signal from ITIM and ITSM motifs**. Previous studies demonstrated that BTLA inhibited T cell function by suppressing effector cytokine production and cell proliferation upon TCR triggering. Thus far, no study has focused on comprehensively understanding BTLA signaling on CD8 T cell function in both human and murine setting.

In this study, we generated retroviral constructs containing wild type BTLA (WT BTLA), BTLA with inactivating mutation of ITIM and ITSM motifs (ΔITSM),

and BTLA with an activating mutation of Grb2 motif (ΔGrb2), and overexpressed those constructs in BTLA knockout OT.1 mouse T cells (BTLA-KO-OT.1). To dissect the function of BTLA, we performed tumor killing assays to investigate the role of BTLA in mediating cytotoxic function. In addition, we also evaluated intracellular effector cytokine production and secretion during antigen re-stimulation using either dendritic cells pulsed with OVA peptide or anti-mouse CD3 with HVEM-Fc fusion protein. Furthermore, we assessed the impact of BTLA signaling on the T cell proliferation induced upon antigen re-stimulation using dendritic cells pulsed with OVA peptide to determine proliferative capacity following T cell re-stimulation.

4.2 Results

Generation of retroviral vectors containing wild type BTLA and BTLA mutants for functional study using BTLA-KO-OT.1 mouse T cells.

The functional role of BTLA signaling motifs remains understudied; therefore, site directed mutagenesis was conducted to inactivate BTLA signaling motifs. This was achieved by substitution of tyrosine for phenylalanine in the two different motifs of WT BTLA cytoplasmic tail to generate two different BTLA mutants; the Grb2 mutant ΔGrb2 (Y245F) and the ITIM and ITSM mutant ΔITSM (Y274 and Y299F) (**Figure 4.1A**). We utilized pRVKM retroviral vector with GFP reporter as a gene delivery system to overexpress WT BTLA or its mutants in BTLA-KO-OT.1 mouse T cells (**Figure 4.1B**). Briefly, the splenocytes of BTLA-KO-OT.1 mouse were stimulated with anti-mouse CD3. After 24 hours, the cells were transduced with the retroviruses containing either WT BTLA or the inactivating mutations of BTLA. On day 3, GFP^+ T cells were sorted and expanded for 7 days prior to functional studies (**Figure 4.1C**). Comparable expression of BTLA was observed in BTLA WT and its mutants (**Figure 4.1D**)

A

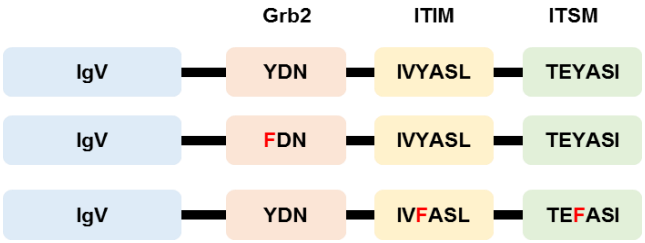
Grb2
ITIM
ITSM
IgV
YDN
IVYASL
TEYASI
IgV
FDN
IVYASL
TEYASI
IgV
YDN
IVFASL
TEFASI

B

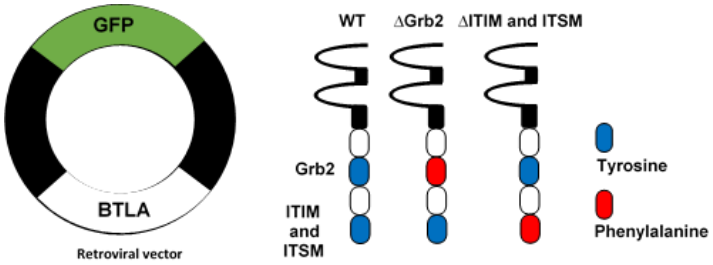
GFP
BTLA
Retroviral vector
WT
ΔGrb2
ΔITIM and ITSM
Grb2
ITIM and ITSM
Tyrosine
Phenylalanine

C

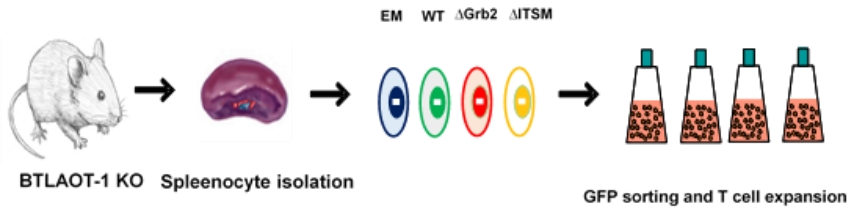
EM
WT
ΔGrb2
ΔITSM
BTLAOT-1 KO
Spleenocyte isolation
GFP sorting and T cell expansion

D

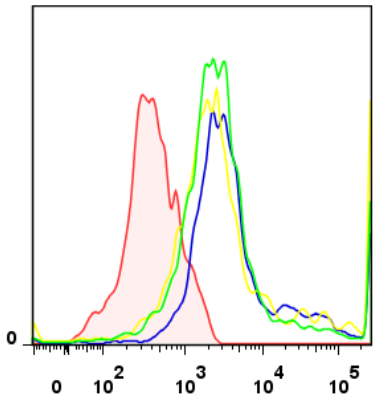
0
0
10^2
10^3
10^4
10^5

Figure 4.1. Generation of retroviral vector containing wild type BTLA and inactivating mutations of BTLA for functional study using BTLA-KO-OT.1 mouse model.

Substitutions of tyrosine for phenylalanine in three different motifs of the cytoplasmic tail of BTLA generated 2 mutant constructs; the Grb2 mutant ΔGrb2 (Y226F), as well as the ITIM and ITSM mutant ΔITSM (Y274 and Y299F) (**A**) Schematic diagram depicts the structure of BTLA WT (Top), BTLA ΔGrb2 (middle), and BTLA ΔITSM (bottom). (**B**) Schematic diagram demonstrates the pRVKM retroviral construct containing GFP and BTLA genes (left). Signaling motifs with Tyrosine and Phenylalanine are indicated in blue and red respectively (right). (**C**) Schematic diagram depicts viral transduction and generation of BTLA-KO-OT.1 mouse T cells overexpressing either BTLA or its mutants. (**D**) Histogram plots showing BTLA expression in BTLA-KO-OT.1 mouse T cells. The cells were gated on GFP positive and AQUA negative cells (live cells). BTLA WT (Yellow), BTLA ΔGrb2 (Green), and BTLA ΔITSM (Blue) positive cells, were gated using empty vector controls (tinted red).

BTLA signaling motifs have no effect on tumor killing capacity.

Our previous result unveiled that the $CD8^+BTLA^+$ TIL subset have superior survival benefit following tumor target killing as opposed to $CD8^+BTLA^-$ subset therefore is able to repeatedly mediate killing of additional tumor targets. This superior serial killing attribute can result from either 1) properties of less-differentiated T cell phenotype or 2) BTLA signaling itself. We set out to further determine whether BTLA signaling pathway might be involved in the superior killing capacity. Here, we conducted *in vitro* assays using murine T lymphocytes and B16 melanoma tumor cells, which express high levels of HVEM (**Figure 4.2A and B**).

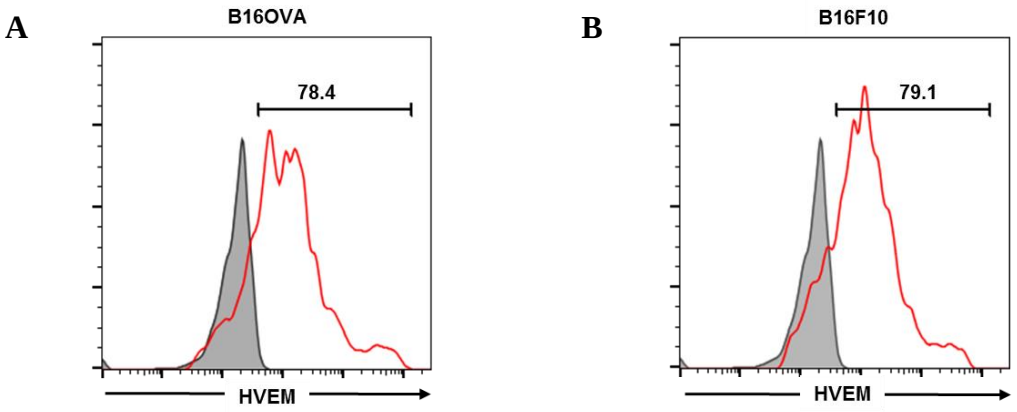

Figure 4.2. Expression level of HVEM in B16 melanoma cell lines.

Histogram plots showing HVEM expression in (**A**) B16 OVA and (**B**) B16F10 mouse melanoma tumor cells. Live tumor cells were defined as AQUA negative. HVEM positive cells (red) were gated using FMO controls (tinted gray).

Virally transduced BTLA-KO-OT.1 mouse T cells overexpressing of WT BTLA, BTLA with mutation of the Grb2 motif (ΔGrb2), BTLA with mutation of ITIM and ITSM motifs (ΔITSM), or empty vector control (EM) were incubated with either B16F10 (negative for OVA antigen) or B16OVA cells (positive for OVA antigen) that were labeled with efluor 670 at an effector to target ratio of 1:1, 1:3, and 1:10. After three hours, apoptotic tumor cells were determined by intracellular staining for cleaved capase-3. We found comparable levels of OVA-specific tumor killing regardless of the presence of WT BTLA or BTLA mutants (T cell: B16OVA, ratio 1:1, P=0.67; ratio 1:3, P=0.46; ratio 1:10, P=0.29; T cells: B16F10; ratio 1:1, P= 0.43; ratio 1:3, P=0.69; ratio 1:10, P=0.47) (**Figure 4.3**).

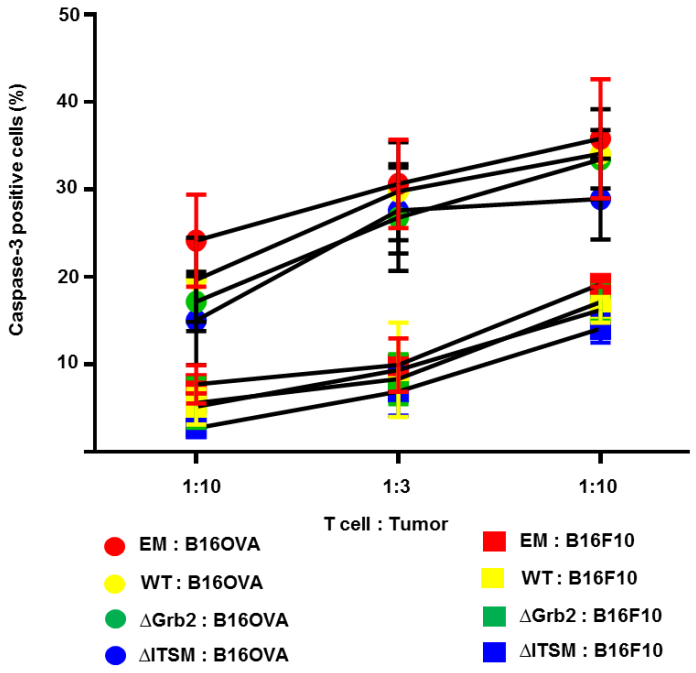

Figure 4.3. In vitro tumor killing capacity of BTLA-KO-OT.1 mouse T cells overexpressing of WT BTLA and it mutants.

B16 OVA (mouse melanoma tumor positive for OVA) or B16F10 (mouse melanoma tumor negative for OVA) were stained with eFluor670® and co-cultured with OT-1 BTLA KO T cells overexpressing WT BTLA or BTLA mutants at the following T cell-to-tumor cell ratios (1:10, 1:3, and 1:1). Tumor cell death is depicted by the percentage of caspase-3 positive cells. *N*=3 independent experiments.

Decrease in TNF-α production in BTLA-KO-OT.1 mouse T cells overexpressing WT BTLA or its mutants.

Because we found the comparable *in vitro* killing tumor capacity of BTLA-KO-OT.1 mouse T cells regardless of BTLA expression, we sought to determine whether overexpression of WT BTLA or its mutants could affect effector cytokine production. In this experiment, we re-stimulated virally transduced T cells overexpressing WT BTLA or its mutants with either dendritic cells alone or pulsed with OVA peptide at an effector to target ratio of 1 to 40. After five hours, the cells were intracellularly stained with IFN-γ and TNF-α. We found almost all effector T cells produced IFN-γ and TNF-α, and comparable percentage of the effector T cells that produced IFN-γ and TNF-α was observed (% of IFN-γ positive cells; P=0.11, % of TNF-α positive cells; P=0.59) (**Figure 4.4A**). However, the quantity of effector cytokines being made by WT BTLA was significantly less than that produced by BTLA negative cells (empty vector) alone when re-stimulated with dendritic cells pulsed with OVA peptide (IFN-γ MFI; EM vs WT, P=0.04, TNF-α MFI; EM vs WT, P=0.0045) (**Figure 4.4B**). This suggests that BTLA signaling negatively impacts effector cytokine production. The suppressive effect of BTLA was completely reverted by the inactivation of ITIM and ITSM motifs, which implies that those motifs are responsible for the BTLA-mediated decrease in IFN-γ and TNF-α effector cytokines upon TCR activation.

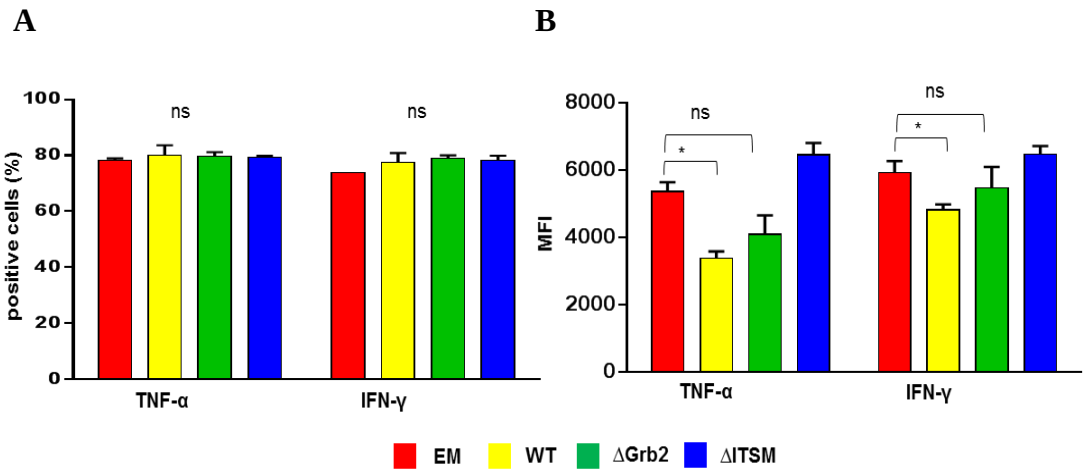

Figure 4.4. Decrease in TNF-α production in BTLA-KO-OT.1 mouse T cells overexpressing of WT BTLA and it mutants.

OT-1 BTLA KO T cells overexpressing WT BTLA or its variants were re-stimulated with dendritic cells pulsed with OVA peptide. TNF-α and IFN-γ production by virally transduced OT-1 BTLA KO T cells was evaluated by intracellular staining. Bar graph depicts the percentage of positive cells (**A**) and mean fluorescence intensity (MFI) (**B**). Each bar represents three independent experiments. (Two-way ANOVA; **P*<0.05).

BTLA signaling motifs affect T cell proliferation.

We have previously demonstrated that $CD8^+BTLA^+$TIL are more proliferative in response to IL-2 and less differentiated. It has been shown that less differentiated T cells were more metabolically active and superior in proliferative capacity. However several studies have demonstrated that BTLA inhibited T cell proliferation upon ligation with HVEM. It was shown that both ITIM and ITSM motifs were required for the full function of BTLA to inhibit T cell proliferation and cytokine production including IFN-γ, IL-2, and IL-10 (193, 217). A recent report indicated that the PD-1 receptor, which consisted of ITIM and ITSM motif, selectively inhibited the Akt and Ras-MEK-ERK pathways. So far, it remains inconclusive whether BTLA utilizes a similar mechanism as PD-1 to inhibit T cells as ITIM and ITSM motifs are commonly shared between these two receptors. Thus, we sought to further determine whether BTLA signaling motifs could play a role in proliferation of $CD8^+$ TIL. BTLA-KO-OT.1 T mouse cells overexpressing BTLA WT or its mutants were labeled with the cell proliferation dye efluor670® and re-stimulated with dendritic cells pulsed with OVA peptide for two days. Upon re-stimulation with dendritic cells pulsed with the cognate peptide most T cells underwent proliferation. However, subtle differences are appreciable between T cells expressing the different BTLA constructs. We observed that BTLA-KO-OT.1 mouse T cells expressing a non-functional inhibitory domain (ΔITSM) had lower mean intensity of fluorescence (MFI) as compared with empty vector control (MFI: ΔITSM versus EM; P=0.012, ΔITSM versus WT; P=0.0057) (**Figure 4.5A and B**). WT BTLA and EM control showed comparable proliferation as no significantly different MFI was observed (MFI: WT versus EM; P=0.30). On the contrary, attenuation of T cell proliferation was observed in T cells expressing a

disrupted Grb2 domain (ΔGrb2), (MFI: ΔGrb2 versus ΔITSM; P=0.0003, ΔGrb2 versus EM; P=0.0008, ΔGrb2 versus WT; P= 0.0009) (**Figure 4.5A and B**). Our findings suggests that Grb2 motif plays a role in enhancing cell proliferation, while ITIM and ITISM motif suppress the proliferative capacity of T cells.

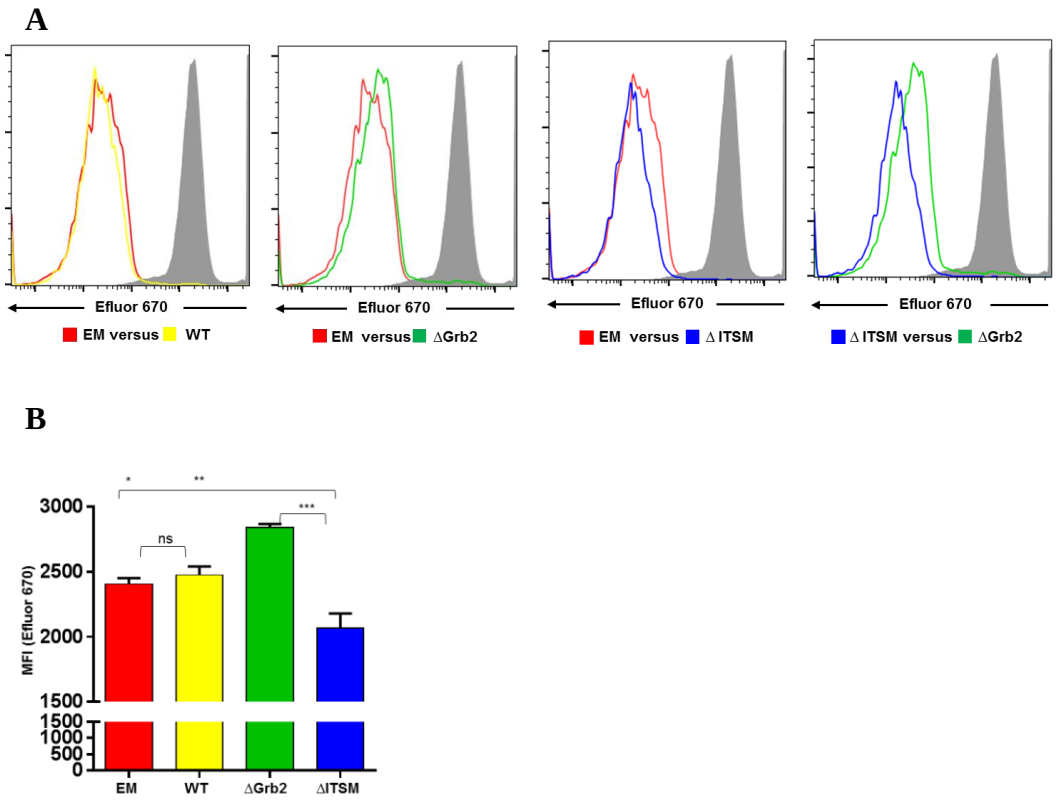

Figure 4.5. ITIM and ITSM motifs of BTLA attenuated T cell proliferation.

OT-1 BTLA KO T cells overexpressing WT BTLA or its variants were labeled with eFluor670® and re-stimulated with dendritic cells pulsed with OVA peptide. Cell proliferation was determined by the dilution of eFluor670®. (**A**) Histogram plots of eFluor670® demonstrate proliferation of OT-1 BTLA KO T cells overexpressing WT BTLA or its variants. (**B**) Bar graph depicts MFI of virally transduced T cells in the same experiment shown in the left panel. N=3 **P* <0.05, ***P* <0.001, ***P<0.0001. All error bars depicts the mean ± s.e.m. All *P*-values were calculated using a two-tailed Student's *t*-test.

Grb2 motif of BTLA enhanced IL-2 production.

Our previous study demonstrated that $CD8^+BTLA^+$TIL subset had increased proliferative capacity due to enhanced IL-2 responsiveness (141). In mouse $CD4^+$T cells, however, it has been shown that engagement of BTLA and HVEM suppressed cytokine production including IFN-γ, IL-2, and IL-10 (193). Thus far, the role of BTLA in cytokine production of CD8 T cells remains unclear. To further investigate whether BTLA signaling motifs might affect the cytokine production, we overexpressed in OT-1 BTLA KO T cells the WT BTLA or its mutants, and re-stimulated with anti-CD3 in the presence of HVEM-Fc fusion protein to engage the BTLA molecules. The supernatants were collected after 24 hours to assess the cytokine secretion using a MILLPLEX multiplex assay.

When ΔGrb2 T cells were re-stimulated with anti-CD3 and HVEM, we found a significant decrease in GM-CSF, IL-6, and IL-10 production as compared with empty vector control (GM-CSF; P=0.0004, IL-6; P=0.02, IL-10; P=0.002), but we did not observe a significant increase in these cytokines in ΔITSM T cells when compared with empty vector control (GM-CSF; P=0.30, IL-6; P=0.72, IL-10; P=0.59) (**Figure 4.6A**).

The only cytokine induced to high levels by the introduction of BTLA was IL-2. The BTLA-dependent IL-2 production was abrogated by the inactivating mutation of Grb2 but unaffected by the inactivating mutations to ITIM/ITSM (WT versus EM; P=0.02, ΔITSM versus EM; P=0.005, WT versus ΔGrb2; P=0.02, ITSM versusΔ Grb2; P=0.01, EM versus Grb2; P=0.79, WT versus ΔITSM; P=0.32) (**Figure 4.6B**). Our data show that BTLA signaling augments the TCR-driven IL-2 production and highlight that Grb2 signaling on BTLA significantly contributes to the IL-2 production following BTLA ligation during T cell activation.

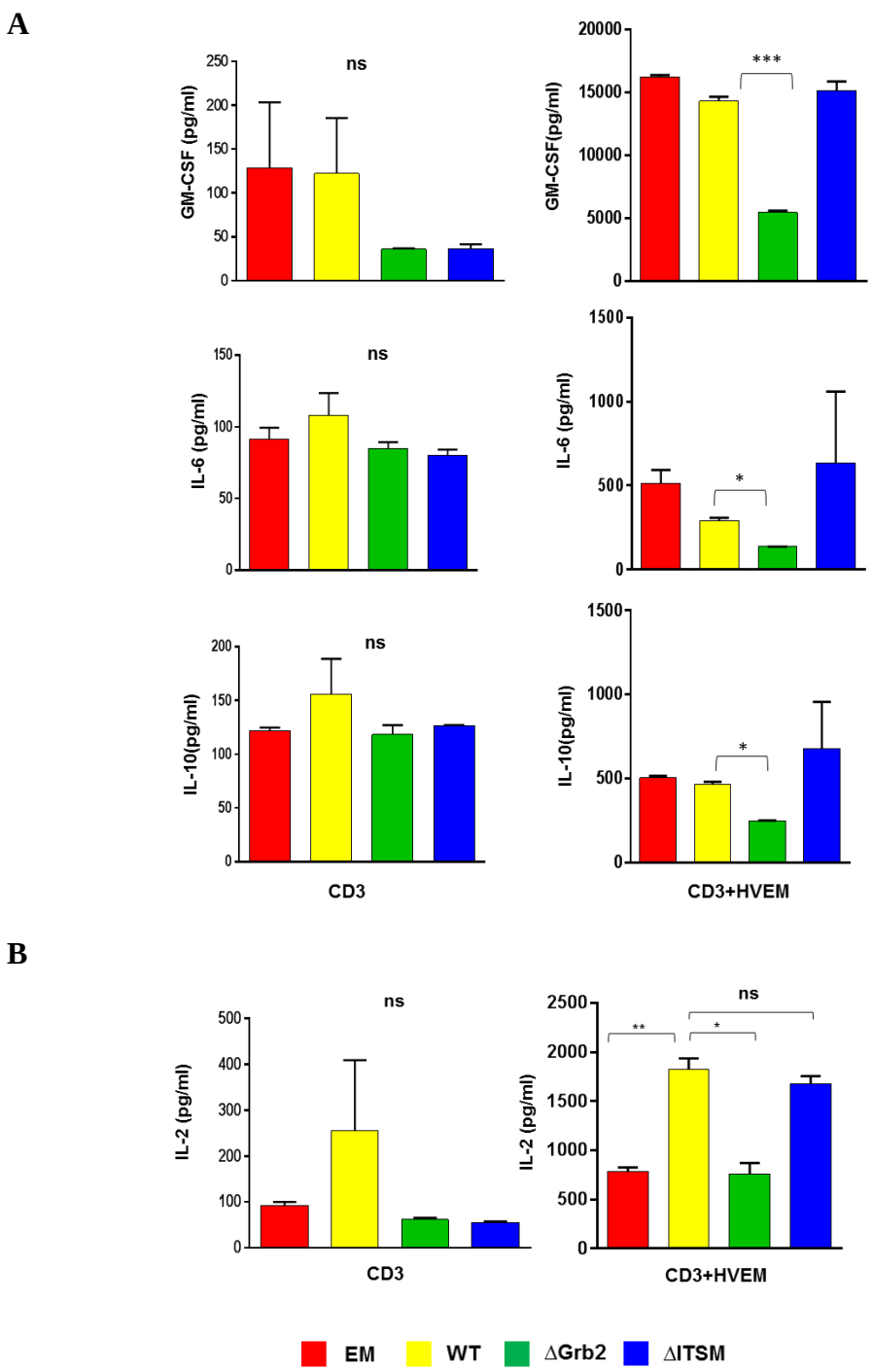

Figure 4.6. Grb2 motif of BTLA augment IL-2 production upon HVEM ligation. Virally transduced OT-1 BTLA KO T cells were stimulated with plate-bound anti-mouse CD3 and HVEM Fc. Supernatants were assessed for cytokine production including (**A**) GM-CSF, IL-6, IL-10, and (**B**) IL-2 using by MILLIPEX MAP Mouse

$CD8^+$ T Cell Magnetic Bead Panel Assays. Each bar graph represents two independent experiments. $*P < 0.05$, $**P < 0.001$. All error bars depicts the mean ± s.e.m. All *P*-value were calculated using a two-tailed Student's *t*-test.

Discussion

It is known that ITIM and ITSM signaling motifs are required for BTLA to inhibit T cell function through the recruiting of phosphatases, SHP-1 and -2. Evidence suggests that Grb2 motif of BTLA might transduce positive signal as an *in vitro* binding assay demonstrated an interaction between Grb2 and p85 subunit of PI3K, suggesting it may happen in physiological conditions. Thus far, it remains inconclusive whether Grb2 motif could play a positive role on T cell function.

Our current study demonstrated that BTLA signaling has no effect on tumor killing capacity even though subtle decreased in TNF-α and IFN-γ was found in BTLA WT. In line with these observations, a recent report showing that BTLA blockade did not improve T cell mediated tumor killing (215). This suggests that BTLA signaling motif might not be directly involved in killing capacity.

We have shown that inactivated ITIM and ITSM motif ameliorated T cell proliferation while malfunction of Grb2 decreased T cell proliferation. Interestingly, we did not observe a significant impact of T cell proliferation when overexpressing BTLA WT. Previous reports demonstrated that $CD8^+$ T cells were less susceptible to BTLA-mediated T cell inhibition as compared to $CD4^+$ T cells in both mouse and human contexts. This may explain our observation of the subtle inhibitory effect of T cell proliferation when overexpressing BTLA WT.

Intriguingly, our result first unveil the importance of Grb2 motif of BTLA in $CD8^+$ T cells. We found that the Grb2 motif of BTLA mediates IL-2 secretion and might not or minimally be affected by SHP1/2-mediated signaling attenuation. Previous report have shown that Grb2-linked SLP-76 and Vav interaction is involved in IL-2 production (218). Of note, Grb2 recruitment was found to be critical for CD28

in mediating IL-2 production. Our work thus demonstrates that BTLA shares features of a co-stimulatory molecule (CD28) as well as inhibitory properties of checkpoint regulators such as PD-1 through its ITIM/ITSM motifs.

CHAPTER 5

Dissecting BTLA signaling pathway in murine T lymphocytes and human tumor infiltrating lymphocytes (TIL)

5.1 Rationale and Hypothesis

Very little is known about the downstream signaling pathways triggered by BTLA. From its structure it is anticipated that ITIM and ITSM motifs will recruit SHP1 and 2 and that Grb2 binding motif will recruit Grb2, but beyond that much is to be learned. Several studies demonstrated that ligation of BTLA and HVEM suppressed T cell proliferation as well as cytokine production such as IL-6, IL-18, and IFN-γ (193, 219). The downstream signaling protein targets of SHP1 and SHP2 of BTLA are not well characterized, but it is suggested that protein involved in proximal TCR activation might be attenuated by BTLA. A recent report has demonstrated that ITIM and ITSM in PD-1 inhibited cytoplasmic proteins of the cell cycle, Cdk-activating phosphatase Cdc25A, PI3K-Akt and Ras-MEK-ERK signaling axis, leading to T cell proliferation inhibition (56). Unlike PD-1, BTLA also harbors Growth factor receptor bound protein 2 (Grb2) motif, commonly shared in co-stimulatory molecules like CD28 with commonly shared YXN sequence. An *in vitro* binding assay using synthetic peptide suggested that Grb2 motif of BTLA could interact with the p85 subunit of PI3K (192, 220). It is known that Grb2 motif of CD28 can activate PI3K-AKT signaling pathway and result in increased cell proliferation and IL-2 production (218, 221). However, it cannot be directly extrapolated that Grb2 motif of BTLA would function similar to that of CD28 as an *in vitro* biochemical assay binding does not reflect physiological binding of cellular protein during BTLA-HVEM interaction. Our previous chapter has demonstrated that mouse BTLA signaling pathway did not affect tumor killing capacity of T cells, but subtly inhibits TNF-α cytokine and IFN-γ production. In addition, an increased proliferation of T cells was observed when ITIM and ITSM motifs were

disrupted, while inactivated Grb2 motifs attenuated T cell proliferation. We observed that IL-2 production was enhanced in WT BTLA as well as with an intact Grb2 motif in the ITIM/ITSM mutant but totally abrogated when a non-functional Grb2 motif was introduced, indicating that Grb2 motif of BTLA could play a role in IL-2 production and cell proliferation. Because we have witnessed that Grb2 motif of BTLA exhibited positive function, we sought to gain a better understanding of the underlying mechanism that might be responsible for its favorable functions. **We hypothesized that the Grb2 motif could exhibit positive signal(s) that are not targeted by ITIM and ITSM during HVEM ligation**. In this study, we further elucidated the downstream signaling pathway of BTLA in BTLA-KO-OT.1 mouse T cells overexpressing WT BTLA and BTLA mutants during TCR activation and HVEM ligation. We used RPPA (Reverse Phase Protein Array) as a high-through put method to determine differential changes in protein production as well as protein phosphorylation. To exclude the bias of the overexpression of WT BTLA and genetically modified BTLA in BTLA knockout mouse, we also investigated the downstream signaling pathway of BTLA in non-modified human TIL.

5.2 Results

Dissecting downstream signaling pathway of mouse BTLA upon HVEM ligation.

We have previously demonstrated the positive effect of Grb2 motif on T cell proliferation and IL-2 production. These findings prompted us to further dissect signaling pathway of BTLA in each signaling motif. We overexpressed WT BTLA and BTLA mutant for either Grb2 or ITIM and ITSM in BTLA-KO-OT.1 murine T cells. Empty vector (EM) was used as a control to determine the basal level of CD3 activation alone. Murine T cells were re-stimulated with plate-bound anti-CD3 with or without the presence of HVEM-Fusion protein. The cell lysates were harvested for protein extraction at 12 hours following re-stimulation. We performed Reverse Phase Protein Array (RPPA), a high-throughput method developed for functional proteomic studies, to evaluate protein changes in both quantity and phosphorylation status upon TCR activation either with or without HVEM ligation.

When we compared the differential protein changes in ΔITSM versus WT BTLA and ΔGrb2 versus WT BTLA, we found that a higher number of the surveyed proteins were significantly changed in ΔITSM as opposed to ΔGrb2. (**Figure 5.1A**) (16 versus 2; $P<0.05$). This analysis was complicated by the fact that each mutant construct bears a mutated (inactivated) motif as well as a functional motif e.g. ΔGrb2 represents the overexpression of an inactive Grb2 motif along with an active ITIM/ITSM motif while ΔITSM construct overexpresses an inactive form of ITIM and ITSM paired with a WT Grb2 motif. We found that the phosphorylation of Akt and a known substrate of AKT, pPRAS40, were significantly attenuated in ΔGrb2 (pAkt S473; P=0.045, pRAS40 T246; P=0.007) (**Figure 5.1B**). This suggests that the Akt pathway was targeted by the

SHP1/2 recruited by the active ITIM/ITSM motif of ΔGrb2 as the net result was a dephosphorylation of these targets, not likely to be influenced by the effect of the Grb2 motif. In contrast, a remarkable enhancement of the phosphorylation levels of multiple targets such as of pSrc at S527, Chk1 at S286, Chk2 at T68, GSK-3b at S9, and of Beta-Catenin at T41 and S45 were observed in ΔITSM (pSrc at S527; *P*=0.005, pA-Raf at S299; *P*=0.01, and pC-Raf at S338; *P*=0.02, pChk1 at S286; P=0.01, pChk2 at T68; P=0.02, GSK-3b at S9; P=0.04, Beta-Catenin at T41 and S45; P=0.04) (**Figure 5.1C**). An increased number of phosphorylated proteins in ΔITIM and ITSM is likely to mainly be due to the defect in recruitment of SHP1 and SHP2 into BTLA cytoplasmic domain caused by the disruption of ITIM and ITSM motifs rather than to the presence of the functional Grb2 motif. To further elucidate whether increased phosphorylation levels of specific targets are due solely to the presence of the Grb2 motif rather than to the deficient ITIM and ITSM motifs, we then compared differential protein changes in ΔITSM (which bears an intact Grb2 motif) versus EM (No BTLA) to isolate the effect of Grb2 on the TCR stimulation alone. We found that only pSrc at S527 and JNK2 were remarkably higher in ΔITSM (**Figure5.1D**). This indicated that those two downstream signaling molecules may be activated through the Grb2 motif and may not be targeted by SHP1 and SHP2. The list of differential protein changes with the following comparisons; ΔGrb2 versus WT, ΔITSM versus WT, and ΔITSM versus EM is demonstrated in **Table 1.**

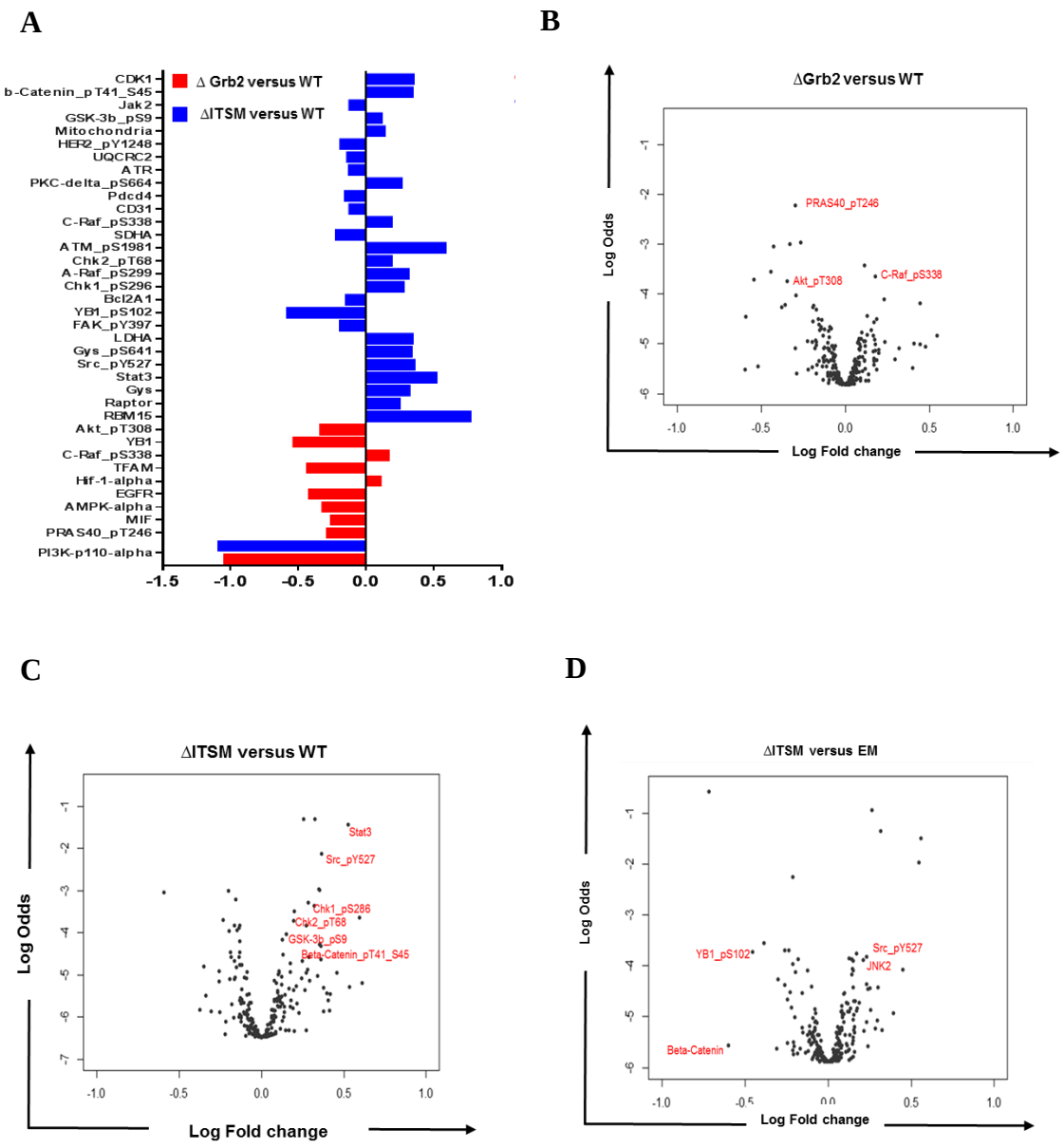

Figure 5.1. Dissecting downstream signaling pathway of mouse BTLA upon HVEM ligation.

OT-1 BTLA KO T cells overexpressing WT BTLA or its variants were re-stimulated with plate-bound anti-CD3 and HVEM-Fc for 8 h prior to harvest. Cells were lysed and the protein supernatant was collected to perform RPPA. (**A)** Bar graph depicts the differential protein expressions with the following comparisons: ΔGrb2 versus WT

(red) and ΔITSM versus WT (blue). Volcano plots depicts fold changes of proteins with the following comparisons: ΔITSM versus EM (**B**) ΔGrb2 versus WT (**C**), and ΔITSM versus WT (**D**). Data shown represent two independent experiments. $P < 0.05$. *P*-value were calculated using Linear models and empirical Bayes methods.

Table 1. Differentially expressed proteins in OT-1 mouse T cells overexpressing either WT BTLA or BTLA mutant re-stimulated with CD3 and HVEM Fc fusion protein at 8 h.

Table demonstrates the list of differential protein changes with the following comparisons; ΔGrb2 versus WT, ΔITSM versus WT, ΔITSM versus EM. Data shown represent two independent experiments. $P < 0.05$. *P*-value were calculated using Linear models and empirical Bayes methods.

Table 1. Differentially expressed proteins in OT-1 mouse T cells overexpressing either WT BTLA or BTLA mutant re-stimulated with CD3 and HVEM Fc fusion protein at 8 h.

	Log fold change	P-value
ΔGrb2 versus WT		
PI3K-p110-alpha-R-C_GBL1115582	-1.0537676	5.836064e-05
PRAS40_pT246-R-V_GBL1115574	-0.2976067	7.643870e-03
MIF-R-C_GBL1116364	-0.2667402	1.815897e-02
AMPK-alpha-R-C_GBL1115509	-0.3295237	1.889904e-02
EGFR-R-V_GBL1115620	-0.4283460	1.969070e-02
Hif-1-alpha-M-C_GBL1116504	0.1131972	3.083201e-02
TFAM-R-V_GBL1116333	-0.4439703	3.552049e-02
C-Raf_pS338-R-V_GBL1115523	0.1775591	4.003768e-02
YB1-R-V_GBL1115569	-0.5434096	4.322444e-02
Akt_pT308-R-V_GBL1116492	-0.3454098	4.509359e-02
ΔITSM versus WT		
PI3K-p110-alpha-R-C_GBL1115582	-1.09610694	4.178212e-05
RBM15-R-V_GBL1115629	0.77592249	3.194537e-04
Raptor-R-V_GBL1115625	0.25530383	2.185063e-03
Gys-R-V_GBL1116482	0.32602047	2.216354e-03
Stat3-R-C_GBL1116311	0.52531068	2.539887e-03
Src_pY527-R-V_GBL1115563	0.36285815	5.045994e-03
Gys_pS641-R-V_GBL1115603	0.34757270	1.207815e-02
LDHA-R-C_GBL1115596	0.35131897	1.222602e-02
FAK_pY397-R-V_GBL1116461	-0.20031315	1.257107e-02
YB1_pS102-R-V_GBL1115584	-0.59051723	1.298821e-02
Bcl2A1-R-V_GBL1116330	-0.15537524	1.530438e-02
Chk1_pS296-R-V_GBL1116335	0.28491931	1.675901e-02
A-Raf_pS299-R-C_GBL1115605	0.32200036	1.787957e-02
Chk2_pT68-R-C_GBL1115522	0.19753223	2.076754e-02
ATM_pS1981-R-V_GBL1116464	0.59568985	2.429322e-02
SDHA-R-V_GBL1116334	-0.23145741	2.537912e-02
C-Raf_pS338-R-V_GBL1115523	0.19658953	2.590506e-02
CD31-M-V_GBL1116506	-0.13128423	2.918579e-02
Pdcd4-R-C_GBL1115583	-0.16554607	2.927126e-02
PKC-delta_pS664-R-V_GBL1115593	0.27087240	2.956589e-02
ATR-R-C_GBL1115590	-0.13505418	3.098111e-02
UQCRC2-M-C_GBL1116412	-0.14721028	3.312001e-02
HER2_pY1248-R-C_GBL1115612	-0.19768054	3.388986e-02
Mitochondria-M-V_GBL1116387	0.14868332	3.679310e-02

Table 1 (continued). Differentially expressed proteins in OT-1 mouse T cells overexpressing either WT BTLA or BTLA mutant re-stimulated with CD3 and HVEM Fc fusion protein at 8 h.

ΔITSM versus WT	**Log fold change**	**P-value**
GSK-3b_pS9-R-V_GBL1115615	0.12487282	4.193362e-02
Jak2-R-V_GBL1116307	-0.13055136	4.349372e-02
b-Catenin_pT41_S45-R-V_GBL1116494	0.35325496	4.731829e-02
CDK1-R-V_GBL1115598	0.36169900	4.952413e-02
ΔITSM versus EM		
PI3K-p110-alpha-R-C_GBL1115582	-0.7194512	0.001134154
Raptor-R-V_GBL1115625	0.2645821	0.001720536
Gys-R-V_GBL1116482	0.3146227	0.002795612
RBM15-R-V_GBL1115629	0.5571886	0.003298385
b-Catenin_pT41_S45-R-V_GBL1116494	0.5471095	0.005618371
Notch3-R-C_GBL1116354	-0.2137534	0.007785951
Vimentin-M-C_GBL1116421	-0.3850135	0.034672688
Stat5a-R-V_GBL1115565	-0.2380353	0.040673318
MMP2-R-V_GBL1115540	-0.2629724	0.040863077
YB1_pS102-R-V_GBL1115584	-0.4568981	0.042068010
ACC_pS79-R-V_GBL1115507	0.1714040	0.043934614
Src_pY527-R-V_GBL1115563	0.2308867	0.046698220
PLK1-R-C_GBL1115575	0.1276333	0.049231222
GCN5L2-R-V_GBL1116463	-0.1807406	0.049610757
JNK2-R-C_GBL1116442	0.1424863	0.049987949

BTLA-HVEM axis in human TIL selectively suppresses MAPK, Akt, and NF-kB pathways, but enhances Src pathway.

Thus far, our data uncovered the positive role of the Grb2 motif of BTLA in mouse T cells in contributing to T cell proliferation and IL-2 production. In addition, RRPA analysis in mouse suggested that Grb2 motif signals through Src at pY527 as a significantly increased level of this phosphorylated protein was present in ΔITSM when compared with both WT and EM. On the other hand, we found that Akt at pT308 and PRAS40, proteins in Akt signaling pathway, were suppressed when Grb2 was mutated as compared to WT BTLA. This suggested that ITIM and ITSM motifs do not suppress all downstream signaling pathways. It has been shown that mouse BTLA signaling motifs are highly conserved with human BTLA. Overexpressing WT BTLA and BTLA mutants allowed us to dissect BTLA signaling at each BTLA motifs. However, downstream signaling pathway of genetically modified BTLA in BTLA might not be physiologically relevant to human T cell signaling pathway. To exclude the bias of BTLA KO mouse T cells, we further investigated BTLA signaling pathway in human BTLA TIL, which is more clinically relevant to our observation in favorable clinical outcome of TIL treated patients with high proportion of $CD8^+BTLA^+$ TIL subset.

In this study, we sorted the $CD8^+BTLA^+$ human TIL subset from five cultured human TIL lines (pre-REP) isolated from melanoma patients treated at M.D. Anderson Cancer. Because TIL from different patients might be variable in their susceptibility to TCR activation, and because the strength of TCR activation could lead to different signaling outcome, we then stimulated with increasing concentration of plate-bound anti-human CD3 at concentrations of 10, 30, 100, 300, and 1000 ng alone or in the presence of

HVEM-Fc, to look at TCR activation with or without BTLA engagement. After activation for two hours, proteins were extracted from the cell lysates, and used to perform RPPA to determine the differential proteins expression in both quantity and phosphorylation status upon T cell activation.

We observed a general decrease in phosphorylation levels of proteins phosphorylated in response to TCR engagement in the presence of HVEM-Fc. We found that the MAPK kinase pathway (pP38 at T180; P=2.08 x 10^{-9}, pP90RSK at T573; P=3.26 x 10^{-4}, pS6 at S235; P= 1.68x10^{-2}), NF-Kb pathway (pNF-Kb p65 at S536; P=3.15 x 10^{-2}), the mTOR pathway (pP70-6K at T389; P=1.7 x 10^{-4}), the Akt pathway (pAKT at S473; P=9.6x10^{-3}), the JNK pathway (pC-Jun at S73; P= 9.38x10^{-3}), and the Beta-catenin pathway (GSK-3a-b pS21; P=9.6x10^{-3}) were significantly decreased in HVEM in comparison to CD3 activation alone. (**Figure 5.2A**). Inhibition of these positive signaling pathways clearly supported the role of BTLA as a co-inhibitory molecule. Consistent with downstream targets of PD-1, we also found that AKT and MAPK pathways were attenuated in BTLA. However activation of specific signaling pathways were also observed when T cell activation happened in the presence of HVEM. Interestingly, we found that the Src signaling pathway was activated due to an increase in pSrc at S416 during HVEM ligation (pSrc at S416; P= 3.36 x 10^{-6}) (**Figure 5.2A**). Our results suggest that the TCR signaling pathway is not completely suppressed by BTLA, but is specifically attenuated in certain pathways as indicated above and specifically potentiated in very select pathways. Unexpectedly, we found that phosphorylation of HER2 at tyrosine 1248 was prominently increased in an anti-CD3 dose-dependent manner regardless of the presence of HVEM (**Figure 5.2B and C**).

This strengthens the notion that not all proteins are affected by the BTLA and HVEM signaling axis. To further comprehensively understand the downstream signaling pathway of human BTLA, we mapped a signaling network with Ingenuity pathway analysis (IPA) utilizing the proteins that were differentially expressed during HVEM ligation **(Figure 5.2D)**. We observed that Src signaling node was exclusively separated from Akt, mTOR, and NF-kB pathway nodes (**Figure 5.2E)**. This likely suggests that some downstream signals from the Grb2 motif and TCR activation are likely not interfered by SHP1/2. The list of differential protein changes in with the following comparisons; CD3+HVEM versus CD3 alone (Dose 100), CD3+HVEM versus CD3 alone (Dose300), CD3+HVEM versus CD3 alone (Dose1000), CD3 alone (Dose 0 versus 30), CD3 alone (Dose 0 versus 100), CD3 alone (Dose 0 versus 300), CD3 alone (Dose 0 versus 1000), CD3+HVEM (Dose 0 versus 30), CD3+HVEM (Dose 0 versus 100) CD3+HVEM (Dose 0 versus 300) CD3+HVEM (Dose 0 versus 1000) is demonstrated in the **Table 2 A, B, and C.**

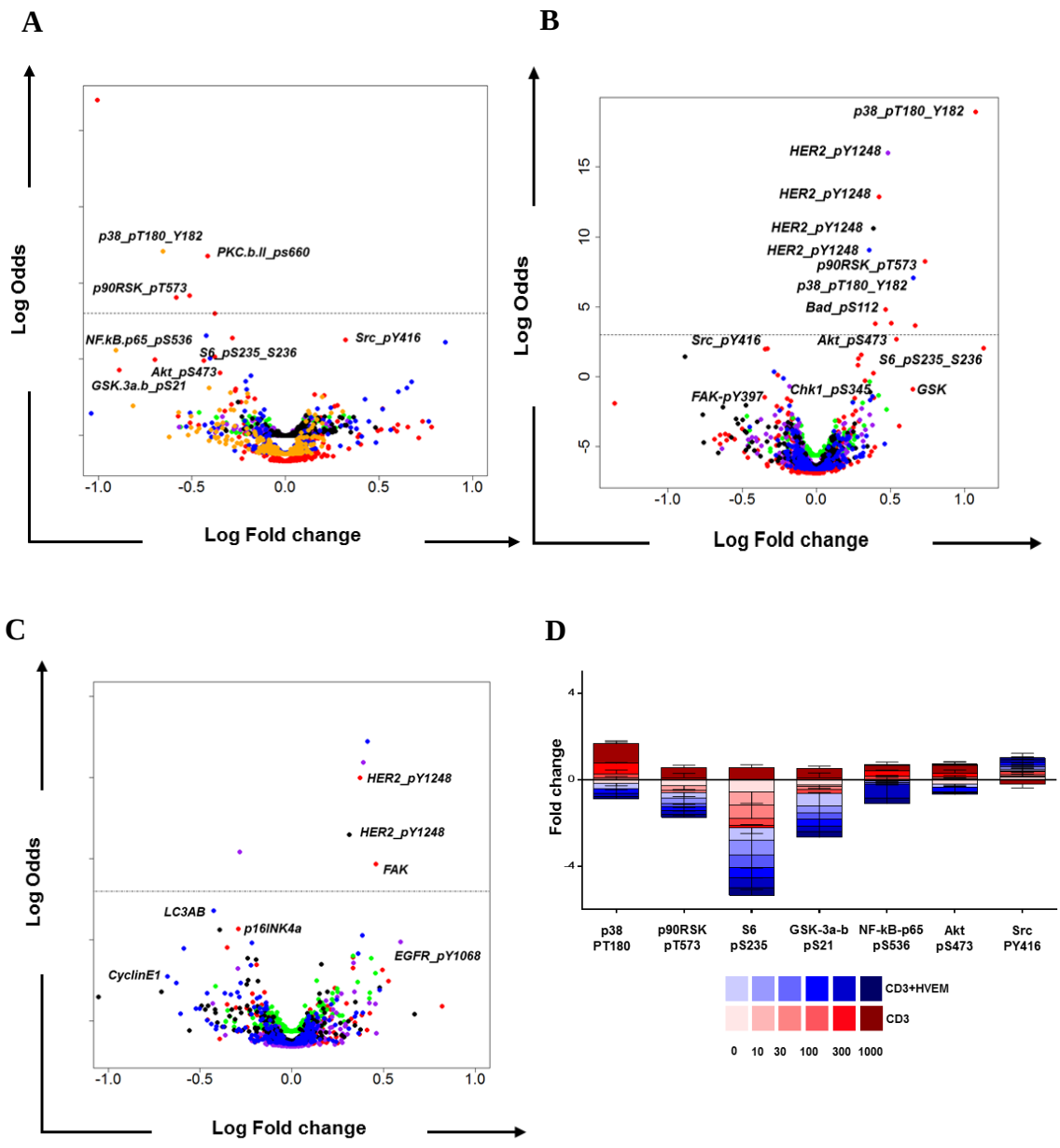
A
B
C
D
E
Log Odds
Log Fold change
p38_pT180_Y182
PKC.b.II_ps660
p90RSK_pT573
NF.kB.p65_pS536
S6_pS235_S236
Src_pY416
Akt_pS473
GSK.3a.b_pS21
HER2_pY1248
Bad_pS112
FAK-pY397
Chk1_pS345
GSK
FAK
LC3AB
p16INK4a
EGFR_pY1068
CyclinE1
Fold change
p38 PT180
p90RSK pT573
S6 pS235
GSK-3a-b pS21
NF-kB-p65 pS536
Akt pS473
Src PY416
CD3+HVEM
CD3
0 10 30 100 300 1000
RELA
Gsk3
PRKCB
AKT1
SRC (family)
RPS6KA1
p70 S6k
RPS6
Legend
Group/Complex
Kinase
Transcription Regulator
Other
Direct interaction
Indirect interaction
Acts on
Inhibits on
Acts/Inhibits on

Figure 5.2. BTLA-HVEM axis in human TIL selectively suppresses Akt, and NF-kB pathways, but enhances Src pathway.

Sorted $CD8^+BTLA^+$ TIL were stimulated with plate-bound anti-CD3 at following concentrations (0, 10, 30, 100, 300, and 1000 ng/ml) alone or with HVEM-Fc for 8 h prior to harvest. Cells were lysed and the protein supernatant was collected to perform RPPA. Volcano plot depicts fold changes of proteins in $CD8^+BTLA^+$TIL upon T cell activation with (**A**) anti-CD3 alone, (**B**) anti-CD3 + HVEM, and (**C**) anti-CD3 in comparison with anti-CD3 + HVEM. (**D**) Bar graph demonstrates proteins that significantly change in comparison between anti-CD3 activation alone (red) and anti-CD3 + HVEM ligation (blue). (**E**) Signaling network from the proteins that significantly change in (**D**) were clustered by Ingenuity Pathway Analysis. N=5, $P < 0.05$. *P*-value were calculated using Linear models and empirical Bayes methods.

Table 2. Differentially expressed proteins in $CD8^{+}BTLA^{+}$TIL re-stimulated with either CD3 or CD3 and HVEM at concentration of 0, 30, 100, 300, and 100 at 8 h

Table demonstrates the list of differential protein changes in with the following comparisons; CD3+HVEM versus CD3 alone (Dose100), CD3+HVEM versus CD3 alone (Dose300), CD3+HVEM versus CD3 alone (Dose1000), CD3 alone (Dose 0 versus 30), CD3 alone (Dose 0 versus 100), CD3 alone (Dose 0 versus 300), CD3 alone (Dose 0 versus 1000), CD3+HVEM (Dose 0 versus 30), CD3+HVEM (Dose 0 versus 100) CD3+HVEM (Dose 0 versus 300) CD3+HVEM (Dose 0 versus 1000). Data shown represent five TIL lines. N=5, P <0.05. P-value were calculated using Linear models and empirical Bayes methods.

Table 2A. Differentially expressed proteins in $CD8^+BTLA^+$TIL re-stimulated with either CD3 or CD3 and HVEM at concentration of 0, 30, 100, 300, and 100 at 8 h

	Log fold change	P-value
CD3+HVEM versus CD3 alone (Dose100)		
GPBB.R.V_GBL1122116	0.8555653	0.01800838
p38_pT180_Y182.R.V_GBL1121998	-0.4030583	0.03829165
CD3+HVEM versus CD3 alone (Dose300)		
p38_pT180_Y182.R.V_GBL1121998	-0.6544899	5.908173e-05
NF.kB.p65_pS536.R.C_GBL1121996	-0.9045702	3.154015e-02
CD3+HVEM versus CD3 alone (Dose1000)		
p38_pT180_Y182.R.V_GBL1121998	-1.0040382	2.089641e-09
PKC.b.II_pS660.R.V_GBL1122088	-0.4154961	3.921504e-05
YB1_pS102.R.V_GBL1122037	-0.5119427	3.268774e-04
p90RSK_pT573.R.C_GBL1122101	-0.5823908	3.268774e-04
Bad_pS112.R.V_GBL1121957	-0.3764103	7.738640e-04
Hif.1.alpha.M.C_GBL1122215	-0.2835044	3.368133e-03
Src_pY416.R.V_GBL1122013	0.3219323	3.368133e-03
c.Jun_pS73.R.V_GBL1122272	-0.3778729	9.382127e-03
GSK.3a.b_pS21_S9.R.V_GBL1122282	-0.6958194	9.619107e-03
Akt_pS473.R.V_GBL1122267	-0.4338686	9.619107e-03
S6_pS235_S236.R.V_GBL1122011	-0.8881963	1.685525e-02
CD3 alone (Dose 0 versus 30)		
HER2_pY1248.R.C_GBL1122070	0.4855243	4.248393e-09
CD3 alone (Dose 0 versus 100)		
HER2_pY1248.R.C_GBL1122070	0.3855653	1.438851e-06
GPBB.R.V_GBL1122116	-0.8828316	1.188161e-02
CD3 alone (Dose 0 versus 300)		
HER2_pY1248.R.C_GBL1122070	0.3577353	7.798521e-06
p38_pT180_Y182.R.V_GBL1121998	0.6541823	2.982066e-05
p16INK4a.R.V_GBL1122112	-0.2825169	2.159478e-02
HES1.R.V_GBL1122148	-0.2216701	2.631820e-02

Table 2B. Differentially expressed proteins in $CD8^{+}BTLA^{+}$TIL re-stimulated with either CD3 or CD3 and HVEM at concentration of 0, 30, 100, 300, and 100 at 8 h

	Log fold change	P-value
CD3 alone (Dose 0 versus 1000)		
p38_pT180_Y182.R.V_GBL1121998	1.0757191	3.002318e-10
HER2_pY1248.R.C_GBL1122070	0.4240169	7.277417e-08
p90RSK_pT573.R.C_GBL1122101	0.7340010	5.278553e-06
FAK.R.C_GBL1121979	0.4678432	1.294449e-04
YB1_pS102.R.V_GBL1122037	0.5055596	2.426017e-04
Bad_pS112.R.V_GBL1121957	0.3991817	2.426017e-04
HER2.M.V_GBL1122226	0.6678777	2.426017e-04
Akt_pS473.R.V_GBL1122267	0.5425173	5.814298e-04
S6_pS235_S236.R.V_GBL1122011	1.1279666	8.810221e-04
p16INK4a.R.V_GBL1122112	-0.3265606	8.810221e-04
Src_pY416.R.V_GBL1122013	-0.3429326	8.810221e-04
PKC.b.II_pS660.R.V_GBL1122088	0.3052046	1.206663e-03
Hif.1.alpha.M.C_GBL1122215	0.2850831	1.464922e-03
MEK1_pS217_S221.R.V_GBL1122071	0.2810258	2.243427e-03
c.Jun_pS73.R.V_GBL1122272	0.3869022	3.748423e-03
Bid.R.C_GBL1122269	-0.2585016	4.012587e-03
Pdcd4.R.C_GBL1122036	0.3287594	5.809354e-03
GSK.3a.b_pS21_S9.R.V_GBL1122282	0.6531518	1.033092e-02
FAK_pY397.R.V_GBL1122111	-0.3464483	1.706239e-02
Annexin.VII.M.V_GBL1122204	0.3889564	1.706239e-02
p70.S6K_pT389.R.V_GBL1122001	0.2603769	1.706239e-02
MEK1.R.V_GBL1122290	-0.1943432	1.706239e-02
Cox2.R.C_GBL1122107	-0.1705135	2.006613e-02
Myosin.IIa_pS1943.R.V_GBL1122096	-1.3589428	2.242156e-02
Myosin.11.R.V_GBL1122090	-0.2640302	2.659773e-02
MCT4.R.V_GBL1122301	-0.2318147	3.155032e-02
Chk1_pS345.R.C_GBL1122046	0.2649744	3.529039e-02
HER3.R.V_GBL1122170	-0.1859548	3.995997e-02
MEK2.R.V_GBL1122113	-0.1887894	4.325005e-02
Rictor_pT1135.R.V_GBL1122087	0.2460314	4.366397e-02
MIG6.M.V_GBL1122201	-0.1615994	4.856163e-02
CD31.M.V_GBL1122218	0.1874872	4.856163e-02

Table 2C. Differentially expressed proteins in $CD8^+BTLA^+$TIL re-stimulated with either CD3 or CD3 and HVEM at concentration of 0, 30, 100, 300, and 100 at 8 h

	Log fold change	P-value
CD3+HVEM (Dose 0 versus 30)		
HER2_pY1248.R.C_GBL1122070	0.3899450	1.105288e-06
Rab11.R.E_GBL1122074	-0.2834234	1.713254e-04
EGFR_pY1068.R.C_GBL1122278	0.5953123	3.704580e-02
CD3+HVEM (Dose 0 versus 100)		
HER2_pY1248.R.C_GBL1122070	0.3146506	0.000110571
CD3+HVEM (Dose 0 versus 300)		
HER2_pY1248.R.C_GBL1122070	0.4133938	2.725237e-07
LC3A.B.R.C_GBL1122300	-0.4248823	7.798027e-03
Dvl3.R.V_GBL1122051	0.3864097	2.657925e-02
HES1.R.V_GBL1122148	-0.2175110	3.269281e-02
Cyclin.E1.M.V_GBL1122219	-0.5887974	3.810823e-02
E.Cadherin.R.V_GBL1122077	0.3640928	4.438662e-02
CD3+HVEM (Dose 0 versus 1000)		
HER2_pY1248.R.C_GBL1122070	0.3735338	2.979160e-06
FAK.R.C_GBL1121979	0.4586727	3.676352e-04
p16INK4a.R.V_GBL1122112	-0.2893436	1.604959e-02
LC3A.B.R.C_GBL1122300	-0.3517036	4.125150e-02

Discussion

BTLA is a unique co-stimulatory molecule that contains both positive (Grb2) and negative (ITIM and ITSM) signaling motifs. Although a previous study demonstrated that Grb2 displayed potential interaction with Grb2 and p85 subunit of PI3K, downstream signaling pathway of BTLA remains under investigation.

Because we have shown that Grb2 motif enhanced IL-2 production and T cell proliferation, we then sought to gain in depth in downstream signaling pathway in both human and mouse $CD8^{+}$T cells. When we compared differential protein expression of BTLA mutants (ΔGrb2 and ΔITIM and ITSM) using WT as a reference, we observed that Akt signaling was remarkably suppressed when Grb2 was mutated. This suggests that the intact effect of ITIM and ITSM specifically targets Akt pathway. In previous study, it has been suggested that PD-1, which also consists of ITIM and ITSM motifs, inhibited Akt and MAPK signaling pathways during TCR activation (56). This suggests that an inhibitory effect of BTLA similarly shares downstream targets with PD-1. However, we found that Src phosphorylation was enhanced when ITIM and ITSM malfunction. Because Src might be enhanced due to either unleashed TCR activation through disrupted negative regulation or through Grb2 activation, ΔITIM and ITSM differential protein expression was then also compared with both WT and EM to distinguish these two effects. We found that Src phosphorylation remains consistently present when using WT and EM as a reference, suggesting that Grb2 could activate Src signaling pathway. In fact, a recent report has provided a direct interaction between Grb2 and Src in NIH3T3 cells upon stimulated with Fibronectin. Additionally, it has

been shown that overexpression of Grb2 augments phosphorylation of Src at 416, but the opposite result was obtained when Grb2 expression was disrupted (222).

Consistently, we found that Src enhancement was also observed in human $CD8^+BTLA^+$ TIL activated with anti-CD3 and HVEM. In fact, we also observed an attenuation of MAPK, NF-κB, and Akt signaling pathways in $CD8^+BTLA^+$ TIL during engagement with anti-CD3 and HVEM as compared to anti-CD3 alone. This data suggests that BTLA signaling pathways in both human and mouse share common downstream targets.

CHAPTER 6

Investigating the functional role of BTLA signaling pathway in *in vivo* tumor control

6.1 Rationale and Hypothesis

We have uncovered that $CD8^+BTLA^+$TIL subset exhibited superior tumor control in tumor bearing NSG mouse when compared with $CD8^+BTLA^-$TIL subset, but no difference in tumor killing capacity was observed in *in vitro* setting. It remains unclear whether persistence of $CD8^+BTLA^+$TIL results from either the intrinsic function of less differentiated phenotype or BTLA signaling itself.

We observed that BTLA signaling pathway did not contribute in tumor killing capacity regardless of the changes introduced in BTLA signaling motifs. However, the effector cytokine production such as IFN-γ and TNF-α were attenuated when Grb2 motif was attenuated. Intriguingly, we found an increased IL-2 production and T cell proliferation when ITIM and ITSM were defective, suggesting the positive function of the Grb2 motif.

Consistently, we observed an attenuation of the Akt pathway with enhanced Src phosphorylation in $CD8^+$ activated with anti-CD3 and HVEM in both human and mouse setting, suggesting that BTLA provides dual signals both positive and negative. **We hypothesize that positive signal transduced by Grb2 motif could improve TIL function and lead to better tumor control.**

To determine to the functional role of the Grb2 and ITIM/ITSM motifs of BTLA in human $CD8^+$TIL, we used the NSG mouse model for adoptive transfer to investigate the role of $CD8^+BTLA^-$TIL overexpressing WT BTLA, BTLA with mutation of Grb2 or ITIM and ITSM during a study of *in vivo* tumor challenge.

6.2 Results

Generation of retroviral vectors containing wild type human BTLA and human BTLA mutants for functional study using NSG mouse model.

Because we have witnessed a dual role for BTLA as a co-stimulatory and co-inhibitory receptor in human and mouse T cells, we next sought to dissect the potential contributions of the Grb2 motif and the ITIM/ITSM motifs of BTLA in $CD8^+$ TIL mediated *in vivo* tumor control. To study the functional role of human BTLA signaling motifs, we generated WT BTLA and mutants of the human Grb2 and ITIM/ITSM motifs by substitution of tyrosine for phenylalanine using a site directed mutagenesis method and thus generated ΔGrb2 mutant (Y226F and Y243F) and ΔITIM and ITSM mutant (Y257F and Y282F) (**Figure 6.1A**). We used pRVKM retroviral vector with GFP reporter as a gene delivery system to overexpress WT BTLA and its mutants in human $CD8^+BTLA^-$TIL. Comparable expression of BTLA was observed in BTLA WT and its mutant (**Figure 6.1B**). Briefly, sorted $CD8^+BTLA^-$TIL were activated with anti-human CD3 for 2 days. The cells were transduced with either WT BTLA or BTLA mutants (ΔGrb2 or ΔITIM and ITSM). Over the next 14 days the cells were propagated using the rapid expansion protocol (RFP). Because not all cells were transduced with retroviruses, the GFP positive cells were further sorted and propagated for another 14 days prior to perform *in vitro* functional assays and adoptive TIL transfer (**Figure 6.1C**).

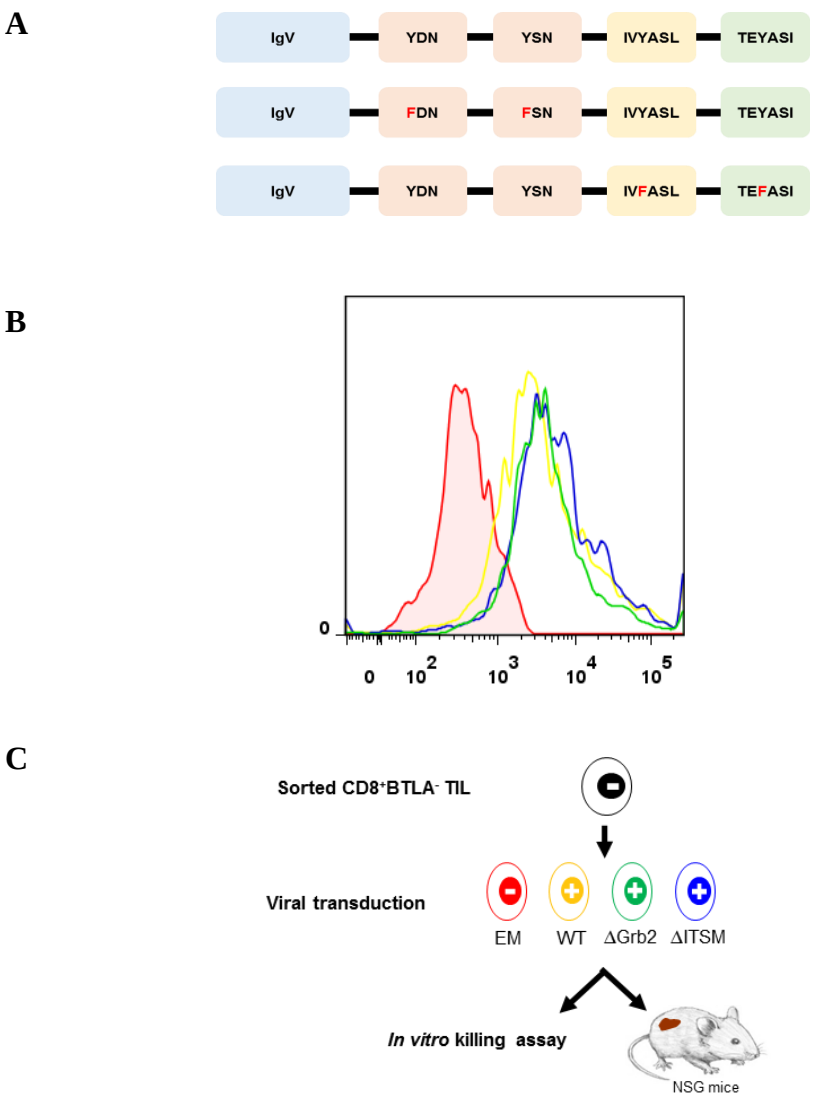

Figure 6.1. BTLA singling motifs had no effect on *in vitro* tumor killing capacity. Substitutions of tyrosine for phenylalanine were made in three different motifs of human BTLA cytoplasmic tail; ΔGrb2 mutants (Y226F and Y243F), Δ ITIM and ITSM mutants (Y243F, Y257F, and Y282F) (**A**) Schematic diagram depicts the structure of BTLA WT (Top), BTLA ΔGrb2 (middle), and BTLA ΔITSM (bottom). (**B**) (**C**) Schematic diagram depicts NSG mouse model for adoptive T cell transfer. $CD8^{+}BTLA^{-}$were virally transduced with WT BTLA or its variants, and propagated by

REP protocol for 14 days. The cells were then sorted based on GFP expression and further expanded by REP protocol for another 14 days. Ten million virally transduced TIL were intravenously injected into tumor bearing mice previously subcutaneously implanted with autologous tumor line.

BTLA signaling motifs have no effect on *in vitro* tumor killing capacity.

We previously showed the comparable *in vitro* tumor killing capacity between $CD8^+BTLA^+$TIL and $CD8^+BTLA^-$TIL; however, we observed superior *in vivo* tumor control of $CD8^+BTLA^+$TIL using the NSG mouse model. In addition, we also found that $CD8^+BTLA^+$TIL subset circulated in the peripheral blood at higher frequency as compared to $CD8^+BTLA^-$TIL subset counterpart. This finding is consistent with our clinical observation demonstrating that the $CD8^+BTLA^+$TIL subset persisted longer in the body following adoptive transfer in comparison to the $CD8^+BTLA^-$TIL subset. Using BTLA-KO mouse T cells overexpressing WT BTLA or its mutants, we also found that BTLA signaling motifs did not affect tumor killing capacity even though effector cytokine production (IFN-γ and TNF-α) were significantly decreased when Grb2 motif was mutated, in the presence of high levels of ITIM/ITSM. To further determine whether BTLA signaling motif could contribute to the *in vitro* tumor killing capacity, we co-incubated sorted $CD8^+BTLA^-$TIL (TIL#2549) overexpressing either WT BTLA or mutant BTLA with the autologous tumor. We consistently observed that the *in vitro* tumor killing capacity was comparable regardless of the presence of BTLA or its mutants (**Figure 6.2**). (1:1, BTLA-EM (23.2%) vs BTLA-WT (23.8%) BTLA-ΔGrb2 (28.0%) vs BTLA- ΔITIM and ITSM (26.5%); 1:3, BTLA-EM (8.2%) vs BTLA-WT (8.5%) vs BTLA-ΔGrb2 (14.8%) vs BTLA- ΔITIM and ITSM (10.5%); 1:10, BTLA-EM (4.5%) vs BTLA-WT (3.2%) vs BTLA-ΔGrb2 (5.6%) vs BTLA-ΔITIM and ITSM (4.7%).

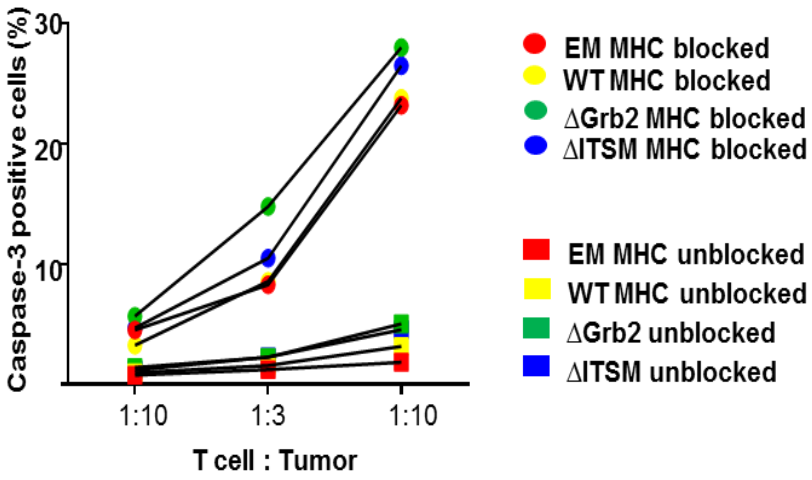

Figure 6.2. BTLA signaling motifs had no effect on *in vitro* tumor killing capacity. Autologous melanoma tumor line 2549 labeled with eFluor670® was co-cultured with TIL at the following TIL-to-tumor cell ratios (1:10, 1:3, and 1:1). Tumor cell death is evaluated by the percentage of caspase-3 positive tumor cells.

Overexpression of inactivated ITIM and ITSM motifs in TIL enhanced tumor burden control in NSG mouse model.

Because we found the comparable *in vitro* killing tumor capacity of cells regardless of WT BTLA and it BTLA mutant expression, we sought to determine whether overexpression of WT BTLA and its mutant could affect *in vivo* tumor control.

For *in vivo* tumor experiment, TIL overexpressing BTLA WT or BTLA mutants were adoptively transferred into NSG tumor-bearing mice, and tumor burden was measured every other day. We found that the transfer of TIL transduced with empty vector ($BTLA^-$) or TIL transduced with BTLA WT did not control the tumor and were not significantly different from the non-treated group (NTx). However, the transfer of TIL with a disrupted ITIM/ITSM domain (ΔITSM) resulted in greater tumor control than the empty vector or non-treated groups early on day 2 (EM vs NTx; P= 0.08, Δ ITSM vs NTx; P= 0.01, WT vs NTx; P=0.24, ΔGrb2 vs NTx; P= 0.92) (**Figure 6.3A, B, and C**). However, the group that received TIL transduced with BTLA bearing a malfunctioning Grb2 motif (ΔGrb2) exhibited significantly worst tumor control as opposed to those receiving TIL with empty vector control (EM) (EM VS WT; P=0.48, EM VS ΔGrb2; P=0.04) (**Figure 6.3A, B, and C**). We found that only $BTLA^-$ overexpressing ΔITIM and ITSM and empty vector control exhibited significantly higher frequency in the blood on day 2 following transfer, while ΔGrb2 and WT overexpressing TIL were not detected following TIL transfer.

Our result suggests that malfunction of Grb2 attenuated TIL function and impaired tumor control. We observed that MEL526 tumor cells grown in NSG mice

were explanted and stained for HVEM expression which was found to be still present (**Figure 6.4**). In addition, HVEM expression is highly abundant in 2549 tumor cells as well as other primary melanoma tumor cells (**Figure 6.5A and B**). This indicated that melanoma tumor cells potentially provided a suppressive signal through BTLA expressed by TIL in the tumor bed.

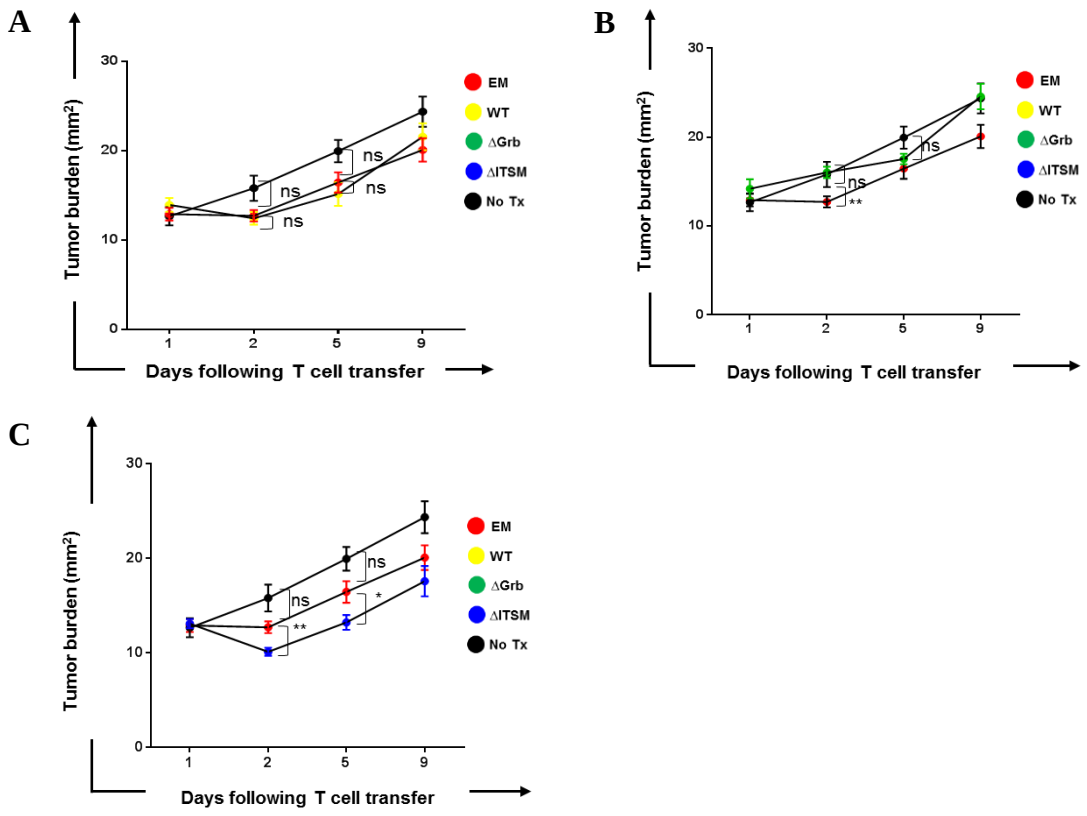

Figure 6.3. Overexpression of inactivated ITIM and ITSM motifs in TIL enhanced tumor burden control in NSG mouse model.

Ten million virally transduced TIL were intravenously injected into tumor-bearing mice previously implanted subcutaneously with autologous tumor line 2549. Tumor burden was measured using calipers and diameter graphed as mm^2. *N*= 5-8 animals per group. **P* <0.05 and ***P* <0.001. Error bars are expressed as mean ± s.e.m. *P*-values were calculated using a two-tailed Student's t-test. The graphs show tumor volumes in NSG mice adoptively transferred with TIL with following comparison; (**A**) Δ ITSM versus EM versus No Tx (**B**) Δ Grb versus EM versus No Tx (**C**) WT versus EM versus No Tx.

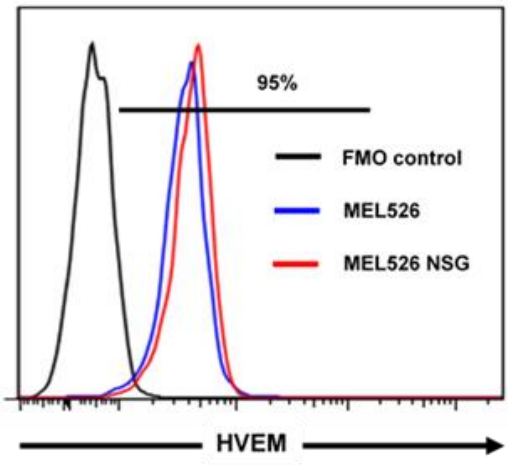

Figure 6.4. Sustained expression of HVEM following injection into NSG mice.

Histogram plots demonstrating HVEM expression in MEL526 tumor cells (blue) and MEL526 tumor cells isolated from NSG mice following engraftment for 10 days (red). Live tumor cells were defined as AQUA negative and MCSP positive. The HVEM positive population was gated using an FMO control (black).

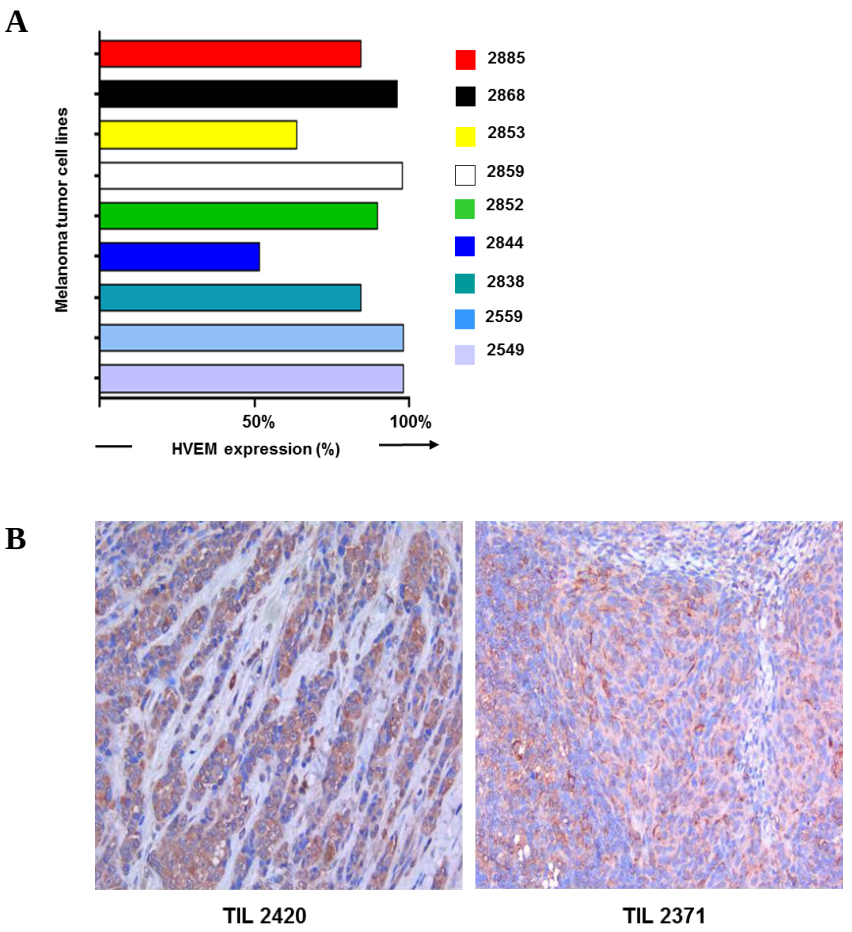

Figure 6.5. HVEM expression in 10 primary melanoma cell lines derived at MDACC.

(**A**) Bar graph demonstrates the percentage of HVEM expression in 10 primary melanoma cell lines derived at MDACC. Live tumor cells were defined as AQUA negative and MCSP positive. HVEM expression was determined using fluorescence minus one controls. (**B**) Representative immunohistochemistry (IHC) of HVEM expression in paired melanoma tumor biopsies (TIL# 2420 and 2371).

Discussion

We have shown that BTLA can provide positive function through Grb2 motif. In this study, we have demonstrated that use of TIL overexpressing a disrupted ITIM/ITSM motif to treat NSG tumor-bearing mice resulted in superior tumor control as compared to EM control and non-treated group. Moreover, the mice received a malfunctioned Grb2 motif had worse tumor control than the control groups. This result indicates that Grb2 could play a role in mediating tumor control.

Although we have also shown that BTLA WT also transduced positive co-signaling function of T cells such as boosting IL-2 secretion, it remains unclear why WT BTLA transduced TIL failed to exhibit tumor control in the NSG tumor bearing mice. It is possible that the repetitive expansion of TIL for two consecutive 14-day rapid expansions naturally triggers TIL to further differentiate. Thus, overexpression of BTLA in TIL containing a large proportion of late-differentiated attributes might not reflect the normal biology of human $CD8^{+}$T cell. As such, the high levels of SHP-1 present in late differentiated $CD8^{+}$T cells potentially gain more interaction with ITIM and ITSM and result in skewing BTLA toward its inhibitory function.

Generally, co-stimulatory molecules expressed by T cells receive signals from their ligands presented by APCs, but not the tumor cells since it usually lacks expression of these ligands. Instead, high expression of ligands for co-inhibitory molecules by tumor cells can suppress T cell function upon ligation with co-inhibitory molecules highly presented by T cell upon activation. Since overexpression of modified BTLA mediated superior tumor control, this is a proof of concept suggesting that

engagement of BTLA by HVEM on tumor cells could improve TIL function at the tumor site.

CHAPTER 7

Functional role of BTLA in T cell priming and memory recall response

7.1 Rationale and Hypothesis

Unlike human BTLA, mouse BTLA is not considered as a differentiation maker as its expression is not detected in mouse naïve T cell, but up-regulated upon TCR stimulation in a similar fashion than other co-inhibitory molecules such as PD-1 and CTLA-4. Although the kinetic of expression of mouse BTLA is different from human, we have showed that expression of BTLA was highly enriched in memory T cell in both human and mouse. A recent study in patients with active pulmonary tuberculosis showed that BTLA is highly expressed by the memory T cell subset and linked with a protective immune response against mycobacterial infection. A survival role of BTLA has been indicated in a mouse model for acute graft versus host disease (GVHD) (201). BTLA KO donor lymphocytes failed to engraft in host body due to impaired re-expression of IL-7R, a critical receptor for homeostasis of naïve T cells and memory T cell development. Additionally, BTLA-HVEM ligation was shown to promote T cell expansion and survival during bacterial infection in a listeria model (204). From these findings, we hypothesize that BTLA could play a role in memory T cell development. To this end, we utilize a mouse model for vaccination to examine the generation of memory T cells and the memory recall response following vaccination. In this study, we vaccinated C57BL/6 mice with gp100 melanoma peptide following the adoptive transfer of bulk splenocytes from either Pmel-1 BTLA WT or Pmel-1 BTLA KO mouse, transgenic for the TCR recognizing the gp100 peptide used for vaccination. Pmel-1 T cells were tracked in peripheral blood following priming and boosting to determine memory recall response following vaccination.

7.2 Results

Memory recall response is defective in BTLA deficient T cells.

We and others showed that BTLA is mainly expressed by the memory T cell subset in both human and mouse. Previous studies have implied the association of BTLA and memory T cell generation in several disease models including GVHD, bacterial infection, and cancer. In this study, we sought to conduct an experiment to determine the role of BTLA in memory recall response using mouse model for vaccination. Pmel-1 mice were crossed with C57BL/6 BTLA KO mice to generate Pmel-1 BTLA KO mice. Half million of splenocytes from either Pmel-1 WT or Pmel-1 BTLA KO were adoptively transferred into c57BL/6 recipient mice. On the following day, mice were vaccinated with gp100 peptide together with anti-mouse CD40. Imiquimod cream 5% was also applied on the vaccination site to boost the innate immune response. Additionally, IL-2 was also provide to support *in vivo* T cell proliferation following vaccination. The frequency of Pmel-1 T cells was determined in peripheral blood every other day after vaccination (**Figure 7A and B**). On day 20 following the first priming, we observed significantly higher frequency of Pmel-1 WT in peripheral blood when compared with Pmel-1 BTLA KO. The frequency of both Pmel-1 WT and Pmel-1 BTLA KO declined and disappeared by day 30. Boost vaccination was performed on day 60 following the first priming. We observed that Pmel-1 WT T cells were detected in the peripheral blood within two days following boosting. However, the frequency of Pmel-1 BTLA KO T cells remained unchanged (**Figure 7C**). To determine the long term memory response, we determined the existence of Pmel-1 T cells in the spleen on day 120. We found significantly higher percentage of Pmel-1 WT T cells in spleen as

compared to Pmel-1 BTLA KO T cells (**Figure 7D**). This result suggests that BTLA is critical for generation of a memory T cell pool in both priming and memory recall response. Our finding has strengthen the notion that BTLA is not only a T cell differentiation marker, but its function is also important in memory T cell development.

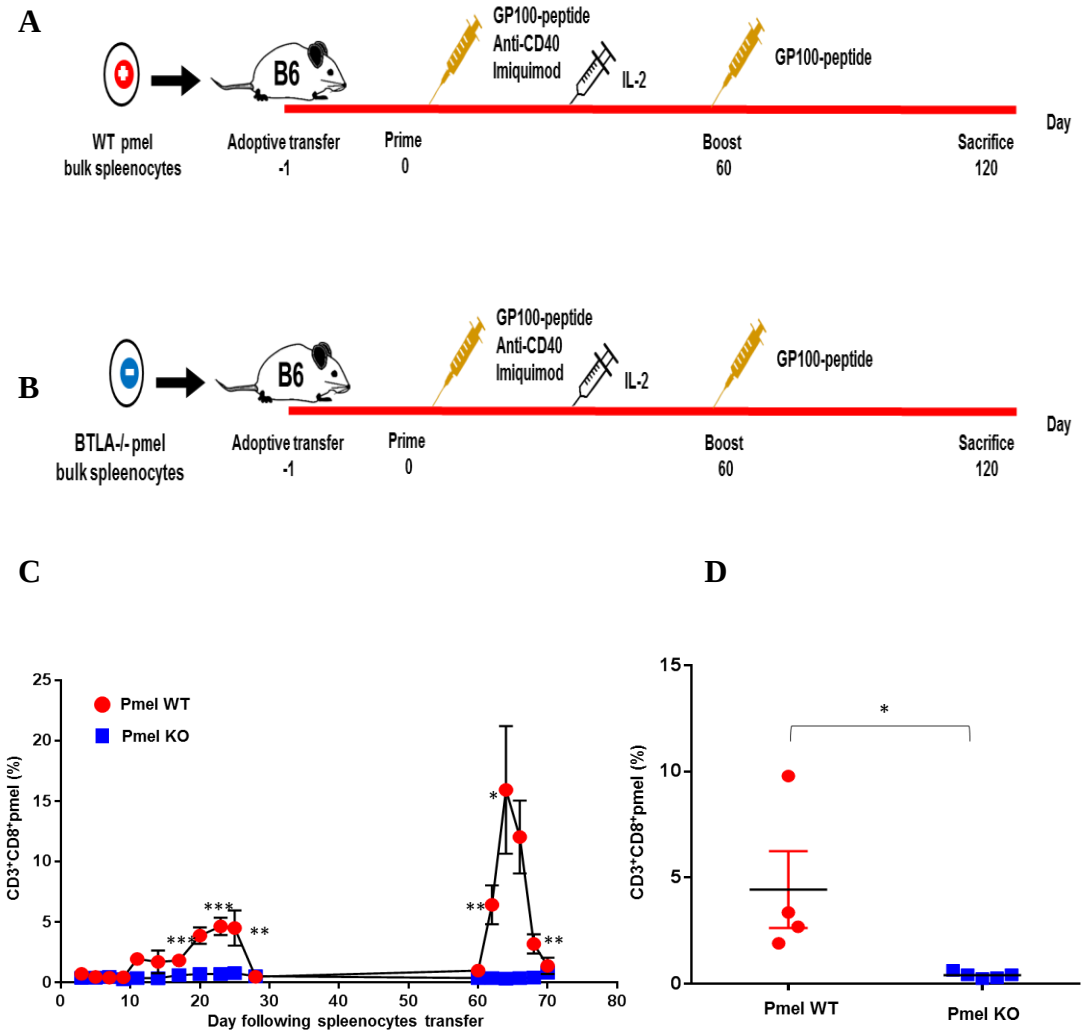

Figure 7. Defect of memory recall response of BTLA deficient T cells.

Schematic diagram depicting experimental design of mouse model for vaccination. A non-myeloablative dose (350 cGy) of radiation is given to induce lymphopenia. The next day, half a million of either (**A**) Pmel-1 Thy 1.1. wild type splenocytes or (**B**) Pmel-1 BTLA KO splenocytes were adoptively transferred into C57BL/6 mouse recipients (i.v.). On the following day, the recipients were vaccinated with gp100 peptide (100µg) together with anti-CD40 (50 µg) and imiquimod (50 mg).

Recombinant human IL-2 at 1.2 $X10^6$ IU was administered once, and 6 x 10^5 IU twice daily for the next 2 days (i.p.). Peripheral blood was collected every other day to determine the frequency of circulating Pmel-1 Thy 1.1 T cells. On day 60, the mice were vaccinated with gp100 peptide, and peripheral blood was collected every other day until Pmel-1 T cells were no longer detected. On day 120, the mice were euthanized, and spleens were collected to determine the presence of Pmel-1 Thy 1.1 T cells. (**C**) Plot graph depicts the percentage of $CD3^+CD8^+Pmel^+$ T cells in the peripheral blood following the priming (first peak from day 15 to day 30) and boosting (second peak from day 60 to 70). The frequency of $CD3^+CD8^+Pmel^+$T cells was significantly higher in C57BL/6 mouse recipients receiving Pmel-1 Thy 1.1. wild type splenocytes as compared to those receiving Pmel-1 Thy 1.1. BTLA KO splenocytes. (**D**) Comparison of the percentage of $CD3^+CD8^+Pmel^+$ T cell in spleen on day 120 of mice receiving either Pmel-1 Thy 1.1. wild type splenocytes or Pmel-1 Thy 1.1. BTLA KO splenocytes. Pmel-1 Thy 1.1. BTLA KO splenocytes failed to develop memory recall response following vaccination and boosting.

Discussion

Generation of memory T cells is critical for highly effective immune response. In this study, we found that mouse transferred with BTLA deficient splenocytes before vaccination failed to develop antigen-specific $CD8^+$ memory T cells, suggesting that BTLA plays a pivotal role in memory T cell development. It is known that BTLA is a co-inhibitory molecule; however, our data has shown that BTLA can also mediate positive signal through its Grb2 motif. It has been clearly shown that optimal antigenic and co-stimulatory signals are involved in memory T cell development, particularly during naïve T cell priming. The weak TCR signal has been shown to inhibit memory T cell development; on the contrary, extremely strong signal resulted in skewing toward terminally differentiated effector T cell development (138). We have shown that BTLA contains motifs that can transduce both positive and negative signal. This data suggest that BTLA (unlike PD-1) induces both pro-survival positive signals but also inhibitory signals through the recruitment of SHP1 and 2. Thus, BTLA acts more like a rheostat reducing TCR signaling during strong antigenic stimulation while also inducing cell survival signaling. This rheostat property of BTLA could play an important role for memory T cell development in producing a balanced TCR signal favoring memory T cell generation.

CHAPTER 8

Overall discussion and future directions

8.1 Overall discussion

Our clinical observation on the association of an improved outcome to TIL ACT in melanoma patients with the infusion of higher numbers of $CD8^+BTLA^+$ TIL has brought up an intriguing question of how this co-inhibitory molecule could benefit TIL therapy as its known function is to inhibit T cell function. Recent literature uncovered another role of BTLA as a T cell differentiation marker. It has been shown that BTLA is highly enriched in naïve and central memory T cells, but down-regulated upon T cell expansion and differentiation (142). Several studies in T cell therapy and cancer immunology clearly demonstrated that adoptive transfer of less differentiated T cell improves T cell persistence, resulting in superior anti-tumor immunity and tumor burden control. Similarly, we also observe that $CD8^+BTLA^+$TIL subset persisted in the peripheral blood longer than its $CD8^+BTLA^-$TIL subset counterpart, indicating that the less differentiated $CD8^+BTLA^+$TIL subset indeed play a role in clinical outcome (121, 141, 143, 223-227).

In this study, while we have demonstrated that $CD8^+BTLA^+$TIL and $CD8^+BTLA^-$TIL subsets had comparable in *vitro* tumor killing capacity, $CD8^+BTLA^+$TIL displayed superior in vivo tumor control using NSG tumor bearing mouse model with increased persistence following transfer in MART-1 antigen-specific setting, which reproduced the exclusive advantage of $CD8^+BTLA^+$ in ACT treated patients. We did not fully understand why the *in vitro* tumor killing observations did not agree with the *in vivo* tumor burden control. We hypothesized that *in vitro* tumor killing was performed in a bulk setting between tumor cells and T cells during such a short time (3 h) that it might not fully predict the fate of T cell following subsequent killing of multiple tumor targets, which occurred in mouse model as well as in melanoma patients. To this end,

we sought to use a nanowell array-based cytolysis assay conducted at the single cell level in order to study the dynamic interactions between tumor targets and effector T cells at high-throughput setting. Our data demonstrated that $CD8^+BTLA^+$TIL were more active at seeking the tumor, but once a contact is established with the target they took more time than their $BTLA^-$ counterpart to produce apoptosis of the target cell. In fact, we observed that $CD8^+BTLA^-$TIL subset was more effective in tumor killing only at early time point (first 250 mins) as compared to $CD8^+BTLA^+$TIL counterpart. However, after careful analysis of the ability of the T cells to kill more than one target, we found that the $CD8^+BTLA^+$TIL subset conferred superior ability for repetitive killing of multiple tumor targets.

We have demonstrated that $CD8^+BTLA^+$TIL manifested enhanced mitochondrial function and spare respiratory capacity (SRC) and preferentially used an oxidative phosphorylation (OXPHOS) pathway for energy generation, which was more efficient than the glycolysis pathway utilized by T effector cells (228, 229). A recent study indicated that increased SRC was strongly associated with a superior bioenergetic capacity, which helped improve T cell survival and motility under hypoxic conditions (230). This property could help explain both the decreased time in finding a tumor target and increased resistance to apoptosis following engagement and subsequent killing of multiple tumor targets. Our result demonstrates for the first time that $CD8^+BTLA^+$ subset is a "serial killing T cell". The potentially intrinsic property of this subset provides an intriguing possibility for why infusion of large numbers of $CD8^+BTLA^+$TIL positively correlates with clinical response to TIL ACT in metastatic melanoma patients. This supports the notion that the minimally differentiated

phenotype of $CD8^+BTLA^+$TIL has less capacity for rapid tumor cytolysis as compared with more differentiated, and short-lived, $CD8^+BTLA^-$TIL, but is more bioenergetically efficient.

The use of $CD8^+BTLA^+$ and $CD8^+BTLA^-$ is impossible to discrete the intrinsic property of less differentiated T cell from BTLA signaling pathway. Because gene silencing of BTLA using lentiviral vector exhibits relatively low efficiency of gene delivery in TIL, this obstacle limits our understanding of the role of BTLA signaling pathway in less differentiated T cells.

Thus, we utilize the genetically modified BTLA constructs to dissect the dichotomy of positive and negative signaling motifs of BTLA, Grb2 and ITIM and ITISM respectively. We did not observe any major differences in the *in vitro* killing capacity and cytotoxic cytokine production between BTLA KO T cells versus BTLA KO T cells overexpressing BTLA WT or its mutants, this suggests that BTLA signaling does not affect tumor killing capability. Our findings are consistent with the previous report showing that the BTLA blockade in gamma delta T cells had no effect on the tumor lysis.

We observed a slight decrease in T cell proliferation in WT as compared with EM, and the inhibitory effect was even more pronounced when the Grb2 motif was defective. In contrast, malfunction of ITIM and ITSM motifs significantly enhanced T cell proliferation. Previous studies in both human and mouse settings indicated that $CD8^+$ T cells were intrinsically less susceptible to BTLA-mediated inhibition as compared to $CD4^+$ T cells. This might explain the minimal inhibition of WT as compared to EM in $CD8^+$ T cells in terms of proliferation. In addition, we noticed that T cells with deficient

Grb2 motifs remarkably decreased IL-2 production. Interestingly, we found that production of IL-2 in BTLA WT was significantly higher than empty vector control. A previous report has shown that Grb2-linked SLP-76 and Vav interaction was involved in IL-2 production. This suggested that the presence of Grb2 is potentially linked to IL-2 production without influence from ITIM and ITSM (218, 231, 232). Our previous work had shown higher IL-2 production in $BTLA^{+}CD8^{+}$ TIL and the current study reveals that the Grb2 motif of BTLA is responsible for the BTLA-dependent IL-2 production which makes the Grb2 motif functionally active and critically important in T cell proliferation.

Because we found a positive role for the Grb2 motif of BTLA, we further wondered whether there was a distinct downstream signaling pathway exhibited from Grb2 motif. When comparing the differentially expressed proteins in activated T cells transduced with the different BTLA constructs and comparing with BTLA WT, we noticed that the Akt signaling pathway was remarkably attenuated in BTLA ΔGrb2, while the phosphorylation of Src was enhanced in BTLA ΔITSM. A previous report demonstrated that ITIM and ITSM motifs of PD-1 inhibited signals through Akt and MAPK. This suggested that the Akt pathway in BTLA was likely targeted by SHP1/2, similar to what was found in PD-1. From our data, it is clear that the phosphorylation of Src increased when ITIM and ITSM domain is abrogated, but this could result from either the effect of Grb2 signal transduction or the deficient dephosphorylation of SHP1/2 recruited through ITIM and ITSM motifs. It was not possible to distinguish the overlapping downstream signaling pathway when BTLA WT was used as a reference to compare with ΔITSM. Instead, we found an increased phosphorylation of Src when

directly comparing ΔITSM to EM, suggesting that Grb2 motif is potentially responsible for the increased Src phosphorylation. It has been demonstrated that the interaction between cells stimulated with Fibronectin (222). Overexpression of Grb2 in osteoclasts was also shown to promote phosphorylation of Src at Y416 and the opposite result was obtained when Grb2 expression was disrupted.

Our data in mouse BTLA signaling are in line with signaling in human TIL as we observed attenuation of MAPK, NF-kB, and Akt signaling proteins, but phosphorylation of Src was enhanced when stimulated with anti-CD3 and HVEM as compared to CD3 alone. This suggested that the downstream signaling pathway of BTLA in mice and humans possibly share similar targets.

As is consistent with the positive function of the Grb2 motif, we demonstrated that TIL overexpressing disrupted ITIM and ITSM had superior *in vivo* tumor burden control while the disruption of Grb2 domain led to the least effective tumor control. It is possible that the signals from the Grb2 motif helped mediate tumor control at tumor sites where TIL interacted with melanoma cells highly expressing HVEM. The fact that the BTLA WT group in this experiment did not control the tumor better than the empty vector group may have to do with the preparation of the cells. The TIL need to undergo two 14-day rapid expansions successively to allow for vector transduction first following by sorting and secondary expansion of the vector positive population. At the end of this four week expansion process the T cell product will be more differentiated whereby we will have late differentiated TIL expressing BTLA and therefore trump the usual "less differentiated" phenotype of the $BTLA^+$ TIL.

Our study sheds light on a dual role of BTLA as both a co-stimulatory and co-inhibitory molecule. The integration of the positive and negative signals transduced by BTLA will promote survival and IL-2 secretion while reducing proliferation and effector cytokine production. In addition, inherited properties of minimally differentiated phenotype of $BTLA^+$ subset display enhanced apoptosis resistance and efficient bioenergetics provide survival advantage following subsequent tumor killing. Since BTLA expression is regulated by the differentiation status of the T cell such that it is only expressed at early stages of differentiation, it is not expected to impact the survival or function of late effector T cells. This places BTLA in a different category than other checkpoint blockade molecules such as PD-1 or CTLA-4, which are up-regulated following T cell activation (184, 233). In general, co-stimulatory molecules expressed by T cells receive signals from their ligands presented by antigen-presenting cells (APCs). Tumor cells generally lack expression of those co-stimulatory molecule ligands. In contrast, tumor cells highly expressing co-inhibitory ligands can suppress T cell function in tumor environments upon ligation with co-inhibitory molecules such as PD-1 and TIM-3. In contrast, BTLA's ligand, HVEM, is expressed widely by melanoma tumor cells. This findings support the concept that intrinsic attribute of less differentiated $CD8^+BTLA^+$ subset together with engagement of HVEM on melanoma cells could provide a costimulatory signal to $BTLA^+CD8^+$ TIL to promote IL-2 secretion, survival and anti-tumor function.

8.2 Future directions

Our data reveal that BTLA provides advantage in both intrinsic attribute of less differentiated T cells as well as signaling pathway. These properties help T cell to resist apoptosis and mediate killing of multiple tumor targets with enhanced IL-2 production and cell proliferation. Overall our findings partially explain the observation of better clinical outcome of melanoma patients infused with high proportion of $CD8^{+}BTLA^{+}$TIL subset (134). Both intrinsic properties of BTLA and its positive signaling pathway through Grb2 motif could contribute to superior clinical responses. On the basis of this finding, I propose two strategies that might potentially improve the efficacy of ACT; I) De-acceleration of T cell differentiation during REP II) Overexpression of BTLA or other inhibitory molecules with genetically modified endo domain.

De-acceleration of T cell differentiation during REP

Several studies have demonstrated that the transfer of less differentiated T cells improved *in vivo* tumor control. In consistent with our clinical observation, patients treated with TIL of a less differentiated T cell phenotype ($CD8^{+}BTLA^{+}$) exhibited superior clinical response with enhanced persistence following TIL transfer as compared to $CD8^{+}BTLA^{-}$ counterpart. During massive T cell expansion, the effect of anti-CD3 activation together with IL-2 promote T cells to undergo proliferation and differentiation (234). Repetitive T cell activation can initiate terminal differentiation resulting in telomere shortening and defect in proliferation, and become clonal deletion eventually (137). This could explain our findings demonstrating that less differentiated TIL subset with high expression of BTLA persist longer than those of more

differentiated phenotype. Thus, an approach to attenuate T cell differentiation during T cell expansion is desirable for T cell therapy. Several strategies have been reported to target cellular signaling pathways that promote T cell differentiation. It has been shown that sustained Akt activation enhanced mTOR phosphorylation and down-regulation of IL-7R expression (235). This resulted in promoting terminal differentiation of effector CD8+ T cells and impaired development of memory T cell pools. On the other hand, inhibition of Akt signaling pathway has been shown to up-regulate CD62L expression and enhance gene signature of human memory T cell (236). In addition, Akt inhibition also altered T cell metabolism by augmenting mitochondrial spare respiratory capacity and oxidative phosphorylation pathway, which is mainly utilized by memory T cells. Adoptive transfer of human TIL previously expanded with Akt inhibitor has demonstrated superior *in vivo* persistence and tumor burden control using NSG mouse model. Consistently, another study also demonstrated that inhibition of Akt signaling pathway can attenuate differentiation of minor histocompatibility antigens (MiHAs) specific $CD8^+$ T cells following rapid expansion for 14 days. In addition, Akt-inhibited MiHA specific CD8+ T cells also exhibited superior anti-tumor capacity following adoptive T cell transfer (237). This suggest that sustained Akt signaling pathway can promote terminal differentiation of T cell by altering transcriptome, metabolism, phenotype, and function.

It has been shown that inhibition of mammalian Target of Rapamycin complex 1 (mTORC1) and activation of Wnt signaling pathway can promote the *in vitro* generation of stem cell-like memory T cells (Tscm). $CD4^+$Tscm cells expanded with mTORC1 inhibitor (Rapamycin) conferred longer term persistence following adoptive

transfer. Furthermore, expanded Tscm also preferentially utilized mitochondria fatty oxidation rather than glycolysis, which is preferably used by effector T cells. The study of mTORC1 gene silencing using siRNA also showed enhanced differentiation of $CD8^+$ T cells into memory phenotype and augmented potent antitumor effect. Interestingly, the combination of 4-1BB aptamer with mTORC1 gene silencing, was found to be synergistically inhibiting mTOR activity and resulted in improved antitumor immunity (238). In vaccination model, it has been demonstrated that using OX-40 agonist in combination with mTOR inhibitor (Rapamycin) boosted the generation of memory T cell pool and protective immunity following Vaccinia Vaccine challenge (239).

Overall current studies demonstrate the advantage of suppressing Akt-mTOR pathway in the generation of less differentiated T cell phenotype and stem-cell like phenotype. It appears that the inhibition of Akt and mTOR can alter the metabolic pathway to mitochondria oxidative phosphorylation, which is much more bioenergetically efficient as compared to the glycolysis pathway. More importantly, expanded T cell with either Akt inhibitor or mTOR inhibitor exhibited superior persistence following adoptive transfer with enhanced antitumor immunity. Therefore, targeting Akt and mTOR could be an effective strategy to help generate less differentiated TIL and stem cell like phenotype.

Overexpression of co-inhibitory molecules with modified endodomain

Less differentiated T cells have intrinsic attributes that enhance survival following tumor cell killing such as apoptosis resistance, superior IL-2 production, and enhanced replicative proliferation. We have demonstrated that the transduction of BTLA bearing

non-functional ITIM and ITSM motifs transduced positive signals with enhanced IL-2 production and T cell proliferation. Thus, intrinsic attribute and positive signaling of BTLA are critical to TIL function and linked to positive clinical response in ACT treated patients. It is known that tumor microenvironment is immunosuppressive. Engagement of co-inhibitory molecules on T cell and their ligand expressed by tumor cells attenuates T function. Using tumor NSG mouse model for adoptive transfer, we have shown that $CD8^{+}BTLA^{-}$ overexpressing BTLA with inactivated ITIM and ITSM motifs conferred superior *in vivo* tumor control, while overexpression of BTLA WT in TIL failed to improve tumor control as compared to non-treatment group. This suggests that engagement of BTLA and HVEM in tumor site affect TIL function in mediating tumor control (**Figure 8A**). This proof of principle allows us to generate a strategy to modify the endodomain of inhibitory molecules by substitution with endodomain of positive co-stimulatory molecule such as CD40, CD27, CD28, 4-1BB, and etc. (**Figure 8B**). Because co-stimulatory molecule only transduces its downstream signal during TCR activation, this context acts selectively and specifically upon engagement of T cell and tumor cell.

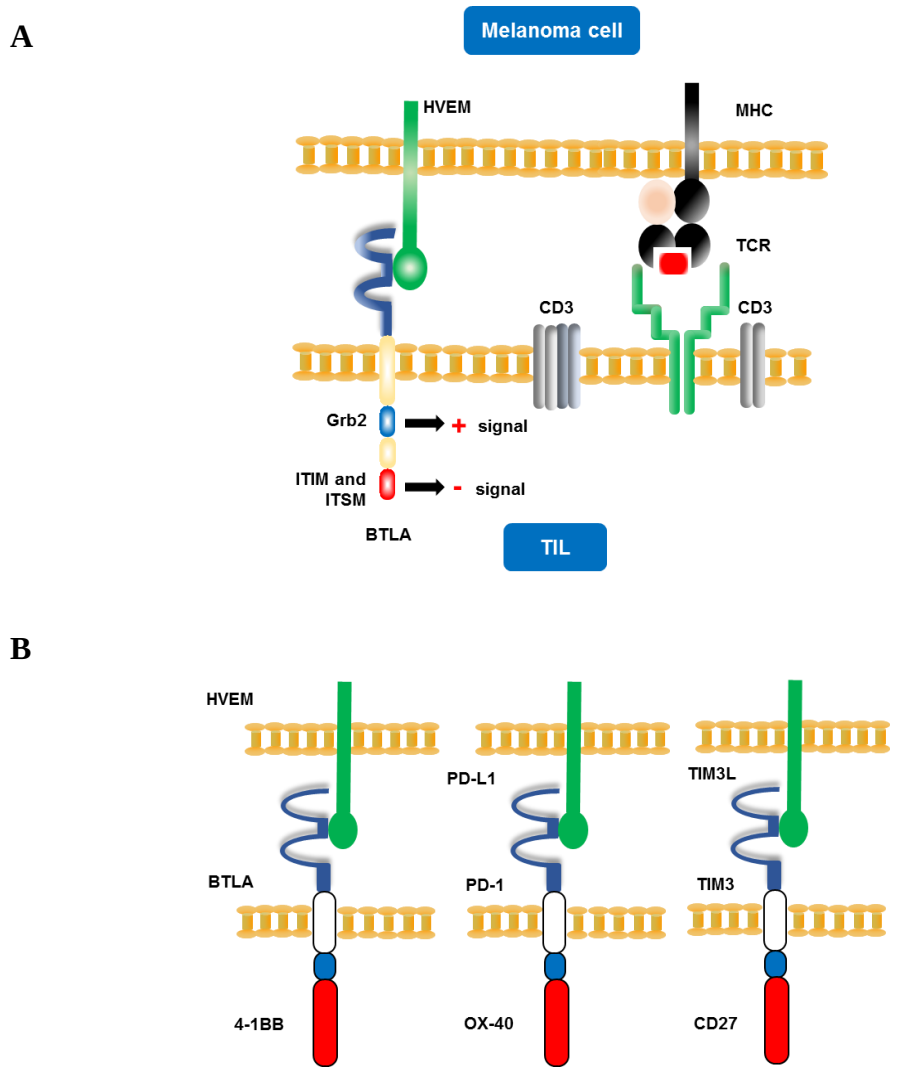

Figure 8. Overexpression of co-inhibitory molecules with modified endodomain. **(A)** Schematic diagram depicts the interaction between TIL and melanoma tumor cell targets. Engagement between BTLA expressed by TIL and HVEM expressed by melanoma tumor cells exhibits both a positive and negative signal. (**B**) Schematic diagram demonstrates interaction between the TIL and melanoma tumor cell targets. Engagement between co-inhibitory molecules with modified endodomain expressed by TIL and HVEM expressed by melanoma tumor cells exhibits positive signals that promote TIL effector function.

CHAPTER 9: MATERIALS and METHODS

Materials and Methods

Reagents.

Cell lines. Platinum E cell line, 526 Melanoma tumor line, and autologous tumor cell line #2549 were maintained in Roswell Park Memorial Institute (RPMI) supplemented with 10% fetal bovine serum (FBS) (Gemini bio product), 10 mM HEPES (Gibco™), 10 mM Penicillin-streptomycin (Gibco™), and 10 mM Glutamine (Gibco™), and 0.05 mM Beta-mercaptoethanol(Gibco™). Platinum-E retro packing cell line was purchased from Cellbiolabs. MEL 526 tumor line was obtained from Dr Steven A. Rosenberg at the National Cancer Institute. B16F10 and B16OVA cell lines were generously provided by Dr. Willem Overwijk (MD Anderson Cancer Center). Autologous primary melanoma tumor cell line #2549 was generated at M.D. Anderson Cancer Center from a tumor sample of a patient enrolled on an ongoing adoptive T cell therapy study (IRB #2004-0069, lab06-0755).

Patient tumor sample acquisition. Tumor samples were obtained from patients with Stage IIIc and Stage IV melanoma undergoing surgery at The University of Texas MD Anderson Cancer Center according to an Institutional Review Board-approved protocol and with patient consent (IRB# LAB06-0755)

Generation of tumor infiltrating lymphocytes (TIL). Fragments from melanoma tumors were cut into 1 to 2 millimeters. Each fragment was placed into a single wells in 24-well-culture plates (Falcon) and maintained with RPMI supplemented with 10% heat inactivated Human AB serum (Gemini bio product), IL-2 6000 IU/ml (Aldesleukin, Novartis), 10 mM HEPES, 10 mM Penicillin-streptomycin (Gibco™), and 10 mM Glutamine (Gibco™).

Animal. The NOD/SCIDγc$^{-/-}$ (NSG) mice were obtained from the Jackson Laboratory. NOD/SCIDγc$^{-/-}$ (NSG) mice were given autoclaved food and acidified autoclaved water. The BTLA-OT.1 KO mouse were kindly provided from Dr. Roza Nurieva (MD Anderson Cancer Center). All mice were housed in a specific pathogen-free facility at The University of Texas M.D. Anderson Cancer Center.

Retroviral constructs of BTLA wild type and mutants. Human BTLA and murine BTLA were amplified from MGC fully sequenced human BTLA and murine BTLA (Open biosystem) respectively by PCR with primers hBTLA-F and R and mBTLA-F and R. The PCR products were cloned into pRVKM retroviral vectors. To generate BTLA mutants, we substituted tyrosine for phenyl alanine in either Grb2 motifs or ITIM and ITSM motifs of BTLA cytoplasmic tails. These included human ΔGrb2 mutants (Y226F and Y243F), human Δ ITIM and ITSM mutants (Y243F, Y257F, and Y282F), murine ΔGrb2 mutants (Y245F), and murine Δ ITIM and ITSM mutants (Y274F, and Y299F). Sequence of all constructs were validated by DNA sequencing.

DNA sequencing of mouse and human BTLA and their mutants

TAT and TTC are genetic codes of tyrosine and phenylalanine respectively. Red, Blue, and Green represent either tyrosine or phenylalanine of Grb2, ITIM, and ITSM motifs respectively.

Wild type human BTLA

ATGAAGACATTGCCTGCCATGCTTGGAACTGGGAAATTATTTTGGGTCTTC

TTCTTAATCCCATATCTGGACATCTGGAACATCCATGGGAAAGAATCATG

TGATGTACAGCTTTATATAAAGAGACAATCTGAACACTCCATCTTAGCAG

GAGATCCCTTTGAACTAGAATGCCCTGTGAAATACTGTGCTAACAGGCCT

CATGTGACTTGGTGCAAGCTCAATGGAACAACATGTGTAAAACTTGAAGA

TAGACAAACAAGTTGGAAGGAAGAGAAGAACATTTCATTTTTCATTCTAC

ATTTTGAACCAGTGCTTCCTAATGACAATGGGTCATACCGCTGTTCTGCAA

ATTTTCAGTCTAATCTCATTGAAAGCCACTCAACAACTCTTTATGTGACAG

ATGTAAAAAGTGCCTCAGAACGACCCTCCAAGGACGAAATGGCAAGCAG

ACCCTGGCTCCTGTATAGTTTACTTCCTTTGGGGGGATTGCCTCTACTCAT

CACTACCTGTTTCTGCCTGTTCTGCTGCCTGAGAAGGCACCAAGGAAAGC

AAAATGAACTCTCTGACACAGCAGGAAGGGAAATTAACCTGGTTGATGCT

CACCTTAAGAGTGAGCAAACAGAAGCAAGCACCAGGCAAAATTCCCAAG

TACTGCTATCAGAAACTGGAATTTATGATAATGACCCTGACCTTTGTTTCA

GGATGCAGGAAGGGTCTGAAGTTTATTCTAATCCATGCCTGGAAGAAAAC

AAACCAGGCATTGTTTATGCTTCCCTGAACCATTCTGTCATTGGACTGAAC

TCAAGACTGGCAAGAAATGTAAAAGAAGCACCAACAGAATATGCATCCA

TATGTGTGAGGAGTGGTGGCGGAAGTGACTACAAGGACGACGATGACAA

GTAA

ΔITIM and ITSM human BTLA

ATGAAGACATTGCCTGCCATGCTTGGAACTGGGAAATTATTTTGGGTCTTC

TTCTTAATCCCATATCTGGACATCTGGAACATCCATGGGAAAGAATCATG

TGATGTACAGCTTTATATAAAGAGACAATCTGAACACTCCATCTTAGCAG

GAGATCCCTTTGAACTAGAATGCCCTGTGAAATACTGTGCTAACAGGCCT

CATGTGACTTGGTGCAAGCTCAATGGAACAACATGTGTAAAACTTGAAGA

TAGACAAACAAGTTGGAAGGAAGAGAAGAACATTTCATTTTTCATTCTAC

ATTTTGAACCAGTGCTTCCTAATGACAATGGGTCATACCGCTGTTCTGCAA

ATTTTCAGTCTAATCTCATTGAAAGCCACTCAACAACTCTTTATGTGACAG

ATGTAAAAAGTGCCTCAGAACGACCCTCCAAGGACGAAATGGCAAGCAG

ACCCTGGCTCCTGTATAGTTTACTTCCTTTGGGGGGATTGCCTCTACTCAT

CACTACCTGTTTCTGCCTGTTCTGCTGCCTGAGAAGGCACCAAGGAAAGC

AAAATGAACTCTCTGACACAGCAGGAAGGGAAATTAACCTGGTTGATGCT

CACCTTAAGAGTGAGCAAACAGAAGCAAGCACCAGGCAAAATTCCCAAG

TACTGCTATCAGAAACTGGAATTTATGATAATGACCCTGACCTTTGTTTCA

GGATGCAGGAAGGGTCTGAAGTTTATTCTAATCCATGCCTGGAAGAAAAC

AAACCAGGCATTGTTTTCGCTTCCCTGAACCATTCTGTCATTGGACTGAAC

TCAAGACTGGCAAGAAATGTAAAAGAAGCACCAACAGAATTCGCATCCA

TATGTGTGAGGAGTGGTGGCGGAAGTGACTACAAGGACGACGATGACAA

GTAA

ΔGrb2 human BTLA

ATGAAGACATTGCCTGCCATGCTTGGAACTGGGAAATTATTTTGGGTCTTC

TTCTTAATCCCATATCTGGACATCTGGAACATCCATGGGAAAGAATCATG

TGATGTACAGCTTTATATAAAGAGACAATCTGAACACTCCATCTTAGCAG

GAGATCCCTTTGAACTAGAATGCCCTGTGAAATACTGTGCTAACAGGCCT

CATGTGACTTGGTGCAAGCTCAATGGAACAACATGTGTAAAACTTGAAGA

TAGACAAACAAGTTGGAAGGAAGAGAAGAACATTTCATTTTTCATTCTAC

ATTTTGAACCAGTGCTTCCTAATGACAATGGGTCATACCGCTGTTCTGCAA

ATTTTCAGTCTAATCTCATTGAAAGCCACTCAACAACTCTTTATGTGACAG

ATGTAAAAAGTGCCTCAGAACGACCCTCCAAGGACGAAATGGCAAGCAG

ACCCTGGCTCCTGTATAGTTTACTTCCTTTGGGGGGATTGCCTCTACTCAT

CACTACCTGTTTCTGCCTGTTCTGCTGCCTGAGAAGGCACCAAGGAAAGC

AAAATGAACTCTCTGACACAGCAGGAAGGGAAATTAACCTGGTTGATGCT

CACCTTAAGAGTGAGCAAACAGAAGCAAGCACCAGGCAAAATTCCCAAG

TACTGCTATCAGAAACTGGAATTTTCGATAATGACCCTGACCTTTGTTTCA

GGATGCAGGAAGGGTCTGAAGTTTTCTCTAATCCATGCCTGGAAGAAAAC

AAACCAGGCATTGTTTATGCTTCCCTGAACCATTCTGTCATTGGACTGAAC

TCAAGACTGGCAAGAAATGTAAAAGAAGCACCAACAGAATATGCATCCA

TATGTGTGAGGAGTGGTGGCGGAAGTGACTACAAGGACGACGATGACAA

GTAA

Wild type mouse BTLA

ATGAAGACAGTGCCTGCCATGCTTGGGACTCCTCGGTTATTTAGGGAATT

CTTCATCCTCCATCTGGGCCTCTGGAGCATCCTTTGTGAGAAAGCTACTAA

GAGGAATGATGAAGAGTGTCCAGTGCAACTTACTATTACGAGGAATTCCA

AACAGTCTGCCAGGACAGGAGAGTTATTTAAAATTCAATGTCCTGTGAAA

TACTGTGTTCATAGACCTAATGTGACTTGGTGTAAGCACAATGGAACAAT

CTGTGTACCCCTTGAGGTTAGCCCTCAGCTATACACTAGTTGGGAAGAAA

ATCAATCAGTTCCGGTTTTTGTTCTCCACTTTAAACCAATACATCTCAGTG

ATAATGGGTCGTATAGCTGTTCTACAAACTTCAATTCTCAAGTTATTAATA

GCCATTCAGTAACCATCCATGTGACAGAAAGGACTCAAAACTCTTCAGAA

CACCCACTAATAACAGTATCTGACATCCCAGATGCCACCAATGCCTCAGG

ACCATCCACCATGGAAGAGAGGCCAGGCAGGACTTGGCTGCTTTACACCT

TGCTTCCTTTGGGGGCATTGCTTCTGCTCCTTGCCTGTGTCTGCCTGCTCTG

CTTTCTGAAAAGGATCCAAGGGAAAGAAAAGAAGCCTTCTGACTTGGCAG

GAAGGGACACTAACCTGGTTGATATTCCAGCCAGTTCCAGGACAAATCAC

CAAGCACTGCCATCAGGAACTGGAATTTATGATAATGATCCCTGGTCTAG

CATGCAGGATGAATCTGAATTGACAATTAGCTTGCAATCAGAGAGAAACA

ACCAGGGCATTGTTTATGCTTCTTTGAACCATTGTGTTATTGGAAGGAATC

CAAGACAGGAAAACAACATGCAGGAGGCACCCACAGAATATGCATCCAT

TTGTGTGAGAAGTGGTGGCGGAAGTGACTACAAGGACGACGATGACAAG

TAA

ΔITIM and ITSM mouse BTLA

ATGAAGACAGTGCCTGCCATGCTTGGGACTCCTCGGTTATTTAGGGAATT

CTTCATCCTCCATCTGGGCCTCTGGAGCATCCTTTGTGAGAAAGCTACTAA

GAGGAATGATGAAGAGTGTCCAGTGCAACTTACTATTACGAGGAATTCCA

AACAGTCTGCCAGGACAGGAGAGTTATTTAAAATTCAATGTCCTGTGAAA

TACTGTGTTCATAGACCTAATGTGACTTGGTGTAAGCACAATGGAACAAT

CTGTGTACCCCTTGAGGTTAGCCCTCAGCTATACACTAGTTGGGAAGAAA

ATCAATCAGTTCCGGTTTTTGTTCTCCACTTTAAACCAATACATCTCAGTG

ATAATGGGTCGTATAGCTGTTCTACAAACTTCAATTCTCAAGTTATTAATA

GCCATTCAGTAACCATCCATGTGACAGAAAGGACTCAAAACTCTTCAGAA

CACCCACTAATAACAGTATCTGACATCCCAGATGCCACCAATGCCTCAGG

ACCATCCACCATGGAAGAGAGGCCAGGCAGGACTTGGCTGCTTTACACCT

TGCTTCCTTTGGGGGCATTGCTTCTGCTCCTTGCCTGTGTCTGCCTGCTCTG

CTTTCTGAAAAGGATCCAAGGGAAAGAAAAGAAGCCTTCTGACTTGGCAG

GAAGGGACACTAACCTGGTTGATATTCCAGCCAGTTCCAGGACAAATCAC

CAAGCACTGCCATCAGGAACTGGAATTTATGATAATGATCCCTGGTCTAG

CATGCAGGATGAATCTGAATTGACAATTAGCTTGCAATCAGAGAGAAACA

ACCAGGGCATTGTTTTCGCTTCTTTGAACCATTGTGTTATTGGAAGGAATC

CAAGACAGGAAAACAACATGCAGGAGGCACCCACAGAATTCGCATCCAT

TTGTGTGAGAAGTGGTGGCGGAAGTGACTACAAGGACGACGATGACAAG

TAA

ΔGrb2 mouse BTLA

ATGAAGACAGTGCCTGCCATGCTTGGGACTCCTCGGTTATTTAGGGAATT

CTTCATCCTCCATCTGGGCCTCTGGAGCATCCTTTGTGAGAAAGCTACTAA

GAGGAATGATGAAGAGTGTCCAGTGCAACTTACTATTACGAGGAATTCCA

AACAGTCTGCCAGGACAGGAGAGTTATTTAAAATTCAATGTCCTGTGAAA

TACTGTGTTCATAGACCTAATGTGACTTGGTGTAAGCACAATGGAACAAT

CTGTGTACCCCTTGAGGTTAGCCCTCAGCTATACACTAGTTGGGAAGAAA

ATCAATCAGTTCCGGTTTTTGTTCTCCACTTTAAACCAATACATCTCAGTG

ATAATGGGTCGTATAGCTGTTCTACAAACTTCAATTCTCAAGTTATTAATA

GCCATTCAGTAACCATCCATGTGACAGAAAGGACTCAAAACTCTTCAGAA

CACCCACTAATAACAGTATCTGACATCCCAGATGCCACCAAT

GCCTCAGGACCATCCACCATGGAAGAGAGGCCAGGCAGGACTTGGCTGC

TTTACACCTTGCTTCCTTTGGGGGCATTGCTTCTGCTCCTTGCCTGTGTCTG

CCTGCTCTGCTTTCTGAAAAGGATCCAAGGGAAAGAAAAGAAGCCTTCTG

ACTTGGCAGGAAGGGACACTAACCTGGTTGATATTCCAGCCAGTTCCAGG

ACAAATCACCAAGCACTGCCATCAGGAACTGGAATTTTCGATAATGATCC

CTGGTCTAGCATGCAGGATGAATCTGAATTGACAATTAGCTTGCAATCAG

AGAGAAACAACCAGGGCATTGTTTATGCTTCTTTGAACCATTGTGTTATTG

GAAGGAATCCAAGACAGGAAAACAACATGCAGGAGGCACCCACAGAATA

TGCATCCATTTGTGTGAGAAGTGGTGGCGGAAGTGACTACAAGGACGACG

ATGACAAGTAA

TAT and TTC are genetic codes of tyrosine and phenylalanine respectively. Red, Blue, and Green represent either tyrosine or phenylalanine of Grb2, ITIM, and ITSM motifs respectively.

Amino acid sequencing of mouse and human BTLA and their mutants

Wild type human BTLA

MKTLPAMLGTGKLFWVFFLIPYLDIWNIHGKESCDVQLYIKRQSEHSILAGDP

FELECPVKYCANRPHVTWCKLNGTTCVKLEDRQTSWKEEKNISFFILHFEPVL

PNDNGSYRCSANFQSNLIESHSTTLYVTDVKSASERPSKDEMASRPWLLYSLL

PLGGLPLLITTCFCLFCCLRRHQGKQNELSDTAGREINLVDAHLKSEQTEAST

RQNSQVLLSETGIYDNDPDLCFRMQEGSEVYSNPCLEENKPGIVYASLNHSVI

GLNSRLARNVKEAPTEYASICVRSGGGSDYKDDDDK.

Δ*ITIM and ITSM human BTLA*

MKTLPAMLGTGKLFWVFFLIPYLDIWNIHGKESCDVQLYIKRQSEHSILAGDP

FELECPVKYCANRPHVTWCKLNGTTCVKLEDRQTSWKEEKNISFFILHFEPVL

PNDNGSYRCSANFQSNLIESHSTTLYVTDVKSASERPSKDEMASRPWLLYSLL

PLGGLPLLITTCFCLFCCLRRHQGKQNELSDTAGREINLVDAHLKSEQTEAST

RQNSQVLLSETGIYDNDPDLCFRMQEGSEVYSNPCLEENKPGIVFASLNHSVI

GLNSRLARNVKEAPTEFASICVRSGGGSDYKDDDDK.

Δ*Grb2 human BTLA*

MKTLPAMLGTGKLFWVFFLIPYLDIWNIHGKESCDVQLYIKRQSEHSILAGDP

FELECPVKYCANRPHVTWCKLNGTTCVKLEDRQTSWKEEKNISFFILHFEPVL

PNDNGSYRCSANFQSNLIESHSTTLYVTDVKSASERPSKDEMASRPWLLYSLL

PLGGLPLLITTCFCLFCCLRRHQGKQNELSDTAGREINLVDAHLKSEQTEAST

RQNSQVLLSETGIFDNDPDLCFRMQEGSEVFSNPCLEENKPGIVYASLNHSVI

GLNSRLARNVKEAPTEYASICVRSGGGSDYKDDDDK.

Wild type mouse BTLA

MKTVPAMLGTPRLFREFFILHLGLWSILCEKATKRNDEECPVQLTITRNSKQS

ARTGELFKIQCPVKYCVHRPNVTWCKHNGTICVPLEVSPQLYTSWEENQSVP

VFVLHFKPIHLSDNGSYSCSTNFNSQVINSHSVTIHVTERTQNSSEHPLITVSDI

PDATNASGPSTMEERPGRTWLLYTLLPLGALLLLLACVCLLCFLKRIQGKEK

KPSDLAGRDTNLVDIPASSRTNHQALPSGTGIYDNDPWSSMQDESELTISLQS

ERNNQGIVYASLNHCVIGRNPRQENNMQEAPTEYASICVRSGGGSDYKDDD

DK.

Δ*ITIM and ITSM mouse BTLA*

MKTVPAMLGTPRLFREFFILHLGLWSILCEKATKRNDEECPVQLTITRNSKQS

ARTGELFKIQCPVKYCVHRPNVTWCKHNGTICVPLEVSPQLYTSWEENQSVP

VFVLHFKPIHLSDNGSYSCSTNFNSQVINSHSVTIHVTERTQNSSEHPLITVSDI

PDATNASGPSTMEERPGRTWLLYTLLPLGALLLLLACVCLLCFLKRIQGKEK

KPSDLAGRDTNLVDIPASSRTNHQALPSGTGIYDNDPWSSMQDESELTISLQS

ERNNQGIVFASLNHCVIGRNPRQENNMQEAPTEFASICVRSGGGSDYKDDDD

K.

Δ*Grb2 mouse BTLA*

MKTVPAMLGTPRLFREFFILHLGLWSILCEKATKRNDEECPVQLTITRNSKQS

ARTGELFKIQCPVKYCVHRPNVTWCKHNGTICVPLEVSPQLYTSWEENQSVP

VFVLHFKPIHLSDNGSYSCSTNFNSQVINSHSVTIHVTERTQNSSEHPLITVSDI

PDATNASGPSTMEERPGRTWLLYTLLPLGALLLLLACVCLLCFLKRIQGKEK

KPSDLAGRDTNLVDIPASSRTNHQALPSGTGIFDNDPWSSMQDESELTISLQSE

RNNQGIVFASLNHCVIGRNPRQENNMQEAPTEYASICVRSGGGSDYKDDDD

K.

Y and F are amino acid codes of tyrosine and phenylalanine respectively. Red, Blue, and Green represent either tyrosine or phenylalanine of Grb2, ITIM, and ITSM motifs respectively.

Amino acid sequencing of human co-stimulatory molecules containing Grb2 motif

Human CD28

MLRLLLALNLFPSIQVTGNKILVKQSPMLVAYDNAVNLSYNEKSNGTIIHVKG

KHLCPSPLFPGPSKPFWVLVVVGGVLACYSLLVTVAFIIFWVRSKRSRLLHSD

YMNMTPRRPGPTRKHYQPYAPPRDFAAYRS

Human ICOS

MKSGLWYFFLFCLRIKVLTGEINGSANYEMFIFHNGGVQILCKYPDIVQQFK

MQLLKGGQILCDLTKTKGSGNTVSIKSLKFCHSQLSNNSVSFFLYNLDHSHA

NYYFCNLSIFDPPPFKVTLTGGYLHIYESQLCCQLKFWLPIGCAAFVVVCILGC

ILICWLTKKKYSSSVHDPNGEYMFMRAVNTAKKSRLTDVTL

Amino acid sequencing of co-inhibitory molecule containing ITIM and ITSM motif

Human PD-1

MQIPQAPWPVVWAVLQLGWRPGWFLDSPDRPWNPPTFSPALLVVTEGDNAT

FTCSFSNTSESFVLNWYRMSPSNQTDKLAAFPEDRSQPGQDCRFRVTQLPNG

RDFHMSVVRARRNDSGTYLCGAISLAPKAQIKESLRAELRVTERRAEVPTAH

PSPSPRPAGQFQTLVVGVVGGLLGSLVLLVWVLAVICSRAARGTIGARRTGQ

PLKEDPSAVPVFSVDYGELDFQWREKTPEPPVPCVPEQTEYATIVFPSGMGTS

SPARRGSADGPRSAQPLRPEDGHCSWPL

Table 3. Primers used to amplify mouse and human BTLA

Human	
hBTLA-F	CACACAAGATCTATGAAGACATTGCTGCCATGCTT
hBTLA-R	CACACACTCGAGTTAACTCCTCACACATATGGATGC
Mouse	
mBTLA-F	CACACAAGATCTATGAAGACAGTGCCTGCCATGCT
mBTLA-R	CACACACTCGAGTTACTTGTCATCGTCCTTGTAGTCA

Retrovirus generation and transduction of human TIL. Plate-E cells were transfected with pRVKM retroviral vectors and RD114 plasmids using PolyJet (Signagen Laboratories) according to manufacturer's protocol for 60 h. The supernatants were harvested and concentrated using Vivaspin-20 (Vivaproducts), then added onto a plate pre-coated with Retronectin (Takara clontech) and centrifuged at 2000 g for 2 h. Pre-activated $CD8^{+}BTLA^{-}$ with anti-human CD3 at a concentration of 300 ng/mL (Clone OKT3, BD Pharmingen^{TM}) were then added and centrifuged at 1000 g for 10 min. On the next day, the cells were propagated using the Rapid expansion protocol (REP) with irradiated PBMC and hIL-2 (Proleukin, Novartis) at 6000 IU for 14 d as previously described (141). Transduced cells were then sorted based on GFP expression and propagated with the REP protocol.

Retroviral transduction in mouse T cells. pRVKM retroviral vectors and pEco plasmids were co-transfected into Plate-E cells using using PolyJet (Signagen Laboratories). The supernatants were harvested 60 h later and concentrated using Vivaspin-20 (Vivaproducts). Splenocytes from BTLA-KO OT.1 mice were cultured with RPMI1640 with 10% FBS and hIL-2 at 300IU/ml, and activated with anti-mouse CD3 at concentration of 0.3 ug/ml (Clone 145-2C11, BD Pharmingen^{TM}) for 24 h. The cells were then infected with a concentrated retrovirus and further expanded in RPMI1640 with 10% FBS and hIL-2 for 3 days. The cells were sorted based on the expression of GFP using a FACSAria (BD Bioscience) and propagated with hIL-2 at 300 IU/ml for 5 days.

Reverse phase protein array. Murine BTLA KO OT.1 cells overexpressing BTLA WT or mutants were re-stimulated with either 10 ng/ml anti-mouse CD3 (Clone 145-2C11, BD Pharmingen^{TM}) alone or with recombinant Fc mouse HVEM (R&D systems) plate-bound for 12 h prior to harvest with cell lysis buffer (kindly provided by RPPA core facility at The University of Texas M.D. Anderson Cancer Center). The cell lysates were centrifuged at 14,000 rpm for 10 minutes at 4 °C. For human TIL, four TIL lines were stained with anti-CD8 (clone RPA-T8, BD Biosciences), anti-BTLA (clone J168, BD Bioscience), and Sytox blue (Molecular Probe^{TM}) under aseptic condition. The cells were sorted based on expression of $CD8^{+}BTLA^{-}$ using FACSAria (BD Biosciences). On the next day, sorted TIL were re-stimulated with anti-human CD3 (clone OKT-3, BD Bioscience) with or without recombinant Fc mouse HVEM (R&D systems) for 30 minutes. The cells were harvested as previously described above.

Surface marker staining

TIL were washed twice with 2 ml FWB for 5 minutes at 1400 rpm. The cell were stained with T cell surface markers with the cocktail antibody of anti-human CD3 (clone BD Pharmingen), anti-human CD8(clone BD Pharmingen), anti-BTLA (clone J168, BD Pharmingen). Amcyan Aqua (Molecular Probes, Life Technologies) was used to selectively gate live cells. Staining was performed on ice for 25 minutes. The cells were washed twice with FWB to remove an excessed unbound antibodies for 5 minutes at 1400 rpm. The samples were fixed with 1% para-formaldehyde solution prior to acquire acquire using a BD FACScanto II flow cytometer machine. For tetramer staining, the cells were washed with FWB previously described, and stained with a MART-1 peptide HLA-A0201 tetramer (Beckman-Coulter) prior to normally stain with surface markers.

Intracellular cytokine staining. Overexpressing BTLA WT or mutants in BTLA-/- OT-1 T cells were re-activated with either DC pulsed with OVA peptide (SIINFEKL) (Polysciences) or DC alone at a ratio of 1 to 40 in the presence of BD™ GolgiStop™ according to the manufacturer's instruction. After 4 hours, cells were fixed and permeabilized using BD Cytofix/Cytoperm^{TM} kits (BD Biosciences Cat: 554722) and subsequently stained with anti-mouse IFN-γ and anti-mouse TNF-α (BD Pharmigen).

Cytokine multiplex assays. Murine BTLA KO OT.1 cells overexpressing BTLA WT or mutants were re-stimulated with either 10 ng/ml anti-mouse CD3 (Clone 145-2C11, BD Pharmingen^{TM}) alone or with recombinant Fc mouse HVEM (R&D systems) plate-bound for 24 h. Supernatants were collected to quantify the secreted cytokines using a MILLPLEX multiplex assay according to manufacturer protocol (Millipore).

Killing assays. T cells were co-cultured with tumor cells labeled with efluor670® at ratio of 1 to 1, 1 to 3, and 1 to 10. After 3 h, the cells were fixed and permeabilized (BD Cytofix/Cytoperm), then stained with anti-cleaved caspase-3 (clone CPP32, BD Biosciences), and analyzed by a BD FACSCanto II (BD Biosciences). The data was analyzed using FlowJo software (TreeStar).

Cell proliferation assay. Murine BTLA-/- OT-1 expressing BTLA WT or mutants were labeled with efluor670® and re-stimulated with DC alone or DC pulsed with OVA peptide (SIINFEKL) at a ratio of 1 to 40 for 48 h prior to being analyzed using a BD FACSCanto II (BD Biosciences). The data was analyzed using FlowJo software (TreeStar).

Nanowell array-based cytolytic assay. TIL and Tumor cells were labeled with 1 μmol/L of red fluorescence dye (PKH26, Sigma) and 1 μl of green fluorescence dye (PKH68, Sigma) respectively. The cells were loaded onto nanowell at concentration of $1x10^6$/mL. Target cell cytolysis mediated by TIL was monitored using a Carl Zeiss Axio Observer fitted with Hamamatsu EM-CCD camera using 10 x 0.3 NA objective. Apoptotic cells became green when stained with Annexin V conjugated with Alexa 647as previously described.

Adoptive Transfer and IL-2 treatment. The NOD/SCIDγc$^{-/-}$ (NSG) mice in each experiment contained 5 to 8, 10-12 week-old female mice per group. We were subcutaneously engrafted with either 10 x 10^6 526 melanoma tumors or 10 x 10^6 autologous melanoma tumors. On day 12, either 5 $x10^6$ sorted $CD8^+BTLA^+$ or sorted $CD8^+BTLA^-$ were adoptively transferred into tumor-bearing mice through the tail vein. In the virally transduced TIL experiment, either sorted $CD8^+GFP^+$WT, $CD8^+GFP^+\Delta$

Grb2, $CD8^{+}GFP^{+}\Delta$ ITSM, or CD8+GFP+empty vector controls were transferred instead. Recombinant human IL-2 (Proleukin, Novartis) was administered intraperitoneally at a concentration of 6 $x10^{5}$ I.U. immediately after TIL transfer twice daily for three day. Tumor size was measured every other day using calipers. Mice were sacrificed when tumors exceeded 15 mm diameter. Peripheral blood was collected every other day, washed with 1X PBS twice, and lysed with ACK lysis buffer. The cells were stained for human surface markers, CD45, CD8, and Aqua (viability) for 20 minutes on ice. After, the cells were washed with 1XPBS twice prior to acquire using a BD FACScanto II flow cytometer machine. The data was analyzed using FlowJo software (TreeStar).

Statistical Analysis

For all survival curve analysis data, we used the log rank test to compare distribution of two groups. We applied Linear Models and Empirical Bayes Methods to compare the differential protein expression from RPPA data sets. Difference in the percentage of positive cells producing IFN-γ and TNF-α was analyzed using an ANOVA, and a two-tailed Student's t-test was used to determine statistical significance for other analyses.

CHAPTER 10: REFERENCES

1. Hanahan D, Weinberg RA. The hallmarks of cancer. Cell. 2000;100:57-70.

2. Hanahan D, Weinberg RA. Hallmarks of cancer: the next generation. Cell. 2011;144:646-74.

3. McCarthy EF. The toxins of William B. Coley and the treatment of bone and soft-tissue sarcomas. Iowa Orthop J. 2006;26:154-8.

4. Ichim CV. Revisiting immunosurveillance and immunostimulation: Implications for cancer immunotherapy. J Transl Med. 2005;3:8.

5. Outzen HC, Custer RP, Eaton GJ, Prehn RT. Spontaneous and induced tumor incidence in germfree "nude" mice. J Reticuloendothel Soc. 1975;17:1-9.

6. Burnet M. Cancer; a biological approach. I. The processes of control. Br Med J. 1957;1:779-86.

7. Smyth MJ, Dunn GP, Schreiber RD. Cancer immunosurveillance and immunoediting: the roles of immunity in suppressing tumor development and shaping tumor immunogenicity. Advances in immunology. 2006;90:1-50.

8. Dunn GP, Old LJ, Schreiber RD. The immunobiology of cancer immunosurveillance and immunoediting. Immunity. 2004;21:137-48.

9. Dunn GP, Old LJ, Schreiber RD. The three Es of cancer immunoediting. Annu Rev Immunol. 2004;22:329-60.

10. Jager E, Knuth A. The discovery of cancer/testis antigens by autologous typing with T cell clones and the evolution of cancer vaccines. Cancer Immun. 2012;12:6.

11. Manjili MH. Revisiting cancer immunoediting by understanding cancer immune complexity. J Pathol. 2011;224:5-9.

12. Hellstrom KE, Hellstrom I. Evidence that tumor antigens enhance tumor growth in vivo by interacting with a radiosensitive (suppressor?) cell population. Proc Natl Acad Sci U S A. 1978;75:436-40.

13. Abelev GI, Perova SD, Khramkova NI, Postnikova ZA, Irlin IS. Production of embryonal alpha-globulin by transplantable mouse hepatomas. Transplantation. 1963;1:174-80.

14. Gershon RK, Kondo K. Cell interactions in the induction of tolerance: the role of thymic lymphocytes. Immunology. 1970;18:723-37.

15. Steinman RM, Cohn ZA. Identification of a novel cell type in peripheral lymphoid organs of mice. I. Morphology, quantitation, tissue distribution. J Exp Med. 1973;137:1142-62.

16. Wigzell H. Quantitative Titrations of Mouse H-2 Antibodies Using Cr-51-Labelled Target Cells. Transplantation. 1965;3:423-31.

17. Morgan DA, Ruscetti FW, Gallo R. Selective in vitro growth of T lymphocytes from normal human bone marrows. Science. 1976;193:1007-8.

18. Ruscetti FW, Morgan DA, Gallo RC. Functional and morphologic characterization of human T cells continuously grown in vitro. J Immunol. 1977;119:131-8.

19. Ruscetti FW, Morgan DA, Gallo RC. Functional and morphologic characterization of human T cells continuously grown in vitro. J. Immunol. 1977. 119: 131-138. J Immunol. 2007;179:1415-22.

20. Winter G, Milstein C. Man-made antibodies. Nature. 1991;349:293-9.

21. Chames P, Van Regenmortel M, Weiss E, Baty D. Therapeutic antibodies: successes, limitations and hopes for the future. Br J Pharmacol. 2009;157:220-33.

22. Grimm EA, Mazumder A, Zhang HZ, Rosenberg SA. Lymphokine-activated killer cell phenomenon. Lysis of natural killer-resistant fresh solid tumor cells by interleukin 2-activated autologous human peripheral blood lymphocytes. J Exp Med. 1982;155:1823-41.

23. Kappler J, Kubo R, Haskins K, Hannum C, Marrack P, Pigeon M, McIntyre B, Allison J, Trowbridge I. The major histocompatibility complex-restricted antigen receptor on T cells in mouse and man: identification of constant and variable peptides. 1983. J Immunol. 2006;176:2683-90.

24. Brunet JF, Denizot F, Luciani MF, Roux-Dosseto M, Suzan M, Mattei MG, Golstein P. A new member of the immunoglobulin superfamily--CTLA-4. Nature. 1987;328:267-70.

25. Brichard V, Van Pel A, Wolfel T, Wolfel C, De Plaen E, Lethe B, Coulie P, Boon T. The tyrosinase gene codes for an antigen recognized by autologous cytolytic T lymphocytes on HLA-A2 melanomas. J Exp Med. 1993;178:489-95.

26. Hege KM, Jooss K, Pardoll D. GM-CSF gene-modifed cancer cell immunotherapies: of mice and men. Int Rev Immunol. 2006;25:321-52.

27. Butterfield LH, Ribas A, Dissette VB, Amarnani SN, Vu HT, Oseguera D, Wang HJ, Elashoff RM, McBride WH, Mukherji B, Cochran AJ, Glaspy JA, Economou JS. Determinant spreading associated with clinical response in dendritic cell-based immunotherapy for malignant melanoma. Clin Cancer Res. 2003;9:998-1008.

28. Hurwitz AA, Yu TF, Leach DR, Allison JP. CTLA-4 blockade synergizes with tumor-derived granulocyte-macrophage colony-stimulating factor for treatment of an experimental mammary carcinoma. Proc Natl Acad Sci U S A. 1998;95:10067-71.

29. Kwon ED, Hurwitz AA, Foster BA, Madias C, Feldhaus AL, Greenberg NM, Burg MB, Allison JP. Manipulation of T cell costimulatory and inhibitory signals for immunotherapy of prostate cancer. Proc Natl Acad Sci U S A. 1997;94:8099-103.

30. Amiri-Kordestani L, Wedam S, Zhang L, Tang S, Tilley A, Ibrahim A, Justice R, Pazdur R, Cortazar P. First FDA approval of neoadjuvant therapy for breast cancer: pertuzumab for the treatment of patients with HER2-positive breast cancer. Clin Cancer Res. 2014;20:5359-64.

31. Singh I, Amin H, Rah B, Goswami A. Targeting EGFR and IGF 1R: a promising combination therapy for metastatic cancer. Front Biosci (Schol Ed). 2013;5:231-46.

32. Centers for Disease C, Prevention. FDA licensure of bivalent human papillomavirus vaccine (HPV2, Cervarix) for use in females and updated HPV vaccination recommendations from the Advisory Committee on Immunization Practices (ACIP). MMWR Morb Mortal Wkly Rep. 2010;59:626-9.

33. Galon J, Pages F, Marincola FM, Thurin M, Trinchieri G, Fox BA, Gajewski TF, Ascierto PA. The immune score as a new possible approach for the classification of cancer. J Transl Med. 2012;10:1.

34. Royal RE, Levy C, Turner K, Mathur A, Hughes M, Kammula US, Sherry RM, Topalian SL, Yang JC, Lowy I, Rosenberg SA. Phase 2 trial of single agent Ipilimumab (anti-CTLA-4) for locally advanced or metastatic pancreatic adenocarcinoma. J Immunother. 2010;33:828-33.

35. Sipuleucel-T: APC 8015, APC-8015, prostate cancer vaccine--Dendreon. Drugs R D. 2006;7:197-201.

36. Hodi FS, O'Day SJ, McDermott DF, Weber RW, Sosman JA, Haanen JB, Gonzalez R, Robert C, Schadendorf D, Hassel JC, Akerley W, van den Eertwegh AJ, Lutzky J, Lorigan P, Vaubel JM, Linette GP, Hogg D, Ottensmeier CH, Lebbe C, Peschel C, Quirt I, Clark JI, Wolchok JD, Weber JS, Tian J, Yellin MJ, Nichol GM, Hoos A, Urba WJ. Improved survival with ipilimumab in patients with metastatic melanoma. N Engl J Med. 2010;363:711-23.

37. Robert C, Thomas L, Bondarenko I, O'Day S, Weber J, Garbe C, Lebbe C, Baurain JF, Testori A, Grob JJ, Davidson N, Richards J, Maio M, Hauschild A, Miller WH, Jr., Gascon P, Lotem M, Harmankaya K, Ibrahim R, Francis S, Chen TT, Humphrey R, Hoos A, Wolchok JD. Ipilimumab plus dacarbazine for previously untreated metastatic melanoma. N Engl J Med. 2011;364:2517-26.

38. Topalian SL, Hodi FS, Brahmer JR, Gettinger SN, Smith DC, McDermott DF, Powderly JD, Carvajal RD, Sosman JA, Atkins MB, Leming PD, Spigel DR, Antonia SJ, Horn L, Drake CG, Pardoll DM, Chen L, Sharfman WH, Anders RA, Taube JM,

McMiller TL, Xu H, Korman AJ, Jure-Kunkel M, Agrawal S, McDonald D, Kollia GD, Gupta A, Wigginton JM, Sznol M. Safety, activity, and immune correlates of anti-PD-1 antibody in cancer. N Engl J Med. 2012;366:2443-54.

39. Brahmer JR, Drake CG, Wollner I, Powderly JD, Picus J, Sharfman WH, Stankevich E, Pons A, Salay TM, McMiller TL, Gilson MM, Wang C, Selby M, Taube JM, Anders R, Chen L, Korman AJ, Pardoll DM, Lowy I, Topalian SL. Phase I study of single-agent anti-programmed death-1 (MDX-1106) in refractory solid tumors: safety, clinical activity, pharmacodynamics, and immunologic correlates. J Clin Oncol. 2010;28:3167-75.

40. Kochenderfer JN, Dudley ME, Kassim SH, Somerville RP, Carpenter RO, Stetler-Stevenson M, Yang JC, Phan GQ, Hughes MS, Sherry RM, Raffeld M, Feldman S, Lu L, Li YF, Ngo LT, Goy A, Feldman T, Spaner DE, Wang ML, Chen CC, Kranick SM, Nath A, Nathan DA, Morton KE, Toomey MA, Rosenberg SA. Chemotherapy-refractory diffuse large B-cell lymphoma and indolent B-cell malignancies can be effectively treated with autologous T cells expressing an anti-CD19 chimeric antigen receptor. J Clin Oncol. 2015;33:540-9.

41. Hadrup S, Donia M, Thor Straten P. Effector CD4 and CD8 T cells and their role in the tumor microenvironment. Cancer Microenviron. 2013;6:123-33.

42. Pardoll DM. The blockade of immune checkpoints in cancer immunotherapy. Nat Rev Cancer. 2012;12:252-64.

43. Batlevi CL, Matsuki E, Brentjens RJ, Younes A. Novel immunotherapies in lymphoid malignancies. Nat Rev Clin Oncol. 2016;13:25-40.

44. Harper K, Balzano C, Rouvier E, Mattei MG, Luciani MF, Golstein P. CTLA-4 and CD28 activated lymphocyte molecules are closely related in both mouse and human as to sequence, message expression, gene structure, and chromosomal location. J Immunol. 1991;147:1037-44.

45. Krummel MF, Allison JP. CD28 and CTLA-4 have opposing effects on the response of T cells to stimulation. J Exp Med. 1995;182:459-65.

46. Pentcheva-Hoang T, Egen JG, Wojnoonski K, Allison JP. B7-1 and B7-2 selectively recruit CTLA-4 and CD28 to the immunological synapse. Immunity. 2004;21:401-13.

47. Chuang E, Fisher TS, Morgan RW, Robbins MD, Duerr JM, Vander Heiden MG, Gardner JP, Hambor JE, Neveu MJ, Thompson CB. The CD28 and CTLA-4 receptors associate with the serine/threonine phosphatase PP2A. Immunity. 2000;13:313-22.

48. Inobe M, Schwartz RH. CTLA-4 engagement acts as a brake on CD4+ T cell proliferation and cytokine production but is not required for tuning T cell reactivity in adaptive tolerance. J Immunol. 2004;173:7239-48.

49. Sojka DK, Hughson A, Fowell DJ. CTLA-4 is required by CD4+CD25+ Treg to control CD4+ T-cell lymphopenia-induced proliferation. Eur J Immunol. 2009;39:1544-51.

50. van Elsas A, Hurwitz AA, Allison JP. Combination immunotherapy of B16 melanoma using anti-cytotoxic T lymphocyte-associated antigen 4 (CTLA-4) and granulocyte/macrophage colony-stimulating factor (GM-CSF)-producing vaccines

induces rejection of subcutaneous and metastatic tumors accompanied by autoimmune depigmentation. J Exp Med. 1999;190:355-66.

51. Prieto PA, Yang JC, Sherry RM, Hughes MS, Kammula US, White DE, Levy CL, Rosenberg SA, Phan GQ. CTLA-4 blockade with ipilimumab: long-term follow-up of 177 patients with metastatic melanoma. Clin Cancer Res. 2012;18:2039-47.

52. Galluzzi L, Kroemer G, Eggermont A. Novel immune checkpoint blocker approved for the treatment of advanced melanoma. Oncoimmunology. 2014;3:e967147.

53. Chung KY, Gore I, Fong L, Venook A, Beck SB, Dorazio P, Criscitiello PJ, Healey DI, Huang B, Gomez-Navarro J, Saltz LB. Phase II study of the anti-cytotoxic T-lymphocyte-associated antigen 4 monoclonal antibody, tremelimumab, in patients with refractory metastatic colorectal cancer. J Clin Oncol. 2010;28:3485-90.

54. Ishida Y, Agata Y, Shibahara K, Honjo T. Induced expression of PD-1, a novel member of the immunoglobulin gene superfamily, upon programmed cell death. EMBO J. 1992;11:3887-95.

55. Chemnitz JM, Parry RV, Nichols KE, June CH, Riley JL. SHP-1 and SHP-2 associate with immunoreceptor tyrosine-based switch motif of programmed death 1 upon primary human T cell stimulation, but only receptor ligation prevents T cell activation. J Immunol. 2004;173:945-54.

56. Patsoukis N, Brown J, Petkova V, Liu F, Li L, Boussiotis VA. Selective effects of PD-1 on Akt and Ras pathways regulate molecular components of the cell cycle and inhibit T cell proliferation. Sci Signal. 2012;5:ra46.

57. Chen L, Han X. Anti-PD-1/PD-L1 therapy of human cancer: past, present, and future. J Clin Invest. 2015;125:3384-91.

58. Wherry EJ, Ha SJ, Kaech SM, Haining WN, Sarkar S, Kalia V, Subramaniam S, Blattman JN, Barber DL, Ahmed R. Molecular signature of CD8+ T cell exhaustion during chronic viral infection. Immunity. 2007;27:670-84.

59. Ha SJ, Mueller SN, Wherry EJ, Barber DL, Aubert RD, Sharpe AH, Freeman GJ, Ahmed R. Enhancing therapeutic vaccination by blocking PD-1-mediated inhibitory signals during chronic infection. J Exp Med. 2008;205:543-55.

60. Zou W, Wolchok JD, Chen L. PD-L1 (B7-H1) and PD-1 pathway blockade for cancer therapy: Mechanisms, response biomarkers, and combinations. Sci Transl Med. 2016;8:328rv4.

61. Patsoukis N, Li L, Sari D, Petkova V, Boussiotis VA. PD-1 increases PTEN phosphatase activity while decreasing PTEN protein stability by inhibiting casein kinase 2. Mol Cell Biol. 2013;33:3091-8.

62. Pilon-Thomas S, Mackay A, Vohra N, Mule JJ. Blockade of programmed death ligand 1 enhances the therapeutic efficacy of combination immunotherapy against melanoma. J Immunol. 2010;184:3442-9.

63. Deng L, Liang H, Burnette B, Beckett M, Darga T, Weichselbaum RR, Fu YX. Irradiation and anti-PD-L1 treatment synergistically promote antitumor immunity in mice. J Clin Invest. 2014;124:687-95.

64. Postow MA, Callahan MK, Wolchok JD. Immune Checkpoint Blockade in Cancer Therapy. J Clin Oncol. 2015;33:1974-82.

65. Johnson DB, Peng C, Sosman JA. Nivolumab in melanoma: latest evidence and clinical potential. Ther Adv Med Oncol. 2015;7:97-106.

66. Li Q, Normolle DP, Sayre DM, Zeng X, Sun R, Jiang G, Redman BD, Chang AE. Immunological effects of BCG as an adjuvant in autologous tumor vaccines. Clin Immunol. 2000;94:64-72.

67. Morton DL, Hsueh EC, Essner R, Foshag LJ, O'Day SJ, Bilchik A, Gupta RK, Hoon DS, Ravindranath M, Nizze JA, Gammon G, Wanek LA, Wang HJ, Elashoff RM. Prolonged survival of patients receiving active immunotherapy with Canvaxin therapeutic polyvalent vaccine after complete resection of melanoma metastatic to regional lymph nodes. Ann Surg. 2002;236:438-48; discussion 48-9.

68. Small EJ, Schellhammer PF, Higano CS, Redfern CH, Nemunaitis JJ, Valone FH, Verjee SS, Jones LA, Hershberg RM. Placebo-controlled phase III trial of immunologic therapy with sipuleucel-T (APC8015) in patients with metastatic, asymptomatic hormone refractory prostate cancer. J Clin Oncol. 2006;24:3089-94.

69. Coulie PG, Van den Eynde BJ, van der Bruggen P, Boon T. Tumour antigens recognized by T lymphocytes: at the core of cancer immunotherapy. Nat Rev Cancer. 2014;14:135-46.

70. Kaczanowska S, Joseph AM, Davila E. TLR agonists: our best frenemy in cancer immunotherapy. J Leukoc Biol. 2013;93:847-63.

71. Schwartzentruber DJ, Lawson DH, Richards JM, Conry RM, Miller DM, Treisman J, Gailani F, Riley L, Conlon K, Pockaj B, Kendra KL, White RL, Gonzalez R, Kuzel TM, Curti B, Leming PD, Whitman ED, Balkissoon J, Reintgen DS, Kaufman H, Marincola FM, Merino MJ, Rosenberg SA, Choyke P, Vena D, Hwu P. gp100

peptide vaccine and interleukin-2 in patients with advanced melanoma. N Engl J Med. 2011;364:2119-27.

72. Oshita C, Takikawa M, Kume A, Miyata H, Ashizawa T, Iizuka A, Kiyohara Y, Yoshikawa S, Tanosaki R, Yamazaki N, Yamamoto A, Takesako K, Yamaguchi K, Akiyama Y. Dendritic cell-based vaccination in metastatic melanoma patients: phase II clinical trial. Oncol Rep. 2012;28:1131-8.

73. Uram JN, Le DT. Current advances in immunotherapy for pancreatic cancer. Curr Probl Cancer. 2013;37:273-9.

74. Kirner A, Mayer-Mokler A, Reinhardt C. IMA901: a multi-peptide cancer vaccine for treatment of renal cell cancer. Hum Vaccin Immunother. 2014;10:3179-89.

75. Yang B, Jeang J, Yang A, Wu TC, Hung CF. DNA vaccine for cancer immunotherapy. Hum Vaccin Immunother. 2014;10:3153-64.

76. Sardesai NY, Weiner DB. Electroporation delivery of DNA vaccines: prospects for success. Curr Opin Immunol. 2011;23:421-9.

77. Bergman PJ, McKnight J, Novosad A, Charney S, Farrelly J, Craft D, Wulderk M, Jeffers Y, Sadelain M, Hohenhaus AE, Segal N, Gregor P, Engelhorn M, Riviere I, Houghton AN, Wolchok JD. Long-term survival of dogs with advanced malignant melanoma after DNA vaccination with xenogeneic human tyrosinase: a phase I trial. Clin Cancer Res. 2003;9:1284-90.

78. Yuan J, Ku GY, Gallardo HF, Orlandi F, Manukian G, Rasalan TS, Xu Y, Li H, Vyas S, Mu Z, Chapman PB, Krown SE, Panageas K, Terzulli SL, Old LJ, Houghton AN, Wolchok JD. Safety and immunogenicity of a human and mouse gp100 DNA vaccine in a phase I trial of patients with melanoma. Cancer Immun. 2009;9:5.

79. Fioretti D, Iurescia S, Fazio VM, Rinaldi M. DNA vaccines: developing new strategies against cancer. J Biomed Biotechnol. 2010;2010:174378.

80. McNamara MA, Nair SK, Holl EK. RNA-Based Vaccines in Cancer Immunotherapy. J Immunol Res. 2015;2015:794528.

81. Weide B, Carralot JP, Reese A, Scheel B, Eigentler TK, Hoerr I, Rammensee HG, Garbe C, Pascolo S. Results of the first phase I/II clinical vaccination trial with direct injection of mRNA. J Immunother. 2008;31:180-8.

82. Geiger C, Regn S, Weinzierl A, Noessner E, Schendel DJ. A generic RNA-pulsed dendritic cell vaccine strategy for renal cell carcinoma. J Transl Med. 2005;3:29.

83. Bhatia S, Tykodi SS, Thompson JA. Treatment of metastatic melanoma: an overview. Oncology (Williston Park). 2009;23:488-96.

84. Sugamura K, Asao H, Kondo M, Tanaka N, Ishii N, Ohbo K, Nakamura M, Takeshita T. The interleukin-2 receptor gamma chain: its role in the multiple cytokine receptor complexes and T cell development in XSCID. Annu Rev Immunol. 1996;14:179-205.

85. Boyman O, Sprent J. The role of interleukin-2 during homeostasis and activation of the immune system. Nat Rev Immunol. 2012;12:180-90.

86. Rosenberg SA, Dudley ME. Adoptive cell therapy for the treatment of patients with metastatic melanoma. Curr Opin Immunol. 2009;21:233-40.

87. Vetto JT, Papa MZ, Lotze MT, Chang AE, Rosenberg SA. Reduction of toxicity of interleukin-2 and lymphokine-activated killer cells in humans by the administration of corticosteroids. J Clin Oncol. 1987;5:496-503.

88. Niu N, Qin X. New insights into IL-7 signaling pathways during early and late T cell development. Cell Mol Immunol. 2013;10:187-9.

89. Goetz CA, Harmon IR, O'Neil JJ, Burchill MA, Farrar MA. STAT5 activation underlies IL7 receptor-dependent B cell development. J Immunol. 2004;172:4770-8.

90. Michaud A, Dardari R, Charrier E, Cordeiro P, Herblot S, Duval M. IL-7 enhances survival of human CD56bright NK cells. J Immunother. 2010;33:382-90.

91. van Lent AU, Dontje W, Nagasawa M, Siamari R, Bakker AQ, Pouw SM, Maijoor KA, Weijer K, Cornelissen JJ, Blom B, Di Santo JP, Spits H, Legrand N. IL-7 enhances thymic human T cell development in "human immune system" Rag2-/-IL-2Rgammac-/- mice without affecting peripheral T cell homeostasis. J Immunol. 2009;183:7645-55.

92. Jiang Q, Li WQ, Hofmeister RR, Young HA, Hodge DR, Keller JR, Khaled AR, Durum SK. Distinct regions of the interleukin-7 receptor regulate different Bcl2 family members. Mol Cell Biol. 2004;24:6501-13.

93. Alderson MR, Sassenfeld HM, Widmer MB. Interleukin 7 enhances cytolytic T lymphocyte generation and induces lymphokine-activated killer cells from human peripheral blood. J Exp Med. 1990;172:577-87.

94. Gao J, Zhao L, Wan YY, Zhu B. Mechanism of Action of IL-7 and Its Potential Applications and Limitations in Cancer Immunotherapy. Int J Mol Sci. 2015;16:10267-80.

95. Rosenberg SA, Sportes C, Ahmadzadeh M, Fry TJ, Ngo LT, Schwarz SL, Stetler-Stevenson M, Morton KE, Mavroukakis SA, Morre M, Buffet R, Mackall CL,

Gress RE. IL-7 administration to humans leads to expansion of CD8+ and CD4+ cells but a relative decrease of CD4+ T-regulatory cells. J Immunother. 2006;29:313-9.

96. Sportes C, Hakim FT, Memon SA, Zhang H, Chua KS, Brown MR, Fleisher TA, Krumlauf MC, Babb RR, Chow CK, Fry TJ, Engels J, Buffet R, Morre M, Amato RJ, Venzon DJ, Korngold R, Pecora A, Gress RE, Mackall CL. Administration of rhIL-7 in humans increases in vivo TCR repertoire diversity by preferential expansion of naive T cell subsets. J Exp Med. 2008;205:1701-14.

97. Grabstein KH, Eisenman J, Shanebeck K, Rauch C, Srinivasan S, Fung V, Beers C, Richardson J, Schoenborn MA, Ahdieh M, et al. Cloning of a T cell growth factor that interacts with the beta chain of the interleukin-2 receptor. Science. 1994;264:965-8.

98. Fehniger TA, Caligiuri MA. Interleukin 15: biology and relevance to human disease. Blood. 2001;97:14-32.

99. Colpitts SL, Stoklasek TA, Plumlee CR, Obar JJ, Guo C, Lefrancois L. Cutting edge: the role of IFN-alpha receptor and MyD88 signaling in induction of IL-15 expression in vivo. J Immunol. 2012;188:2483-7.

100. Abadie V, Jabri B. IL-15: a central regulator of celiac disease immunopathology. Immunol Rev. 2014;260:221-34.

101. Inoue S, Unsinger J, Davis CG, Muenzer JT, Ferguson TA, Chang K, Osborne DF, Clark AT, Coopersmith CM, McDunn JE, Hotchkiss RS. IL-15 prevents apoptosis, reverses innate and adaptive immune dysfunction, and improves survival in sepsis. J Immunol. 2010;184:1401-9.

102. Spolski R, Leonard WJ. Interleukin-21: a double-edged sword with therapeutic potential. Nat Rev Drug Discov. 2014;13:379-95.

103. Wan CK, Andraski AB, Spolski R, Li P, Kazemian M, Oh J, Samsel L, Swanson PA, 2nd, McGavern DB, Sampaio EP, Freeman AF, Milner JD, Holland SM, Leonard WJ. Opposing roles of STAT1 and STAT3 in IL-21 function in CD4+ T cells. Proc Natl Acad Sci U S A. 2015;112:9394-9.

104. Pene J, Gauchat JF, Lecart S, Drouet E, Guglielmi P, Boulay V, Delwail A, Foster D, Lecron JC, Yssel H. Cutting edge: IL-21 is a switch factor for the production of IgG1 and IgG3 by human B cells. J Immunol. 2004;172:5154-7.

105. Parrish-Novak J, Foster DC, Holly RD, Clegg CH. Interleukin-21 and the IL-21 receptor: novel effectors of NK and T cell responses. J Leukoc Biol. 2002;72:856-63.

106. Liu Z, Yang L, Cui Y, Wang X, Guo C, Huang Z, Kan Q, Liu Z, Liu Y. Il-21 enhances NK cell activation and cytolytic activity and induces Th17 cell differentiation in inflammatory bowel disease. Inflamm Bowel Dis. 2009;15:1133-44.

107. Mittal A, Murugaiyan G, Beynon V, Hu D, Weiner HL. IL-27 induction of IL-21 from human CD8+ T cells induces granzyme B in an autocrine manner. Immunol Cell Biol. 2012;90:831-5.

108. Croce M, Rigo V, Ferrini S. IL-21: a pleiotropic cytokine with potential applications in oncology. J Immunol Res. 2015;2015:696578.

109. Li Y, Yee C. IL-21 mediated Foxp3 suppression leads to enhanced generation of antigen-specific CD8+ cytotoxic T lymphocytes. Blood. 2008;111:229-35.

110. Caligiuri MA. Human natural killer cells. Blood. 2008;112:461-9.

111. Pegram HJ, Andrews DM, Smyth MJ, Darcy PK, Kershaw MH. Activating and inhibitory receptors of natural killer cells. Immunol Cell Biol. 2011;89:216-24.

112. Cheng M, Chen Y, Xiao W, Sun R, Tian Z. NK cell-based immunotherapy for malignant diseases. Cell Mol Immunol. 2013;10:230-52.

113. Liu Y, Wu HW, Sheard MA, Sposto R, Somanchi SS, Cooper LJ, Lee DA, Seeger RC. Growth and activation of natural killer cells ex vivo from children with neuroblastoma for adoptive cell therapy. Clin Cancer Res. 2013;19:2132-43.

114. Pende D, Marcenaro S, Falco M, Martini S, Bernardo ME, Montagna D, Romeo E, Cognet C, Martinetti M, Maccario R, Mingari MC, Vivier E, Moretta L, Locatelli F, Moretta A. Anti-leukemia activity of alloreactive NK cells in KIR ligand-mismatched haploidentical HSCT for pediatric patients: evaluation of the functional role of activating KIR and redefinition of inhibitory KIR specificity. Blood. 2009;113:3119-29.

115. Lim O, Jung MY, Hwang YK, Shin EC. Present and Future of Allogeneic Natural Killer Cell Therapy. Front Immunol. 2015;6:286.

116. Irie RF, DeNunzio FD. Immunotherapy of melanoma: current status and prospects for the future. J Dermatol. 1993;20:65-73.

117. Cheever MA, Greenberg PD, Fefer A. Specific adoptive therapy of established leukemia with syngeneic lymphocytes sequentially immunized in vivo and in vitro and nonspecifically expanded by culture with Interleukin 2. J Immunol. 1981;126:1318-22.

118. Eberlein TJ, Rosenstein M, Spiess P, Wesley R, Rosenberg SA. Adoptive chemoimmunotherapy of a syngeneic murine lymphoma with long-term lymphoid cell lines expanded in T cell growth factor. Cancer Immunol Immunother. 1982;13:5-13.

119. Rosenberg SA. IL-2: the first effective immunotherapy for human cancer. J Immunol. 2014;192:5451-8.

120. Rosenberg SA, Packard BS, Aebersold PM, Solomon D, Topalian SL, Toy ST, Simon P, Lotze MT, Yang JC, Seipp CA, et al. Use of tumor-infiltrating lymphocytes and interleukin-2 in the immunotherapy of patients with metastatic melanoma. A preliminary report. N Engl J Med. 1988;319:1676-80.

121. Wu R, Forget MA, Chacon J, Bernatchez C, Haymaker C, Chen JQ, Hwu P, Radvanyi LG. Adoptive T-cell therapy using autologous tumor-infiltrating lymphocytes for metastatic melanoma: current status and future outlook. Cancer J. 2012;18:160-75.

122. Forget MA, Malu S, Liu H, Toth C, Maiti S, Kale C, Haymaker C, Bernatchez C, Huls H, Wang E, Marincola FM, Hwu P, Cooper LJ, Radvanyi LG. Activation and propagation of tumor-infiltrating lymphocytes on clinical-grade designer artificial antigen-presenting cells for adoptive immunotherapy of melanoma. J Immunother. 2014;37:448-60.

123. Dudley ME, Wunderlich JR, Robbins PF, Yang JC, Hwu P, Schwartzentruber DJ, Topalian SL, Sherry R, Restifo NP, Hubicki AM, Robinson MR, Raffeld M, Duray P, Seipp CA, Rogers-Freezer L, Morton KE, Mavroukakis SA, White DE, Rosenberg SA. Cancer regression and autoimmunity in patients after clonal repopulation with antitumor lymphocytes. Science. 2002;298:850-4.

124. Dudley ME, Wunderlich JR, Yang JC, Hwu P, Schwartzentruber DJ, Topalian SL, Sherry RM, Marincola FM, Leitman SF, Seipp CA, Rogers-Freezer L, Morton KE, Nahvi A, Mavroukakis SA, White DE, Rosenberg SA. A phase I study of

nonmyeloablative chemotherapy and adoptive transfer of autologous tumor antigen-specific T lymphocytes in patients with metastatic melanoma. J Immunother. 2002;25:243-51.

125. Dudley ME, Yang JC, Sherry R, Hughes MS, Royal R, Kammula U, Robbins PF, Huang J, Citrin DE, Leitman SF, Wunderlich J, Restifo NP, Thomasian A, Downey SG, Smith FO, Klapper J, Morton K, Laurencot C, White DE, Rosenberg SA. Adoptive cell therapy for patients with metastatic melanoma: evaluation of intensive myeloablative chemoradiation preparative regimens. J Clin Oncol. 2008;26:5233-9.

126. Gros A, Robbins PF, Yao X, Li YF, Turcotte S, Tran E, Wunderlich JR, Mixon A, Farid S, Dudley ME, Hanada K, Almeida JR, Darko S, Douek DC, Yang JC, Rosenberg SA. PD-1 identifies the patient-specific CD8(+) tumor-reactive repertoire infiltrating human tumors. J Clin Invest. 2014;124:2246-59.

127. Pedron B, Duval M, Elbou OM, Moskwa M, Jambou M, Vilmer E, Sterkers G. Common genomic HLA haplotypes contributing to successful donor search in unrelated hematopoietic transplantation. Bone Marrow Transplant. 2003;31:423-7.

128. Pandolfi F, Boyle LA, Trentin L, Kurnick JT, Isselbacher KJ, Gattoni-Celli S. Expression of HLA-A2 antigen in human melanoma cell lines and its role in T-cell recognition. Cancer Res. 1991;51:3164-70.

129. Kittlesen DJ, Thompson LW, Gulden PH, Skipper JC, Colella TA, Shabanowitz J, Hunt DF, Engelhard VH, Slingluff CL, Jr. Human melanoma patients recognize an HLA-A1-restricted CTL epitope from tyrosinase containing two cysteine residues: implications for tumor vaccine development. J Immunol. 1998;160:2099-106.

130. Topalian SL, Solomon D, Avis FP, Chang AE, Freerksen DL, Linehan WM, Lotze MT, Robertson CN, Seipp CA, Simon P, et al. Immunotherapy of patients with advanced cancer using tumor-infiltrating lymphocytes and recombinant interleukin-2: a pilot study. J Clin Oncol. 1988;6:839-53.

131. Dudley ME, Wunderlich JR, Shelton TE, Even J, Rosenberg SA. Generation of tumor-infiltrating lymphocyte cultures for use in adoptive transfer therapy for melanoma patients. J Immunother. 2003;26:332-42.

132. Dudley ME, Wunderlich JR, Yang JC, Sherry RM, Topalian SL, Restifo NP, Royal RE, Kammula U, White DE, Mavroukakis SA, Rogers LJ, Gracia GJ, Jones SA, Mangiameli DP, Pelletier MM, Gea-Banacloche J, Robinson MR, Berman DM, Filie AC, Abati A, Rosenberg SA. Adoptive cell transfer therapy following non-myeloablative but lymphodepleting chemotherapy for the treatment of patients with refractory metastatic melanoma. J Clin Oncol. 2005;23:2346-57.

133. Goff SL, Dudley ME, Citrin DE, Somerville RP, Wunderlich JR, Danforth DN, Zlott DA, Yang JC, Sherry RM, Kammula US, Klebanoff CA, Hughes MS, Restifo NP, Langhan MM, Shelton TE, Lu L, Kwong ML, Ilyas S, Klemen ND, Payabyab EC, Morton KE, Toomey MA, Steinberg SM, White DE, Rosenberg SA. Randomized, Prospective Evaluation Comparing Intensity of Lymphodepletion Before Adoptive Transfer of Tumor-Infiltrating Lymphocytes for Patients With Metastatic Melanoma. J Clin Oncol. 2016.

134. Radvanyi LG, Bernatchez C, Zhang M, Fox PS, Miller P, Chacon J, Wu R, Lizee G, Mahoney S, Alvarado G, Glass M, Johnson VE, McMannis JD, Shpall E, Prieto V, Papadopoulos N, Kim K, Homsi J, Bedikian A, Hwu WJ, Patel S, Ross MI,

Lee JE, Gershenwald JE, Lucci A, Royal R, Cormier JN, Davies MA, Mansaray R, Fulbright OJ, Toth C, Ramachandran R, Wardell S, Gonzalez A, Hwu P. Specific lymphocyte subsets predict response to adoptive cell therapy using expanded autologous tumor-infiltrating lymphocytes in metastatic melanoma patients. Clin Cancer Res. 2012;18:6758-70.

135. Gajewski TF, Schreiber H, Fu YX. Innate and adaptive immune cells in the tumor microenvironment. Nat Immunol. 2013;14:1014-22.

136. Nicol AJ, Tokuyama H, Mattarollo SR, Hagi T, Suzuki K, Yokokawa K, Nieda M. Clinical evaluation of autologous gamma delta T cell-based immunotherapy for metastatic solid tumours. Br J Cancer. 2011;105:778-86.

137. Obar JJ, Lefrancois L. Memory CD8+ T cell differentiation. Ann N Y Acad Sci. 2010;1183:251-66.

138. Daniels MA, Teixeiro E. TCR Signaling in T Cell Memory. Front Immunol. 2015;6:617.

139. Tomiyama H, Matsuda T, Takiguchi M. Differentiation of human CD8(+) T cells from a memory to memory/effector phenotype. J Immunol. 2002;168:5538-50.

140. Plunkett FJ, Franzese O, Finney HM, Fletcher JM, Belaramani LL, Salmon M, Dokal I, Webster D, Lawson AD, Akbar AN. The loss of telomerase activity in highly differentiated CD8+CD28-CD27- T cells is associated with decreased Akt (Ser473) phosphorylation. J Immunol. 2007;178:7710-9.

141. Haymaker CL, Wu RC, Ritthipichai K, Bernatchez C, Forget MA, Chen JQ, Liu H, Wang E, Marincola F, Hwu P, Radvanyi LG. BTLA marks a less-differentiated

tumor-infiltrating lymphocyte subset in melanoma with enhanced survival properties. Oncoimmunology. 2015;4:e1014246.

142. Legat A, Speiser DE, Pircher H, Zehn D, Fuertes Marraco SA. Inhibitory Receptor Expression Depends More Dominantly on Differentiation and Activation than "Exhaustion" of Human CD8 T Cells. Front Immunol. 2013;4:455.

143. Zhou J, Dudley ME, Rosenberg SA, Robbins PF. Persistence of multiple tumor-specific T-cell clones is associated with complete tumor regression in a melanoma patient receiving adoptive cell transfer therapy. J Immunother. 2005;28:53-62.

144. Gattinoni L, Lugli E, Ji Y, Pos Z, Paulos CM, Quigley MF, Almeida JR, Gostick E, Yu Z, Carpenito C, Wang E, Douek DC, Price DA, June CH, Marincola FM, Roederer M, Restifo NP. A human memory T cell subset with stem cell-like properties. Nat Med. 2011;17:1290-7.

145. Barrett DM, Singh N, Porter DL, Grupp SA, June CH. Chimeric antigen receptor therapy for cancer. Annu Rev Med. 2014;65:333-47.

146. Srivastava S, Riddell SR. Engineering CAR-T cells: Design concepts. Trends Immunol. 2015;36:494-502.

147. Lorentzen CL, Straten PT. CD19-Chimeric Antigen Receptor T Cells for Treatment of Chronic Lymphocytic Leukaemia and Acute Lymphoblastic Leukaemia. Scand J Immunol. 2015;82:307-19.

148. Wang QS, Wang Y, Lv HY, Han QW, Fan H, Guo B, Wang LL, Han WD. Treatment of CD33-directed chimeric antigen receptor-modified T cells in one patient with relapsed and refractory acute myeloid leukemia. Mol Ther. 2015;23:184-91.

149. Tettamanti S, Biondi A, Biagi E, Bonnet D. CD123 AML targeting by chimeric antigen receptors: A novel magic bullet for AML therapeutics? Oncoimmunology. 2014;3:e28835.

150. Morgan RA, Yang JC, Kitano M, Dudley ME, Laurencot CM, Rosenberg SA. Case report of a serious adverse event following the administration of T cells transduced with a chimeric antigen receptor recognizing ERBB2. Mol Ther. 2010;18:843-51.

151. Yee C, Lizee G, Schueneman AJ. Endogenous T-Cell Therapy: Clinical Experience. Cancer J. 2015;21:492-500.

152. Pollack SM, Jones RL, Farrar EA, Lai IP, Lee SM, Cao J, Pillarisetty VG, Hoch BL, Gullett A, Bleakley M, Conrad EU, 3rd, Eary JF, Shibuya KC, Warren EH, Carstens JN, Heimfeld S, Riddell SR, Yee C. Tetramer guided, cell sorter assisted production of clinical grade autologous NY-ESO-1 specific CD8(+) T cells. J Immunother Cancer. 2014;2:36.

153. Lizee G, Overwijk WW, Radvanyi L, Gao J, Sharma P, Hwu P. Harnessing the power of the immune system to target cancer. Annu Rev Med. 2013;64:71-90.

154. Hinrichs CS, Borman ZA, Gattinoni L, Yu Z, Burns WR, Huang J, Klebanoff CA, Johnson LA, Kerkar SP, Yang S, Muranski P, Palmer DC, Scott CD, Morgan RA, Robbins PF, Rosenberg SA, Restifo NP. Human effector CD8+ T cells derived from naive rather than memory subsets possess superior traits for adoptive immunotherapy. Blood. 2011;117:808-14.

155. Li Y, Bleakley M, Yee C. IL-21 influences the frequency, phenotype, and affinity of the antigen-specific CD8 T cell response. J Immunol. 2005;175:2261-9.

156. Locker GY, Hamilton S, Harris J, Jessup JM, Kemeny N, Macdonald JS, Somerfield MR, Hayes DF, Bast RC, Jr., Asco. ASCO 2006 update of recommendations for the use of tumor markers in gastrointestinal cancer. J Clin Oncol. 2006;24:5313-27.

157. Galon J, Mlecnik B, Bindea G, Angell HK, Berger A, Lagorce C, Lugli A, Zlobec I, Hartmann A, Bifulco C, Nagtegaal ID, Palmqvist R, Masucci GV, Botti G, Tatangelo F, Delrio P, Maio M, Laghi L, Grizzi F, Asslaber M, D'Arrigo C, Vidal-Vanaclocha F, Zavadova E, Chouchane L, Ohashi PS, Hafezi-Bakhtiari S, Wouters BG, Roehrl M, Nguyen L, Kawakami Y, Hazama S, Okuno K, Ogino S, Gibbs P, Waring P, Sato N, Torigoe T, Itoh K, Patel PS, Shukla SN, Wang Y, Kopetz S, Sinicrope FA, Scripcariu V, Ascierto PA, Marincola FM, Fox BA, Pages F. Towards the introduction of the 'Immunoscore' in the classification of malignant tumours. J Pathol. 2014;232:199-209.

158. Fridman WH, Pages F, Sautes-Fridman C, Galon J. The immune contexture in human tumours: impact on clinical outcome. Nat Rev Cancer. 2012;12:298-306.

159. Chen L, Flies DB. Molecular mechanisms of T cell co-stimulation and co-inhibition. Nat Rev Immunol. 2013;13:227-42.

160. Bremer E. Targeting of the tumor necrosis factor receptor superfamily for cancer immunotherapy. ISRN Oncol. 2013;2013:371854.

161. Melero I, Murillo O, Dubrot J, Hervas-Stubbs S, Perez-Gracia JL. Multi-layered action mechanisms of CD137 (4-1BB)-targeted immunotherapies. Trends Pharmacol Sci. 2008;29:383-90.

162. Jung HW, Choi SW, Choi JI, Kwon BS. Serum concentrations of soluble 4-1BB and 4-1BB ligand correlated with the disease severity in rheumatoid arthritis. Exp Mol Med. 2004;36:13-22.

163. Lee HW, Park SJ, Choi BK, Kim HH, Nam KO, Kwon BS. 4-1BB promotes the survival of CD8+ T lymphocytes by increasing expression of Bcl-xL and Bfl-1. J Immunol. 2002;169:4882-8.

164. Guinn BA, DeBenedette MA, Watts TH, Berinstein NL. 4-1BBL cooperates with B7-1 and B7-2 in converting a B cell lymphoma cell line into a long-lasting antitumor vaccine. J Immunol. 1999;162:5003-10.

165. Chacon JA, Sarnaik AA, Chen JQ, Creasy C, Kale C, Robinson J, Weber J, Hwu P, Pilon-Thomas S, Radvanyi L. Manipulating the tumor microenvironment ex vivo for enhanced expansion of tumor-infiltrating lymphocytes for adoptive cell therapy. Clin Cancer Res. 2015;21:611-21.

166. Elgueta R, Benson MJ, de Vries VC, Wasiuk A, Guo Y, Noelle RJ. Molecular mechanism and function of CD40/CD40L engagement in the immune system. Immunol Rev. 2009;229:152-72.

167. Saemann MD, Diakos C, Kelemen P, Kriehuber E, Zeyda M, Bohmig GA, Horl WH, Baumruker T, Zlabinger GJ. Prevention of CD40-triggered dendritic cell maturation and induction of T-cell hyporeactivity by targeting of Janus kinase 3. Am J Transplant. 2003;3:1341-9.

168. Ahmadi T, Flies A, Efebera Y, Sherr DH. CD40 Ligand-activated, antigen-specific B cells are comparable to mature dendritic cells in presenting protein antigens

and major histocompatibility complex class I- and class II-binding peptides. Immunology. 2008;124:129-40.

169. Johnson-Leger C, Christensen J, Klaus GG. CD28 co-stimulation stabilizes the expression of the CD40 ligand on T cells. Int Immunol. 1998;10:1083-91.

170. Vonderheide RH, Glennie MJ. Agonistic CD40 antibodies and cancer therapy. Clin Cancer Res. 2013;19:1035-43.

171. Borst J, Hendriks J, Xiao Y. CD27 and CD70 in T cell and B cell activation. Curr Opin Immunol. 2005;17:275-81.

172. Denoeud J, Moser M. Role of CD27/CD70 pathway of activation in immunity and tolerance. J Leukoc Biol. 2011;89:195-203.

173. Dolfi DV, Boesteanu AC, Petrovas C, Xia D, Butz EA, Katsikis PD. Late signals from CD27 prevent Fas-dependent apoptosis of primary CD8+ T cells. J Immunol. 2008;180:2912-21.

174. Claus C, Riether C, Schurch C, Matter MS, Hilmenyuk T, Ochsenbein AF. CD27 signaling increases the frequency of regulatory T cells and promotes tumor growth. Cancer Res. 2012;72:3664-76.

175. Shimizu K, Kurosawa Y, Taniguchi M, Steinman RM, Fujii S. Cross-presentation of glycolipid from tumor cells loaded with alpha-galactosylceramide leads to potent and long-lived T cell mediated immunity via dendritic cells. J Exp Med. 2007;204:2641-53.

176. van de Ven K, Borst J. Targeting the T-cell co-stimulatory CD27/CD70 pathway in cancer immunotherapy: rationale and potential. Immunotherapy. 2015;7:655-67.

177. Sharpe AH, Freeman GJ. The B7-CD28 superfamily. Nat Rev Immunol. 2002;2:116-26.

178. Boomer JS, Green JM. An enigmatic tail of CD28 signaling. Cold Spring Harbor perspectives in biology. 2010;2:a002436.

179. Kerstan A, Hunig T. Cutting edge: distinct TCR- and CD28-derived signals regulate CD95L, Bcl-xL, and the survival of primary T cells. J Immunol. 2004;172:1341-5.

180. Rudd CE, Schneider H. Unifying concepts in CD28, ICOS and CTLA4 co-receptor signalling. Nat Rev Immunol. 2003;3:544-56.

181. Li J, Heinrichs J, Leconte J, Haarberg K, Semple K, Liu C, Gigoux M, Kornete M, Piccirillo CA, Suh WK, Yu XZ. Phosphatidylinositol 3-kinase-independent signaling pathways contribute to ICOS-mediated T cell costimulation in acute graft-versus-host disease in mice. J Immunol. 2013;191:200-7.

182. Chen L. Co-inhibitory molecules of the B7-CD28 family in the control of T-cell immunity. Nat Rev Immunol. 2004;4:336-47.

183. Lee SJ, Jang BC, Lee SW, Yang YI, Suh SI, Park YM, Oh S, Shin JG, Yao S, Chen L, Choi IH. Interferon regulatory factor-1 is prerequisite to the constitutive expression and IFN-γ-induced upregulation of B7-H1 (CD274). FEBS Lett. 2006;580:755-62.

184. Linsley PS, Bradshaw J, Greene J, Peach R, Bennett KL, Mittler RS. Intracellular trafficking of CTLA-4 and focal localization towards sites of TCR engagement. Immunity. 1996;4:535-43.

185. Bjoern J, Juul Nitschke N, Zeeberg Iversen T, Schmidt H, Fode K, Svane IM. Immunological correlates of treatment and response in stage IV malignant melanoma patients treated with Ipilimumab. Oncoimmunology. 2016;5:e1100788.

186. Watanabe N, Gavrieli M, Sedy JR, Yang J, Fallarino F, Loftin SK, Hurchla MA, Zimmerman N, Sim J, Zang X, Murphy TL, Russell JH, Allison JP, Murphy KM. BTLA is a lymphocyte inhibitory receptor with similarities to CTLA-4 and PD-1. Nat Immunol. 2003;4:670-9.

187. Sedy JR, Gavrieli M, Potter KG, Hurchla MA, Lindsley RC, Hildner K, Scheu S, Pfeffer K, Ware CF, Murphy TL, Murphy KM. B and T lymphocyte attenuator regulates T cell activation through interaction with herpesvirus entry mediator. Nat Immunol. 2005;6:90-8.

188. Murphy KM, Nelson CA, Sedy JR. Balancing co-stimulation and inhibition with BTLA and HVEM. Nat Rev Immunol. 2006;6:671-81.

189. Gavrieli M, Sedy J, Nelson CA, Murphy KM. BTLA and HVEM cross talk regulates inhibition and costimulation. Advances in immunology. 2006;92:157-85.

190. Murphy TL, Murphy KM. Slow down and survive: Enigmatic immunoregulation by BTLA and HVEM. Annu Rev Immunol.28:389-411.

191. Bekiaris V, Sedy JR, Macauley MG, Rhode-Kurnow A, Ware CF. The inhibitory receptor BTLA controls gammadelta T cell homeostasis and inflammatory responses. Immunity. 2013;39:1082-94.

192. Gavrieli M, Murphy KM. Association of Grb-2 and PI3K p85 with phosphotyrosile peptides derived from BTLA. Biochem Biophys Res Commun. 2006;345:1440-5.

193. Chemnitz JM, Lanfranco AR, Braunstein I, Riley JL. B and T lymphocyte attenuator-mediated signal transduction provides a potent inhibitory signal to primary human CD4 T cells that can be initiated by multiple phosphotyrosine motifs. J Immunol. 2006;176:6603-14.

194. Shubin NJ, Chung CS, Heffernan DS, Irwin LR, Monaghan SF, Ayala A. BTLA expression contributes to septic morbidity and mortality by inducing innate inflammatory cell dysfunction. J Leukoc Biol. 2012;92:593-603.

195. Shubin NJ, Monaghan SF, Heffernan DS, Chung CS, Ayala A. B and T lymphocyte attenuator expression on CD4+ T-cells associates with sepsis and subsequent infections in ICU patients. Crit Care. 2013;17:R276.

196. Truong W, Hancock WW, Plester JC, Merani S, Rayner DC, Thangavelu G, Murphy KM, Anderson CC, Shapiro AM. BTLA targeting modulates lymphocyte phenotype, function, and numbers and attenuates disease in nonobese diabetic mice. J Leukoc Biol. 2009;86:41-51.

197. Li S, Zhang M, Xiang F, Zhao J, Jiang C, Zhu J. Dendritic cells expressing BTLA induces CD8+ T cell tolerance and attenuates the severity of diabetes. Vaccine. 2011;29:7747-51.

198. Adler G, Steeg C, Pfeffer K, Murphy TL, Murphy KM, Langhorne J, Jacobs T. B and T lymphocyte attenuator restricts the protective immune response against experimental malaria. J Immunol. 2011;187:5310-9.

199. Albring JC, Sandau MM, Rapaport AS, Edelson BT, Satpathy A, Mashayekhi M, Lathrop SK, Hsieh CS, Stelljes M, Colonna M, Murphy TL, Murphy KM. Targeting

of B and T lymphocyte associated (BTLA) prevents graft-versus-host disease without global immunosuppression. J Exp Med. 2010;207:2551-9.

200. Tao R, Wang L, Han R, Wang T, Ye Q, Honjo T, Murphy TL, Murphy KM, Hancock WW. Differential effects of B and T lymphocyte attenuator and programmed death-1 on acceptance of partially versus fully MHC-mismatched cardiac allografts. J Immunol. 2005;175:5774-82.

201. Hurchla MA, Sedy JR, Murphy KM. Unexpected role of B and T lymphocyte attenuator in sustaining cell survival during chronic allostimulation. J Immunol. 2007;178:6073-82.

202. Yang C, Chen Y, Guo G, Li H, Cao D, Xu H, Guo S, Fei L, Yan W, Ning Q, Zheng L, Wu Y. Expression of B and T lymphocyte attenuator (BTLA) in macrophages contributes to the fulminant hepatitis caused by murine hepatitis virus strain-3. Gut. 2013;62:1204-13.

203. Oya Y, Watanabe N, Kobayashi Y, Owada T, Oki M, Ikeda K, Suto A, Kagami S, Hirose K, Kishimoto T, Nakajima H. Lack of B and T lymphocyte attenuator exacerbates autoimmune disorders and induces Fas-independent liver injury in MRL-lpr/lpr mice. Int Immunol. 2011;23:335-44.

204. Yang X, Zhang X, Sun Y, Tu T, Fu ML, Miller M, Fu YX. A BTLA-mediated bait and switch strategy permits Listeria expansion in CD8alpha(+) DCs to promote long-term T cell responses. Cell Host Microbe. 2014;16:68-80.

205. Wherry EJ, Kurachi M. Molecular and cellular insights into T cell exhaustion. Nat Rev Immunol. 2015;15:486-99.

206. Klebanoff CA, Scott CD, Leonardi AJ, Yamamoto TN, Cruz AC, Ouyang C, Ramaswamy M, Roychoudhuri R, Ji Y, Eil RL, Sukumar M, Crompton JG, Palmer DC, Borman ZA, Clever D, Thomas SK, Patel S, Yu Z, Muranski P, Liu H, Wang E, Marincola FM, Gros A, Gattinoni L, Rosenberg SA, Siegel RM, Restifo NP. Memory T cell-driven differentiation of naive cells impairs adoptive immunotherapy. J Clin Invest. 2016;126:318-34.

207. Derre L, Rivals JP, Jandus C, Pastor S, Rimoldi D, Romero P, Michielin O, Olive D, Speiser DE. BTLA mediates inhibition of human tumor-specific CD8+ T cells that can be partially reversed by vaccination. J Clin Invest. 2010;120:157-67.

208. Uchiyama M, Jin X, Matsuda H, Bashuda H, Imazuru T, Shimokawa T, Yagita H, Niimi M. An agonistic anti-BTLA mAb (3C10) induced generation of IL-10-dependent regulatory CD4+ T cells and prolongation of murine cardiac allograft. Transplantation. 2014;97:301-9.

209. Kannan S, Kurupati RK, Doyle SA, Freeman GJ, Schmader KE, Ertl HC. BTLA expression declines on B cells of the aged and is associated with low responsiveness to the trivalent influenza vaccine. Oncotarget. 2015;6:19445-55.

210. Agata Y, Kawasaki A, Nishimura H, Ishida Y, Tsubata T, Yagita H, Honjo T. Expression of the PD-1 antigen on the surface of stimulated mouse T and B lymphocytes. Int Immunol. 1996;8:765-72.

211. Geginat J, Lanzavecchia A, Sallusto F. Proliferation and differentiation potential of human CD8+ memory T-cell subsets in response to antigen or homeostatic cytokines. Blood. 2003;101:4260-6.

212. Shultz LD, Brehm MA, Garcia-Martinez JV, Greiner DL. Humanized mice for immune system investigation: progress, promise and challenges. Nat Rev Immunol. 2012;12:786-98.

213. Liadi I, Singh H, Romain G, Rey-Villamizar N, Merouane A, Adolacion JR, Kebriaei P, Huls H, Qiu P, Roysam B, Cooper LJ, Varadarajan N. Individual Motile CD4(+) T Cells Can Participate in Efficient Multikilling through Conjugation to Multiple Tumor Cells. Cancer immunology research. 2015;3:473-82.

214. Romain G, Senyukov V, Rey-Villamizar N, Merouane A, Kelton W, Liadi I, Mahendra A, Charab W, Georgiou G, Roysam B, Lee DA, Varadarajan N. Antibody Fc engineering improves frequency and promotes kinetic boosting of serial killing mediated by NK cells. Blood. 2014;124:3241-9.

215. Gertner-Dardenne J, Fauriat C, Orlanducci F, Thibult ML, Pastor S, Fitzgibbon J, Bouabdallah R, Xerri L, Olive D. The co-receptor BTLA negatively regulates human Vgamma9Vdelta2 T-cell proliferation: a potential way of immune escape for lymphoma cells. Blood. 2013;122:922-31.

216. Forget MA, Haymaker C, Dennison JB, Toth C, Maiti S, Fulbright OJ, Cooper LJ, Hwu P, Radvanyi LG, Bernatchez C. The beneficial effects of a gas-permeable flask for expansion of Tumor-Infiltrating lymphocytes as reflected in their mitochondrial function and respiration capacity. Oncoimmunology. 2016;5:e1057386.

217. Otsuki N, Kamimura Y, Hashiguchi M, Azuma M. Expression and function of the B and T lymphocyte attenuator (BTLA/CD272) on human T cells. Biochem Biophys Res Commun. 2006;344:1121-7.

218. Wu J, Motto DG, Koretzky GA, Weiss A. Vav and SLP-76 interact and functionally cooperate in IL-2 gene activation. Immunity. 1996;4:593-602.

219. Kobayashi Y, Iwata A, Suzuki K, Suto A, Kawashima S, Saito Y, Owada T, Kobayashi M, Watanabe N, Nakajima H. B and T lymphocyte attenuator inhibits LPS-induced endotoxic shock by suppressing Toll-like receptor 4 signaling in innate immune cells. Proc Natl Acad Sci U S A. 2013;110:5121-6.

220. Gavrieli M, Watanabe N, Loftin SK, Murphy TL, Murphy KM. Characterization of phosphotyrosine binding motifs in the cytoplasmic domain of B and T lymphocyte attenuator required for association with protein tyrosine phosphatases SHP-1 and SHP-2. Biochem Biophys Res Commun. 2003;312:1236-43.

221. Watanabe R, Harada Y, Takeda K, Takahashi J, Ohnuki K, Ogawa S, Ohgai D, Kaibara N, Koiwai O, Tanabe K, Toma H, Sugamura K, Abe R. Grb2 and Gads exhibit different interactions with CD28 and play distinct roles in CD28-mediated costimulation. J Immunol. 2006;177:1085-91.

222. Schlaepfer DD, Hunter T. Evidence for in vivo phosphorylation of the Grb2 SH2-domain binding site on focal adhesion kinase by Src-family protein-tyrosine kinases. Mol Cell Biol. 1996;16:5623-33.

223. Cush SS, Flano E. KLRG1+NKG2A+ CD8 T cells mediate protection and participate in memory responses during gamma-herpesvirus infection. J Immunol. 2011;186:4051-8.

224. Huang J, Khong HT, Dudley ME, El-Gamil M, Li YF, Rosenberg SA, Robbins PF. Survival, persistence, and progressive differentiation of adoptively transferred

tumor-reactive T cells associated with tumor regression. J Immunother. 2005;28:258-67.

225. Li Y, Liu S, Hernandez J, Vence L, Hwu P, Radvanyi L. MART-1-specific melanoma tumor-infiltrating lymphocytes maintaining CD28 expression have improved survival and expansion capability following antigenic restimulation in vitro. J Immunol. 2010;184:452-65.

226. Lugli E, Dominguez MH, Gattinoni L, Chattopadhyay PK, Bolton DL, Song K, Klatt NR, Brenchley JM, Vaccari M, Gostick E, Price DA, Waldmann TA, Restifo NP, Franchini G, Roederer M. Superior T memory stem cell persistence supports long-lived T cell memory. J Clin Invest. 2013;123:594-9.

227. Powell DJ, Jr., Dudley ME, Robbins PF, Rosenberg SA. Transition of late-stage effector T cells to CD27+ CD28+ tumor-reactive effector memory T cells in humans after adoptive cell transfer therapy. Blood. 2005;105:241-50.

228. van der Windt GJ, Everts B, Chang CH, Curtis JD, Freitas TC, Amiel E, Pearce EJ, Pearce EL. Mitochondrial respiratory capacity is a critical regulator of CD8+ T cell memory development. Immunity. 2012;36:68-78.

229. Marie-Andrée Forgeta CH, Jennifer B. Dennisonb, Christopher Totha, Sourindra Maitic, Orenthial J. Fulbrighta, Laurence J.N. Cooperc, Patrick Hwua, Laszlo G. Radvanyiade & Chantale Bernatcheza*. The beneficial effects of a gas-permeable flask for expansion of Tumor-Infiltrating lymphocytes as reflected in their mitochondrial function and respiration capacity. Oncoimmunology. 2015.

230. Dimeloe S, Mehling M, Frick C, Loeliger J, Bantug GR, Sauder U, Fischer M, Belle R, Develioglu L, Tay S, Langenkamp A, Hess C. The Immune-Metabolic Basis

of Effector Memory CD4+ T Cell Function under Hypoxic Conditions. J Immunol. 2016;196:106-14.

231. Jackman JK, Motto DG, Sun Q, Tanemoto M, Turck CW, Peltz GA, Koretzky GA, Findell PR. Molecular cloning of SLP-76, a 76-kDa tyrosine phosphoprotein associated with Grb2 in T cells. J Biol Chem. 1995;270:7029-32.

232. Harada Y, Ohgai D, Watanabe R, Okano K, Koiwai O, Tanabe K, Toma H, Altman A, Abe R. A single amino acid alteration in cytoplasmic domain determines IL-2 promoter activation by ligation of CD28 but not inducible costimulator (ICOS). J Exp Med. 2003;197:257-62.

233. Baitsch L, Legat A, Barba L, Fuertes Marraco SA, Rivals JP, Baumgaertner P, Christiansen-Jucht C, Bouzourene H, Rimoldi D, Pircher H, Rufer N, Matter M, Michielin O, Speiser DE. Extended co-expression of inhibitory receptors by human CD8 T-cells depending on differentiation, antigen-specificity and anatomical localization. PLoS One. 2012;7:e30852.

234. Boyman O, Cho JH, Sprent J. The role of interleukin-2 in memory CD8 cell differentiation. Advances in experimental medicine and biology. 2010;684:28-41.

235. Hand TW, Cui W, Jung YW, Sefik E, Joshi NS, Chandele A, Liu Y, Kaech SM. Differential effects of STAT5 and PI3K/AKT signaling on effector and memory CD8 T-cell survival. Proc Natl Acad Sci U S A. 2010;107:16601-6.

236. Crompton JG, Sukumar M, Roychoudhuri R, Clever D, Gros A, Eil RL, Tran E, Hanada K, Yu Z, Palmer DC, Kerkar SP, Michalek RD, Upham T, Leonardi A, Acquavella N, Wang E, Marincola FM, Gattinoni L, Muranski P, Sundrud MS, Klebanoff CA, Rosenberg SA, Fearon DT, Restifo NP. Akt inhibition enhances

expansion of potent tumor-specific lymphocytes with memory cell characteristics. Cancer Res. 2015;75:296-305.

237. Sukumar M, Liu J, Ji Y, Subramanian M, Crompton JG, Yu Z, Roychoudhuri R, Palmer DC, Muranski P, Karoly ED, Mohney RP, Klebanoff CA, Lal A, Finkel T, Restifo NP, Gattinoni L. Inhibiting glycolytic metabolism enhances CD8+ T cell memory and antitumor function. J Clin Invest. 2013;123:4479-88.

238. Scholz G, Jandus C, Zhang L, Grandclement C, Lopez-Mejia IC, Soneson C, Delorenzi M, Fajas L, Held W, Dormond O, Romero P. Modulation of mTOR Signalling Triggers the Formation of Stem Cell-like Memory T Cells. EBioMedicine. 2016;4:50-61.

239. Bassett JD, Swift SL, VanSeggelen H, Hammill JA, McGray AJ, Evelegh C, Wan Y, Bramson JL. Combined mTOR inhibition and OX40 agonism enhances CD8(+) T cell memory and protective immunity produced by recombinant adenovirus vaccines. Mol Ther. 2012;20:860-9.

CHAPTER 11: VITA

Krit Ritthipichai was born in Phetchabun, Thailand on November 4, 1981, the son of Samuth Noopeuak and Nongluck Noopeuak. He attended Kasetsart University, Bangkok, Thailand. He earned a Doctor of Veterinary Medicine with First Class Honors in March, 2006. In 2007, Krit worked as a research assistant at the department of microbiology and immunology under the guidance of Dr. Porntippa Lekchareounsuk, D.V.M., Ph.D. In August 2008, He entered the University of Maryland, College Park, where he received his Master of Science degree in Veterinary Medical Sciences, specializing in Molecular Virology under the guidance of Dr. Yanjin Zhang, D.V.M., Ph.D. After completing his Master's degree in 2011, he attended the Ph.D program in Immunology at The University of Texas Health Science Center-Houston, Graduate School of Biomedical Sciences, under the mentorship of Drs. Patrick Hwu, Chantale Bernatchez, and Laszlo Radvanyi at the department of Melanoma Medical Oncology, The University of Texas M.D. Anderson Cancer Center.